

UNIVERSITY OF CANTERBURY

MASTERS THESIS

Detailed characterisation of ground
water nitrate/leachate flow in gravelly
deposits using EM and GPR methods
with particular reference to temporal
flow changes

Author:

Matthew David JAMES

Supervisors:

Dr. Travis HORTON

Dr. David NOBES

Dr. Clint RISSMANN

Dr. Mike FINNEMORE

*A thesis submitted in fulfilment of the requirements
for the degree of Master of Science*

in

Engineering Geology

Geological Sciences

January 2015

Declaration of Authorship

I, Matthew David JAMES, declare that this thesis titled, 'Detailed characterisation of ground water nitrate/leachate flow in gravelly deposits using EM and GPR methods with particular reference to temporal flow changes' and the work presented in it are my own. I confirm that:

- This work was done wholly or mainly while in candidature for a research degree at this University.
- Where any part of this thesis has previously been submitted for a degree or any other qualification at this University or any other institution, this has been clearly stated.
- Where I have consulted the published work of others, this is always clearly attributed.
- Where I have quoted from the work of others, the source is always given. With the exception of such quotations, this thesis is entirely my own work.
- I have acknowledged all main sources of help.
- Where the thesis is based on work done by myself jointly with others, I have made clear exactly what was done by others and what I have contributed myself.

Signed: *Matt James*

Date: 25/01/2015

Acknowledgements

I would like to start by thanking David Nobes for all of the help and guidance he has given me over the last year. This would not have been possible without his unwavering attention to detail and commitment to helping me, even when working in China. The speed with which David replies to my emails is unbelievable, and I could not have asked for a more dedicated and helpful supervisor.

To Clint Rissmann, Darren May, Andrew Little, and the Environment Southland team it was a pleasure to meet and work alongside you all. I have grown to love northern Southland; you guys and girls have an amazing workplace. Also congratulations Darren on getting a job at ES!

Thank you Travis Horton for firstly allowing me to turn you into my primary supervisor when David made the move to China, and for then being so relaxed and understanding of what I was trying to achieve. Our progress meetings at the gym were highly productive and kept me on track!

From Southern Geophysical Ltd I would like to thank Mike Finnemore and Christian Ruegg for their help in both my research and work endeavours.

I would like to give a huge thank you to Ben Walling, who as landowner and farmer allowed me undisturbed access to his property throughout the year. I could not have dug those enormous holes without your digger and this research would not have been possible without your permission. The fact that you allowed research to be conducted on your property which could have potentially provided negative feedback for your industry is a brave move. You give great hope for the future of farming alongside environmental research, and I thank you for that.

To my mother, Sarra Hunter-Weston, and my partner, Aleisha Langdale, thank you so much for towing around geophysical equipment in sun, rain, snow, and mud. I assure you that being turned into tractors was worth it, and there is no way I could have done this without your help!

To Tracy and Brian Ross, owners of the Lumsden Motel, thank you for housing me throughout the research. I spent three weeks in Lumsden, and it was always lovely getting back to your motel in the evenings.

Thank you to Meadow Mushrooms for helping me financially, in the last few months you allowed me to maintain a pleasurable standard of living while I was concentrating wholly on writing.

I would also like to make a special mention of Dr. James Burn who provided me with a Toyota Landcruiser to use for my research. I put 15,000 kilometres onto your truck and none of this would have been possible without your generosity.

And finally to everyone at the University of Canterbury, my friends, and family. Thank you so much for your help, friendship, and fun over the last five years. It has been a university life full of great times, and the skiing, partying, travelling, and memories have helped me get to where I am today.

For all the support, thank you.

Abstract

Irthing Road is situated 20 kilometres north of the small town of Lumsden in Northern Southland, New Zealand. Irthing Road is accessed from State Highway 97 and leads north-west for 7 kilometres up the Irthing Creek Valley. The research site is situated 4.4 kilometres from the Irthing Road - State Highway 97 intersection and the area is at 300 metres elevation above sea level on gently south sloping Quaternary alluvial deposits.

The study was initiated by Environment Southland and Southern Geophysical Ltd with the intention of investigating the potential uses of near surface geophysics in the mapping of shallow groundwater contamination, specifically agriculturally sourced nitrates and leachates. The changes in land use and the introduction of high density grazing of dairy cattle on free draining soils in Southland has created cause for concern around the ease at which large volumes of contaminants could potentially gain access to the shallow groundwater system.

The investigation of the Irthing Road field site included: (1) background research into historical land use changes that may have affected the area 2) a study of the Lumsden area geological and hydrogeological setting 3) six trips to the field site throughout the year to collect near surface geophysical data using a Geonics Ltd EM31-MK2, Dualem Inc. DUAL-EM 421s, and Sensors & Software pulseEKKO Pro GPR system; 4) groundwater testing conducted by Environment Southland; 5) an evaluation of the geophysical and groundwater data sets to identify whether leachate concentrations were high enough to register an anomalous response 6) the identification of how the groundwater system at the Irthing Road field site behaves 7) a conclusion as to the effectiveness of all three near surface geophysical techniques in this application.

The major conclusions that emerged from this study are: (1) the groundwater system is transporting a large volume of water beneath the site and this leads to such efficient removal of contaminants that the concentrations are not high enough to register a response in the geophysical data 2) the groundwater system is highly sensitive to rainfall and this is a contributing factor to the variation within the geophysical data 3) the Geonics Ltd EM31-MK2 and Sensors & Software pulseEKKO Pro GPR system returned highly consistent results and have great potential in further contaminated groundwater applications 4) Environment Southlands' DUAL-EM 421s needs more consistency, however the device has a lot of potential once reliability can be ensured 5) further research is needed to determine the contamination flow paths and destinations at a larger, regional scale.

Contents

Declaration of Authorship	i
Acknowledgements	ii
Abstract	iv
Contents	v
List of Figures	viii
1 Introduction	1
1.1 Introduction	1
1.2 Study Background	2
1.3 Project Objectives	2
1.4 Thesis Conceptualisation	3
2 Project Area	5
2.1 Introduction	5
2.2 Location, Climate and Vegetation	5
2.3 Socio-economic Condition	7
2.4 Geological History	10
2.5 Current Geology and Hydrogeology	13
3 Literature Review	17
3.1 Introduction to Shallow Groundwater Contamination	17
3.2 Geophysics in Agriculture	18
3.3 Geophysics to Monitor Shallow Groundwater Contamination from Agri- culture	20
4 Methodology	22
4.1 Introduction	22
4.2 Research Site Selection	24
4.3 Initial Research Site Development	24
4.4 Electromagnetic Methods	28
4.4.1 EM31 Survey	28

4.4.1.1	EM31 Data Processing	31
4.4.2	DUAL-EM Survey	35
4.4.2.1	DUAL-EM Data Processing	37
4.5	Ground Penetrating Radar	38
4.5.1	GPR Data Processing	41
4.6	Groundwater Sampling	46
4.7	Combination of Techniques	46
5	Results and Interpretation	48
5.1	EM-31 Results	48
5.1.1	EM-31 Base Level Initial Results	48
5.1.2	EM-31 Temporal Changes	55
5.2	DUAL-EM Results	61
5.2.1	DUAL-EM Base Level Initial Results	61
5.2.2	DUAL-EM Temporal Changes	67
5.2.3	The use of DUAL-EM as a stand alone method	71
5.3	GPR Results	73
5.3.1	GPR Base Level Initial Results	73
5.3.2	GPR Temporal Changes	84
5.4	Groundwater Sampling	95
5.5	Interpretations based upon all data	95
5.5.1	System Temporal Changes	96
5.5.2	System Behaviour	107
6	Conclusion and Recommendations	108
6.1	Conclusion	108
6.2	Recommendations	110
6.2.1	Future Research Plan	111
A	Appendix 1: Supporting Resources	112
B	Appendix 2: EM31 Results	115
C	Appendix 3: DUAL-EM Results	176
D	Appendix 4: GPR Results	343
D.1	Trip 1	343
D.1.1	Line 0: 100 MHz	343
D.1.2	Line 25: 100 MHz	347
D.1.3	Line 50: 100 MHz	351
D.1.4	Line 75: 100 MHz	355
D.1.5	Line 100: 100 MHz	359
D.1.6	Line 0: 200 MHz	363
D.1.7	Line 50: 200 MHz	367
D.1.8	Line 100: 200 MHz	371
D.2	Trip 2	375
D.2.1	Line 0: 100 MHz	375

D.2.2	Line 25: 100 MHz	379
D.2.3	Line 50: 100 MHz	383
D.2.4	Line 75: 100 MHz	387
D.2.5	Line 100: 100 MHz	391
D.3	Trip 3	395
D.3.1	Line 0: 100 MHz	395
D.3.2	Line 0: 100 MHz Truck Towed	399
D.3.3	Line 100: 200 MHz	403
D.3.4	Line 50: 100 MHz	407
D.4	Trip 5	411
D.4.1	Line 0: 100 MHz	411
D.4.2	Line 25: 100 MHz	415
D.4.3	Line 50: 100 MHz	419
D.4.4	Line 75: 100 MHz	423
D.4.5	Line 100: 100 MHz	427
D.4.6	Line 10 Transverse: 100 MHz	431
D.4.7	Line 150 Transverse: 100 MHz	433
D.4.8	Line 300 Transverse: 100 MHz	435
D.5	Trip 6	437
D.5.1	Line 0: 100 MHz	437
D.5.2	Line 25: 100 MHz	441
D.5.3	Line 50: 100 MHz	445
D.5.4	Line 75: 100 MHz	449
D.5.5	Line 100: 100 MHz	453

List of Figures

2.1	Site Map	6
2.2	Southland Vegetation and Topography (Grant, 2012)	7
2.3	Vegetation at Irthing Road Field Site (DOC, 2010)	7
2.4	Swedes and Bailage Before Stock Arrival - 27 March 2014 (Photo courtesy of D. C. Nobes)	8
2.5	Cows Strip Grazing - 07 June 2014 (Photo courtesy of D. C. Nobes) . . .	9
2.6	QMAP Geological Map with topography (ArcGIS et al., 2012; Turnbull, 2000)	11
2.7	QMAP Geological Map with topography (ArcGIS et al., 2012; Turnbull, 2000)	12
2.8	Close up photo of Irthing field site - Gravelly Soil	14
2.9	Close up photo of Irthing field site - Soil	14
2.10	Close up photo of Irthing field site - Large boulder	15
2.11	Irthing Stream emerging from Irthing Valley upstream of the field site . .	15
2.12	Irthing Stream flowing in Irthing Valley	16
4.1	Table showing the dates of the research trips to Southland.	23
4.2	Topographic map showing Irthing field site line set up. Green box represents the grazing area of wintering cattle, the black arrow is the shallow groundwater flow direction, and the red grid marks the geophysical survey lines.	26
4.3	Survey line set up showing Irthing Valley. This is a Google Earth image from 21/01/2013 taken at 367 metres elevation.	26
4.4	Survey line layout using Google Earth images taken from 21/01/2013 at 700 metres altitude.	27
4.5	Photo along survey line 25 taken from the 290 metre mark looking north. This photo appears to show changes in surface vegetation growth that coincides with the location of old channels shown in the Google Earth images of Figure 4.3 and 4.4 which date back to 21/01/2013	27
4.6	David Nobes running EM31	29
4.7	Matt James running EM31 (Photo courtesy of D. C. Nobes)	30
4.8	Changing raw EM31 .R31 format to .G31 format for processing	31
4.9	Changing the .G31 format to XYZ format using DAT31W	31
4.10	Processing the XYZ file in Microsoft Excel	32
4.11	Interpolating EM31 data using Matlab	33
4.12	Using Grapher 9 software to present EM31 data. This example shows the difference between parallel and perpendicular coil orientations along all five of the survey lines. Error bars represent the ± 0.2 mS/m error of the EM31 device.	34

4.13	Matt James and Darren May running DUAL-EM (Photo courtesy of A. Langdale)	35
4.14	Table showing the Effective Depth of Exploration (DOE) for the various coil spacings and configurations in the DUAL-EM 421s. Sourced from (May, 2014), based upon data from (Triantafilis et al., 2013)	36
4.15	Raw XYZ data from the DUAL-EM after it has been imported into Microsoft Excel.	37
4.16	Sled with 100MHz antennas attached.	38
4.17	Running 100MHz GPR (Photo courtesy of A. Langdale).	39
4.18	Running 200MHz GPR past metal objects can cause interference in the data.	40
4.19	Importing raw GPR data into EKKO View Deluxe.	42
4.20	Editing GPR trace data within EKKO View Deluxe.	42
4.21	Rubberbanding GPR data using EKKO View Deluxe.	43
4.22	CMP Analysis showing the sub surface velocity of 0.9 m/s.	43
4.23	Migrating GPR data using EKKO View Deluxe.	44
4.24	Adding topography to GPR data using EKKO View Deluxe.	44
4.25	Adjusting gains using EKKO View Deluxe.	45
4.26	Final radargram output.	45
4.27	Locations of groundwater sampling pits with photos showing possible changes in surface vegetation across the field area.	47
4.28	GPR radargram with a 100MHz EM31 apparent conductivity overlay.	47
5.1	Comparison of EM31 apparent conductivities recorded with both parallel and perpendicular coil orientation. The results include data from trip 1 and 2. Error bars represent the $\pm 0.2 \text{ mS/m}$ error of the EM31 device.	50
5.2	Comparison of EM31 apparent conductivities recorded during trip 1 with both parallel and perpendicular coil orientation.	51
5.3	Comparison of EM31 apparent conductivities recorded during trip 2 with both parallel and perpendicular coil orientation.	52
5.4	Comparison of EM31 apparent conductivities recorded during trips 1 and 2 using a parallel coil orientation. Error bars represent the $\pm 0.2 \text{ mS/m}$ error of the EM31 device.	53
5.5	Google Earth image with an overlay of the trip 1 EM31 data collected using parallel coil orientation. The blue areas identify high apparent conductivity areas. The arrows represent possible infilled historic flow paths and the green oval marks the central low conductivity zone.	54
5.6	Google Earth image with an overlay of the trip 2 EM31 data collected using parallel coil orientation. The blue areas identify high apparent conductivity areas. The arrows represent possible infilled historic flow paths and the green oval marks the central low conductivity zone.	54
5.7	EM31 data recorded over five trips using a parallel coil orientation. All lines are shown and data from different trips is distinguished using different colours. Error bars represent the $\pm 0.2 \text{ mS/m}$ error of the EM31 device.	56
5.8	EM31 data recorded over five trips using a perpendicular coil orientation. All lines are shown and data from different trips is distinguished using different colours. Error bars represent the $\pm 0.2 \text{ mS/m}$ error of the EM31 device.	57

5.9	EM31 data recorded over five trips using a parallel coil and perpendicular coil orientations along line 0. This data has then been turned into composite plots to compare trends between trips.	58
5.10	EM31 data recorded over five trips using a parallel coil and perpendicular coil orientations along line 25. This data has then been turned into composite plots to compare trends between trips.	58
5.11	EM31 data recorded over five trips using a parallel coil and perpendicular coil orientations along line 50. This data has then been turned into composite plots to compare trends between trips.	59
5.12	EM31 data recorded over five trips using a parallel coil and perpendicular coil orientations along line 75. This data has then been turned into composite plots to compare trends between trips.	60
5.13	EM31 data recorded over five trips using a parallel coil and perpendicular coil orientations along line 100. This data has then been turned into composite plots to compare trends between trips.	60
5.14	DUAL-EM horizontal co-planar 1 apparent conductivity from trip 1. Both parallel and perpendicular coil orientations are shown for the 1 metre coil spacing.	63
5.15	DUAL-EM horizontal co-planar 1 apparent conductivity from trip 2. Both parallel and perpendicular coil orientations are shown for the 1 metre coil spacing.	64
5.16	Comparison of DUAL-EM horizontal co-planar 2 apparent conductivity results from trips 1 and 2. This figure shows data from both coil orientations across three lines using a 2 metre coil spacing.	65
5.17	Comparison of DUAL-EM horizontal co-planar 4 apparent conductivity results from trips 1 and 2. This figure shows data from both coil orientations across three lines using a 4 metre coil spacing.	66
5.18	Comparison of DUAL-EM horizontal co-planar 4 apparent conductivity results across all of the lines from all of the research trips.	67
5.19	composite plot showing the DUAL-EM horizontal co-planar results from trips 1, 2, 5, and 6 along line 0. This data is recorded using a 4 metre coil separation. There is also a composite plot of the EM31 data along line 0 from trip 2. This EM31 plot is intended to be used as a reference to compare techniques.	68
5.20	composite plot showing the DUAL-EM horizontal co-planar results from trips 1, 2, 3, 5, and 6 along line 50. This data is recorded using a 4 metre coil separation. There is also a composite plot of the EM31 data along line 50 from trip 2. This EM31 plot is intended to be used as a reference to compare techniques.	69
5.21	composite plot showing the DUAL-EM horizontal co-planar results from trips 1, 2, 3, 5, and 6 along line 100. This data is recorded using a 4 metre coil separation. There is also a composite plot of the EM31 data along line 100 from trip 2. This EM31 plot is intended to be used as a reference to compare techniques.	69
5.22	100MHz radargram along line 0 from trip 6. This is then overlain with the line 50 EM31 and DUAL-EM data from trip 6.	72
5.23	Radargram showing the 200 MHz results from Trip 1, Line 0.	74
5.24	Comparison of 100 MHz GPR radargrams from trip 1 and 2 along line 0 between the 10 metre and 60 metre marks.	75

5.25	100MHz radargram from trip 1 showing the difference in DOE between the 165 - 245 metre mark and the 250 - 300 metre mark.	76
5.26	100MHz radargram from trip 1 showing the difference in DOE between the 165 - 245 metre mark and the 250 - 300 metre mark.	78
5.27	100MHz radargram from trip 1 showing the point at 150 metres when the DOE appears to plateau and continue at a relatively uniform 6 metres depth.	79
5.28	100MHz radargram from trip 1 showing the increasing depth of penetration along the 50 metre line as the radar travels away from the 10 metre mark.	79
5.29	100 MHz and 200 MHz radargrams from trip 1 showing the extremely poor DOE near the 10 metre mark on the 50 metre line. These two radargrams also show how well the two frequencies compare with one another.	80
5.30	100 MHz radargram from the 75 metre line showing the DOE slowly increasing from the 10 metre mark until the 190 metre mark.	81
5.31	Comparison between the 100 MHz and 200 MHz radargrams showing the areas of lower radar penetration.	82
5.32	100 MHz radargram showing the poor DOE towards the end of the 100 metre line.	83
5.33	A collection of all of the 100 MHz radargrams that were recorded along line 0.	86
5.34	Comparison between two 100 MHz radargrams recorded along line 0. The first is towed by hand, the second is towed using a Toyota Hilux 4WD vehicle.	87
5.35	A collection of all of the 100 MHz radargrams that were recorded along line 25.	88
5.36	A collection of 100 MHz radargram sections from line 25. These sections focus on the area between 250 and 300 metres along the GPR line.	89
5.37	A collection of all of the 100 MHz radargrams that were recorded along line 50.	90
5.38	A collection of 100 MHz radargram sections from line 50. These sections focus on the area between 0 and 50 metres along the GPR line.	91
5.39	A collection of all of the 100 MHz radargrams that were recorded along line 75.	92
5.40	A collection of 100 MHz radargram sections from line 75. These sections focus on the area between 150 and 200 metres along the GPR line.	93
5.41	A collection of all of the 100 MHz radargrams that were recorded along line 100.	94
5.42	100MHz radargram along line 0 from trip 1. This is then overlain with the line 0 EM31 and DUAL-EM data from trip 1.	97
5.43	100MHz radargram along line 0 from trip 2. This is then overlain with the line 0 EM31 and DUAL-EM data from trip 2.	97
5.44	100MHz radargram along line 0 from trip 3. This is then overlain with the line 0 EM31 data from trip 3.	98
5.45	100MHz radargram along line 0 from trip 5. This is then overlain with the line 0 EM31 and DUAL-EM data from trip 5.	98
5.46	100MHz radargram along line 0 from trip 6. This is then overlain with the line 0 EM31 and DUAL-EM data from trip 6.	99

5.47	100MHz radargram along line 50 from trip 1. This is then overlain with the line 50 EM31 and DUAL-EM data from trip 1.	99
5.48	100MHz radargram along line 50 from trip 2. This is then overlain with the line 50 EM31 and DUAL-EM data from trip 2.	100
5.49	100MHz radargram along line 50 from trip 3. This is then overlain with the line 50 EM31 and DUAL-EM data from trip 3.	100
5.50	100MHz radargram along line 50 from trip 5. This is then overlain with the line 50 EM31 and DUAL-EM data from trip 5.	101
5.51	100MHz radargram along line 50 from trip 6. This is then overlain with the line 50 EM31 and DUAL-EM data from trip 6.	101
5.52	100MHz radargram along line 100 from trip 1. This is then overlain with the line 100 EM31 and DUAL-EM data from trip 1.	102
5.53	100MHz radargram along line 100 from trip 2. This is then overlain with the line 100 EM31 and DUAL-EM data from trip 2.	102
5.54	100MHz radargram along line 100 from trip 5. This is then overlain with the line 100 EM31 and DUAL-EM data from trip 5.	103
5.55	100MHz radargram along line 100 from trip 6. This is then overlain with the line 100 EM31 and DUAL-EM data from trip 6.	103
5.56	EM31 and DUAL-EM data recorded in the paddock that contained wintering cows. Reference data from line 0 is also included with each plot. . .	105
5.57	EM31 and DUAL-EM data recorded by walking between the cow paddock and the survey area in an attempt to see any obvious changes in apparent conductivity.	106
A.1	Description of Geological units shown in figure 2.7 (Turnbull, 2000) . . .	112
A.2	Water sampling results from Environment Southland. Sample 20145041: Southern Pit. Sample 20145042: Northern Pit. Sample 20145045: Irthing Stream. Sample 20145046: Creek between cow paddock and survey area. . .	113
A.3	Water sampling results from Environment Southland. Sample 20145043: Crop Paddock Soil Water. Sample 20145044: Survey Area Soil Water. . .	114
D.1	GPR 100MHz complete radargram from line 0	343
D.2	GPR 100MHz 10 - 60 metre radargram section from line 0	344
D.3	GPR 100MHz 60 - 110 metre radargram section from line 0	344
D.4	GPR 100MHz 105 - 155 metre radargram section from line 0	345
D.5	GPR 100MHz 155 - 205 metre radargram section from line 0	345
D.6	GPR 100MHz 205 - 255 metre radargram section from line 0	346
D.7	GPR 100MHz 255 - 300 metre radargram section from line 0	346
D.8	GPR 100MHz complete radargram from line 25	347
D.9	GPR 100MHz 10 - 60 metre radargram section from line 25	347
D.10	GPR 100MHz 60 - 110 metre radargram section from line 25	348
D.11	GPR 100MHz 105 - 155 metre radargram section from line 25	348
D.12	GPR 100MHz 155 - 205 metre radargram section from line 25	349
D.13	GPR 100MHz 205 - 255 metre radargram section from line 25	349
D.14	GPR 100MHz 255 - 300 metre radargram section from line 25	350
D.15	GPR 100MHz complete radargram from line 50	351
D.16	GPR 100MHz 10 - 60 metre radargram section from line 50	351
D.17	GPR 100MHz 60 - 110 metre radargram section from line 50	352

D.18 GPR 100MHz 105 - 155 metre radargram section from line 50	352
D.19 GPR 100MHz 155 - 205 metre radargram section from line 50	353
D.20 GPR 100MHz 205 - 255 metre radargram section from line 50	353
D.21 GPR 100MHz 255 - 300 metre radargram section from line 50	354
D.22 GPR 100MHz complete radargram from line 75	355
D.23 GPR 100MHz 10 - 60 metre radargram section from line 75	355
D.24 GPR 100MHz 60 - 110 metre radargram section from line 75	356
D.25 GPR 100MHz 105 - 155 metre radargram section from line 75	356
D.26 GPR 100MHz 155 - 205 metre radargram section from line 75	357
D.27 GPR 100MHz 205 - 255 metre radargram section from line 75	357
D.28 GPR 100MHz 255 - 300 metre radargram section from line 75	358
D.29 GPR 100MHz complete radargram from line 100	359
D.30 GPR 100MHz 10 - 60 metre radargram section from line 100	359
D.31 GPR 100MHz 60 - 110 metre radargram section from line 100	360
D.32 GPR 100MHz 105 - 155 metre radargram section from line 100	360
D.33 GPR 100MHz 155 - 205 metre radargram section from line 100	361
D.34 GPR 100MHz 205 - 255 metre radargram section from line 100	361
D.35 GPR 100MHz 255 - 300 metre radargram section from line 100	362
D.36 GPR 200MHz complete radargram from line 0	363
D.37 GPR 200MHz 10 - 60 metre radargram section from line 0	363
D.38 GPR 200MHz 60 - 110 metre radargram section from line 0	364
D.39 GPR 200MHz 105 - 155 metre radargram section from line 0	364
D.40 GPR 200MHz 155 - 205 metre radargram section from line 0	365
D.41 GPR 200MHz 205 - 255 metre radargram section from line 0	365
D.42 GPR 200MHz 255 - 300 metre radargram section from line 0	366
D.43 GPR 200MHz complete radargram from line 50	367
D.44 GPR 200MHz 10 - 60 metre radargram section from line 50	367
D.45 GPR 200MHz 60 - 110 metre radargram section from line 50	368
D.46 GPR 200MHz 105 - 155 metre radargram section from line 50	368
D.47 GPR 200MHz 155 - 205 metre radargram section from line 50	369
D.48 GPR 200MHz 205 - 255 metre radargram section from line 50	369
D.49 GPR 200MHz 255 - 300 metre radargram section from line 50	370
D.50 GPR 200MHz complete radargram from line 100	371
D.51 GPR 200MHz 10 - 60 metre radargram section from line 100	371
D.52 GPR 200MHz 60 - 110 metre radargram section from line 100	372
D.53 GPR 200MHz 105 - 155 metre radargram section from line 100	372
D.54 GPR 200MHz 155 - 205 metre radargram section from line 100	373
D.55 GPR 200MHz 205 - 255 metre radargram section from line 100	373
D.56 GPR 200MHz 255 - 300 metre radargram section from line 100	374
D.57 GPR 100MHz complete radargram from line 0	375
D.58 GPR 100MHz 10 - 60 metre radargram section from line 0	376
D.59 GPR 100MHz 60 - 110 metre radargram section from line 0	376
D.60 GPR 100MHz 105 - 155 metre radargram section from line 0	377
D.61 GPR 100MHz 155 - 205 metre radargram section from line 0	377
D.62 GPR 100MHz 205 - 255 metre radargram section from line 0	378
D.63 GPR 100MHz 255 - 300 metre radargram section from line 0	378
D.64 GPR 100MHz complete radargram from line 25	379

D.65 GPR 100MHz 10 - 60 metre radargram section from line 25	379
D.66 GPR 100MHz 60 - 110 metre radargram section from line 25	380
D.67 GPR 100MHz 105 - 155 metre radargram section from line 25	380
D.68 GPR 100MHz 155 - 205 metre radargram section from line 25	381
D.69 GPR 100MHz 205 - 255 metre radargram section from line 25	381
D.70 GPR 100MHz 255 - 300 metre radargram section from line 25	382
D.71 GPR 100MHz complete radargram from line 50	383
D.72 GPR 100MHz 10 - 60 metre radargram section from line 50	383
D.73 GPR 100MHz 60 - 110 metre radargram section from line 50	384
D.74 GPR 100MHz 105 - 155 metre radargram section from line 50	384
D.75 GPR 100MHz 155 - 205 metre radargram section from line 50	385
D.76 GPR 100MHz 205 - 255 metre radargram section from line 50	385
D.77 GPR 100MHz 255 - 300 metre radargram section from line 50	386
D.78 GPR 100MHz complete radargram from line 75	387
D.79 GPR 100MHz 10 - 60 metre radargram section from line 75	387
D.80 GPR 100MHz 60 - 110 metre radargram section from line 75	388
D.81 GPR 100MHz 105 - 155 metre radargram section from line 75	388
D.82 GPR 100MHz 155 - 205 metre radargram section from line 75	389
D.83 GPR 100MHz 205 - 255 metre radargram section from line 75	389
D.84 GPR 100MHz 255 - 300 metre radargram section from line 75	390
D.85 GPR 100MHz complete radargram from line 100	391
D.86 GPR 100MHz 10 - 60 metre radargram section from line 100	391
D.87 GPR 100MHz 60 - 110 metre radargram section from line 100	392
D.88 GPR 100MHz 105 - 155 metre radargram section from line 100	392
D.89 GPR 100MHz 155 - 205 metre radargram section from line 100	393
D.90 GPR 100MHz 205 - 255 metre radargram section from line 100	393
D.91 GPR 100MHz 255 - 300 metre radargram section from line 100	394
D.92 GPR 100MHz complete radargram from line 0	395
D.93 GPR 100MHz 10 - 60 metre radargram section from line 0	396
D.94 GPR 100MHz 60 - 110 metre radargram section from line 0	396
D.95 GPR 100MHz 105 - 155 metre radargram section from line 0	397
D.96 GPR 100MHz 155 - 205 metre radargram section from line 0	397
D.97 GPR 100MHz 205 - 255 metre radargram section from line 0	398
D.98 GPR 100MHz 255 - 300 metre radargram section from line 0	398
D.99 GPR 100MHz complete radargram from line 0	399
D.100GPR 100MHz 10 - 60 metre radargram section from line 0	399
D.101GPR 100MHz 60 - 110 metre radargram section from line 0	400
D.102GPR 100MHz 105 - 155 metre radargram section from line 0	400
D.103GPR 100MHz 155 - 205 metre radargram section from line 0	401
D.104GPR 100MHz 205 - 255 metre radargram section from line 0	401
D.105GPR 100MHz 255 - 300 metre radargram section from line 0	402
D.106GPR 200MHz complete radargram from line 100	403
D.107GPR 200MHz 10 - 60 metre radargram section from line 100	403
D.108GPR 200MHz 60 - 110 metre radargram section from line 100	404
D.109GPR 200MHz 105 - 155 metre radargram section from line 100	404
D.110GPR 200MHz 155 - 205 metre radargram section from line 100	405
D.111GPR 200MHz 205 - 255 metre radargram section from line 100	405

D.112GPR 200MHz 255 - 300 metre radargram section from line 100	406
D.113GPR 100MHz complete radargram from line 50	407
D.114GPR 100MHz 10 - 60 metre radargram section from line 50	407
D.115GPR 100MHz 60 - 110 metre radargram section from line 50	408
D.116GPR 100MHz 105 - 155 metre radargram section from line 50	408
D.117GPR 100MHz 155 - 205 metre radargram section from line 50	409
D.118GPR 100MHz 205 - 255 metre radargram section from line 50	409
D.119GPR 100MHz 255 - 300 metre radargram section from line 50	410
D.120GPR 100MHz complete radargram from line 0	411
D.121GPR 100MHz 10 - 60 metre radargram section from line 0	412
D.122GPR 100MHz 60 - 110 metre radargram section from line 0	412
D.123GPR 100MHz 105 - 155 metre radargram section from line 0	413
D.124GPR 100MHz 155 - 205 metre radargram section from line 0	413
D.125GPR 100MHz 205 - 255 metre radargram section from line 0	414
D.126GPR 100MHz 255 - 300 metre radargram section from line 0	414
D.127GPR 100MHz complete radargram from line 25	415
D.128GPR 100MHz 10 - 60 metre radargram section from line 25	415
D.129GPR 100MHz 60 - 110 metre radargram section from line 25	416
D.130GPR 100MHz 105 - 155 metre radargram section from line 25	416
D.131GPR 100MHz 155 - 205 metre radargram section from line 25	417
D.132GPR 100MHz 205 - 255 metre radargram section from line 25	417
D.133GPR 100MHz 255 - 300 metre radargram section from line 25	418
D.134GPR 100MHz complete radargram from line 50	419
D.135GPR 100MHz 10 - 60 metre radargram section from line 50	419
D.136GPR 100MHz 60 - 110 metre radargram section from line 50	420
D.137GPR 100MHz 105 - 155 metre radargram section from line 50	420
D.138GPR 100MHz 155 - 205 metre radargram section from line 50	421
D.139GPR 100MHz 205 - 255 metre radargram section from line 50	421
D.140GPR 100MHz 255 - 300 metre radargram section from line 50	422
D.141GPR 100MHz complete radargram from line 75	423
D.142GPR 100MHz 10 - 60 metre radargram section from line 75	423
D.143GPR 100MHz 60 - 110 metre radargram section from line 75	424
D.144GPR 100MHz 105 - 155 metre radargram section from line 75	424
D.145GPR 100MHz 155 - 205 metre radargram section from line 75	425
D.146GPR 100MHz 205 - 255 metre radargram section from line 75	425
D.147GPR 100MHz 255 - 300 metre radargram section from line 75	426
D.148GPR 100MHz complete radargram from line 100	427
D.149GPR 100MHz 10 - 60 metre radargram section from line 100	427
D.150GPR 100MHz 60 - 110 metre radargram section from line 100	428
D.151GPR 100MHz 105 - 155 metre radargram section from line 100	428
D.152GPR 100MHz 155 - 205 metre radargram section from line 100	429
D.153GPR 100MHz 205 - 255 metre radargram section from line 100	429
D.154GPR 100MHz 255 - 300 metre radargram section from line 100	430
D.155GPR 100MHz complete radargram from a transverse along line 10	431
D.156GPR 100MHz 0 - 50 metre radargram section from a transverse along line 10	431

D.157	GPR 100MHz 50 - 100 metre radargram section from a transverse along line 10	432
D.158	GPR 100MHz complete radargram from a transverse along line 150	433
D.159	GPR 100MHz 0 - 50 metre radargram section from a transverse along line 150	433
D.160	GPR 100MHz 50 - 100 metre radargram section from a transverse along line 150	434
D.161	GPR 100MHz complete radargram from a transverse along line 300	435
D.162	GPR 100MHz 0 - 50 metre radargram section from a transverse along line 300	435
D.163	GPR 100MHz 50 - 100 metre radargram section from a transverse along line 300	436
D.164	GPR 100MHz complete radargram from line 0	437
D.165	GPR 100MHz 10 - 60 metre radargram section from line 0	438
D.166	GPR 100MHz 60 - 110 metre radargram section from line 0	438
D.167	GPR 100MHz 105 - 155 metre radargram section from line 0	439
D.168	GPR 100MHz 155 - 205 metre radargram section from line 0	439
D.169	GPR 100MHz 205 - 255 metre radargram section from line 0	440
D.170	GPR 100MHz 255 - 300 metre radargram section from line 0	440
D.171	GPR 100MHz complete radargram from line 25	441
D.172	GPR 100MHz 10 - 60 metre radargram section from line 25	441
D.173	GPR 100MHz 60 - 110 metre radargram section from line 25	442
D.174	GPR 100MHz 105 - 155 metre radargram section from line 25	442
D.175	GPR 100MHz 155 - 205 metre radargram section from line 25	443
D.176	GPR 100MHz 205 - 255 metre radargram section from line 25	443
D.177	GPR 100MHz 255 - 300 metre radargram section from line 25	444
D.178	GPR 100MHz complete radargram from line 50	445
D.179	GPR 100MHz 10 - 60 metre radargram section from line 50	445
D.180	GPR 100MHz 60 - 110 metre radargram section from line 50	446
D.181	GPR 100MHz 105 - 155 metre radargram section from line 50	446
D.182	GPR 100MHz 155 - 205 metre radargram section from line 50	447
D.183	GPR 100MHz 205 - 255 metre radargram section from line 50	447
D.184	GPR 100MHz 255 - 300 metre radargram section from line 50	448
D.185	GPR 100MHz complete radargram from line 75	449
D.186	GPR 100MHz 10 - 60 metre radargram section from line 75	449
D.187	GPR 100MHz 60 - 110 metre radargram section from line 75	450
D.188	GPR 100MHz 105 - 155 metre radargram section from line 75	450
D.189	GPR 100MHz 155 - 205 metre radargram section from line 75	451
D.190	GPR 100MHz 205 - 255 metre radargram section from line 75	451
D.191	GPR 100MHz 255 - 300 metre radargram section from line 75	452
D.192	GPR 100MHz complete radargram from line 100	453
D.193	GPR 100MHz 10 - 60 metre radargram section from line 100	453
D.194	GPR 100MHz 60 - 110 metre radargram section from line 100	454
D.195	GPR 100MHz 105 - 155 metre radargram section from line 100	454
D.196	GPR 100MHz 155 - 205 metre radargram section from line 100	455
D.197	GPR 100MHz 205 - 255 metre radargram section from line 100	455
D.198	GPR 100MHz 255 - 300 metre radargram section from line 100	456

Dedicated to everyone I met at university, cheers for the memories.

Chapter 1

Introduction

1.1 Introduction

Animal waste is a normal byproduct of agriculture, particularly dairying. The high nutrient content within animal waste is a good fertilizer, and the application of animal waste as a replacement for commercial fertiliser can save farmers millions of dollars per year. The damage to the environment however of applying too much effluent in vulnerable areas is severe and the understanding of this aspect is only beginning (Garnier et al., 1998).

Excess nutrients can have an impact on groundwater and its quality. Surface water percolates down through the protective soil layers, where mechanical, physiochemical, and microbiological processes degrade contaminants (Kirsch, 2009). The best protection is provided by a thick protective layer with low hydraulic conductivity that leads to high residence time of percolating water and hence allows removal or degradation of contaminants before they reach the groundwater system. The danger occurs when this barrier is either insufficient or has its integrity breached in a natural or manmade way. This is how contaminants from agriculture gain access to shallow groundwater systems that have very little protective layering. A common issue in agriculture is the addition of large volumes of animal waste onto an area that has a high hydraulic conductivity, which allows rapid transport of contaminants into a shallow groundwater system.

The application of geophysics to hydrogeology, generally, and agriculture, specifically, is not new (Allred et al., 2008; Reynolds, 2011), and the application to characterization of groundwater contaminant transport in an agricultural setting has been done before, both for mapping preferential flow paths (Close et al., 2004) and for time lapse mapping of groundwater changes (Versteeg, 2004), albeit usually in controlled lab conditions.

Here, we present preliminary results from a field experiment carried out on a farm in Southland, New Zealand. The farm had been used for low-intensity deer farming, and was recently converted to providing winter forage and grazing for dairy cattle. The focus of our work was to (1) locate potential preferential subsurface flow paths, (2) to determine if there was groundwater contamination, and (3) if so, was it at a level high enough to be of concern.

1.2 Study Background

This research project was initiated in March 2014 after representatives for Environment Southland, Southern Geophysical Ltd, and the University of Canterbury agreed upon a research proposal. The project is designed around understanding leachate flow from agriculture, particularly dairy cattle, in high density grazing situations. Environment Southland is tasked to protect shallow groundwater quality throughout Southland; they have made progress recently through the use of groundwater testing and identification of contaminant source locations. The desire of both Environment Southland and Southern Geophysical Ltd however is to gain a better understanding of the potential uses of near surface geophysics in monitoring and understanding shallow groundwater contamination.

The research schedule consisted of three distinct phases of study and preparation. The initial phase consisted of understanding the hydrogeological conditions of the research area prior to the introduction of heavily concentrated agriculture. Phase two involved the ongoing collection of data throughout the winter months and into mid spring with the intention of using this data in phase three to produce conclusive results. The third phase revolved around producing a thesis that clearly and concisely communicated the results of the research conducted. Conclusions upon the potential benefits of using near surface geophysics to indicate changes in contaminant concentrations and temporal flow of leachates within a shallow aquifer were of utmost importance.

1.3 Project Objectives

This project was created by Environment Southland and Southern Geophysical Ltd with the intention of investigating the potential uses of near surface geophysics in the mapping of shallow groundwater contamination, specifically agricultural contamination.

The primary objective is to test the application of GPR, EM31 and DUAL-EM devices in mapping the concentrations and temporal flow of contaminants in the shallow groundwater. The effectiveness of these results will also dictate what other objectives can be

met, as well as perhaps whether these techniques can be used on a wider scale in New Zealand as a way to better manage water contamination from animal waste

Using the information gathered through the GPR, EM31 and DUAL-EM surveys, it is hoped that a better understanding of the groundwater system and its interaction with the agricultural land use can be achieved. Recommendations on further testing will be an important output of the research. There is potential to apply the knowledge gained to other areas of New Zealand with similar land use and hydrogeological settings.

The project objectives therefore are:

1. Identify whether leachate concentrations are high enough for the GPR, EM31 and DUAL-EM techniques to register an anomalous response.
2. Identify how the groundwater system at the field site in Southland is behaving. This includes the effects of rainfall upon contaminant transport, how rainfall and soil structure affect infiltration speeds, and how the contaminants are moving through the system.
3. Comment upon the effectiveness of all three geophysical techniques with particular reference to commercial application of these techniques for the accurate monitoring of groundwater pollution. Include detailed planning for further testing and how this could positively influence the usefulness of these techniques in a commercial setting. Some suggestion of other possible techniques that could assist in providing a more complete picture will be included in the findings.

1.4 Thesis Conceptualisation

This thesis is formatted as follows to show the progression of the research and how the results affected the recommendations and planning for further investigations:

Chapter 2: Project Area

Chapter 2 outlines the location, climate and vegetation of the study area. This is then built upon by adding the geological history of the area including major geological units and their formation. The current geological and hydrogeological conditions are then discussed. The socio-economic conditions of the study area are also discussed because the past and current land use is very important for this project.

Chapter 3: Literature Review

The third chapter is a collection of research that is deemed highly relevant to this project. This includes an introduction into shallow groundwater contamination from agriculture

and examples from around the world. The history of the use of geophysics in agriculture is then explored. This chapter then concludes with a more focused look on the viability of using geophysics to monitor shallow groundwater contamination from agriculture.

Chapter 4: Methodology

Methodology is divided into six distinct sections based upon how the research was conducted. The first section explains the issues around site selection and how the decisions were made on survey set up. This is then followed by an explanation of the geophysical methods (EM31, DUAL-EM, GPR) used and how the data gained was processed. The final two sections then cover the groundwater sampling regime and how the data from multiple techniques is being combined to present a more complete picture.

Chapter 5: Results and Interpretation

The results are presented in an accurate and unbiased way. This is followed by an interpretation that draws upon almost a year's experience working in this field area. It is important to realise that the interpretation has a personal touch to it regardless of how impersonal the author tries to be so every reader is encouraged to analyse the results and come to their own conclusions. The results discuss the potential for the geophysical techniques to be applied on a commercial basis to shallow groundwater research and monitoring.

Chapter 6: Conclusion and Recommendations

The conclusion begins with a summary of the potential of the geophysical instruments to be used in a commercial application for shallow groundwater research and monitoring. The results of the research and how the project objectives were completed is then outlined. This is followed by recommendations and finally a plan as to how future research may be conducted as to best continue this work in a positive and productive manner.

Chapter 2

Project Area

2.1 Introduction

The following chapter was created using information from interviews, past research and field observations that strive to produce a complete picture of the research area and conditions. This chapter may be left incomplete in certain situations and be edited as needed to ensure privacy to the land owners that so kindly allowed me full access to their properties to conduct this research. If any part of this chapter is removed it will be clearly stated. The aim of the chapter is to outline the current details of the Irthing Road study area and to provide a broad history dating back to the Early Permian when the oldest geological group in this study area was formed. This is designed to provide a broader understanding of the area so that future work on this subject can be designed with reference to the geological and hydrogeological conditions that were encountered at this site. This allows for future testing at both similar and dissimilar sites.

2.2 Location, Climate and Vegetation

Irthing Road is situated approximately 20 kilometres north of the small town of Lumsden in Northern Southland, New Zealand. Irthing Road is accessed from State Highway 97 (Mossburn-Five Rivers Road) and leads north-west for 7 kilometres up the Irthing Creek Valley. The area is at 300 metres elevation above sea level and is gently sloping south towards the Oreti River. The topography and location is clearly shown in figure 2.1 on page 6. The study area is 520 metres to the south-west of Irthing road, with the access gate being 4.4 kilometres from the Irthing Road - State Highway 97 intersection. The research site is situated on the property of Ben Walling.

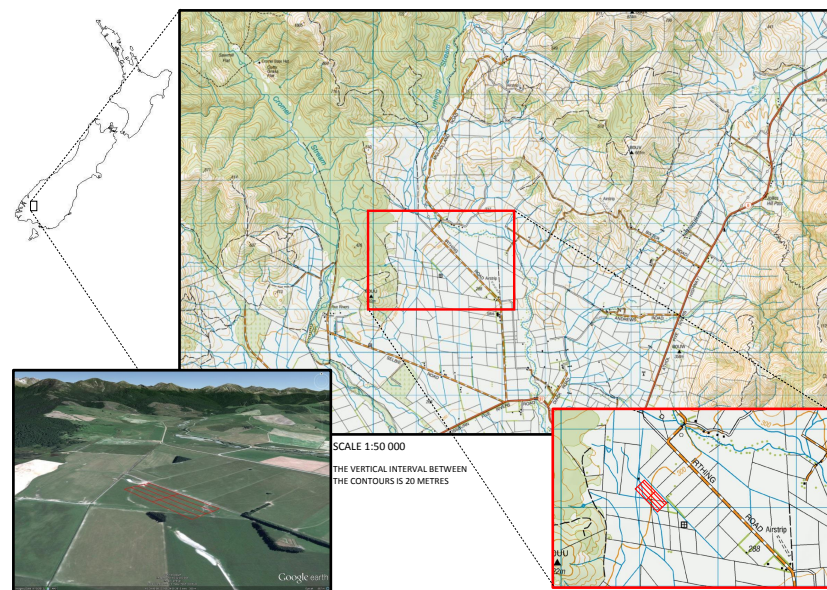


FIGURE 2.1: Site Map

The climate in northern Southland is described as mild and temperate, and is generally drier, calmer, and warmer than coastal areas of Southland (Environment-Southland, 2014). The increased altitude however means that there is a higher chance of snow (Venture-Southland, 2014). Southland on average receives 1600 sunshine hours per year, 1000 mm of rain, and wind speed averages of 15 - 25 kilometres per hour (Venture-Southland, 2014). Northern Southland however receives slightly less than the average 1000 mm of rain per year because a large proportion of the rainfall is on coastal areas or the high topography of Fiordland to the west. The driest months of the year are generally June, July, and August because a predominant southerly flow brings drier air whereas the westerly flows often experienced in December, January, and February bring the wettest conditions (Environment-Southland, 2014). The variation between the driest and wettest months is only 30 - 40 mm so the relatively uniform weather conditions create a great climate for agriculture. The average annual temperature in northern Southland is 9 - 12 degrees (Environment-Southland, 2014).

Before the arrival of humans in Southland the area was heavily forested with some tussock lowlands and valleys. The early Polynesians and European settlers proceeded to burn large areas of lowland Southland and replace the forests with high yield exotic grasses (See Figure 2.2). West Southland, predominantly Fiordland, was exempt from this due to the remoteness and extreme topography. The majority of Northern Southland was however transformed into grasslands and is now primarily used to produce sheep, cattle, and deer with an increasing tendency towards dairy farming. The field site at Irthing Road is high yield exotic grasses with gorse and tussock leading into established

forest as the elevation increases in the valley (Figure 2.3).

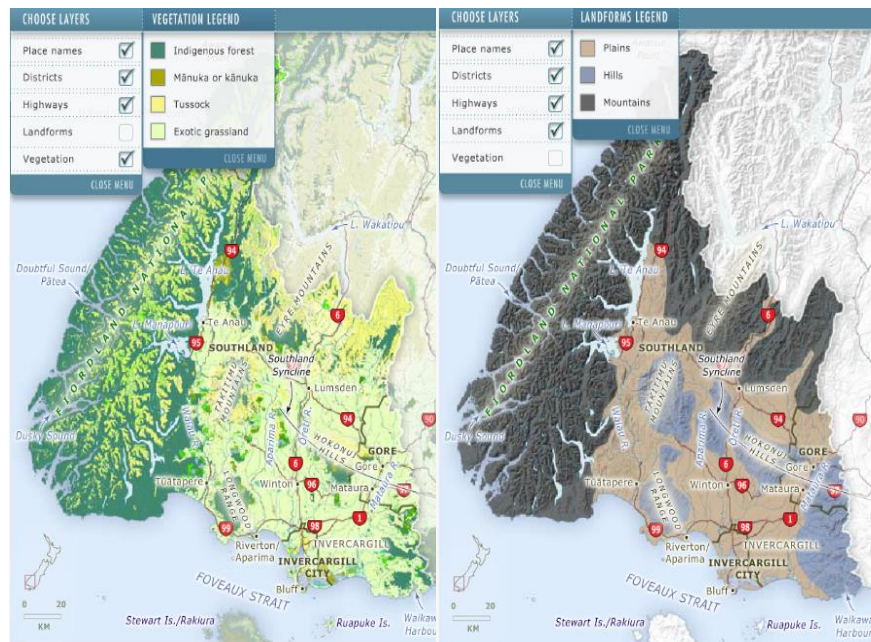


FIGURE 2.2: Southland Vegetation and Topography (Grant, 2012)

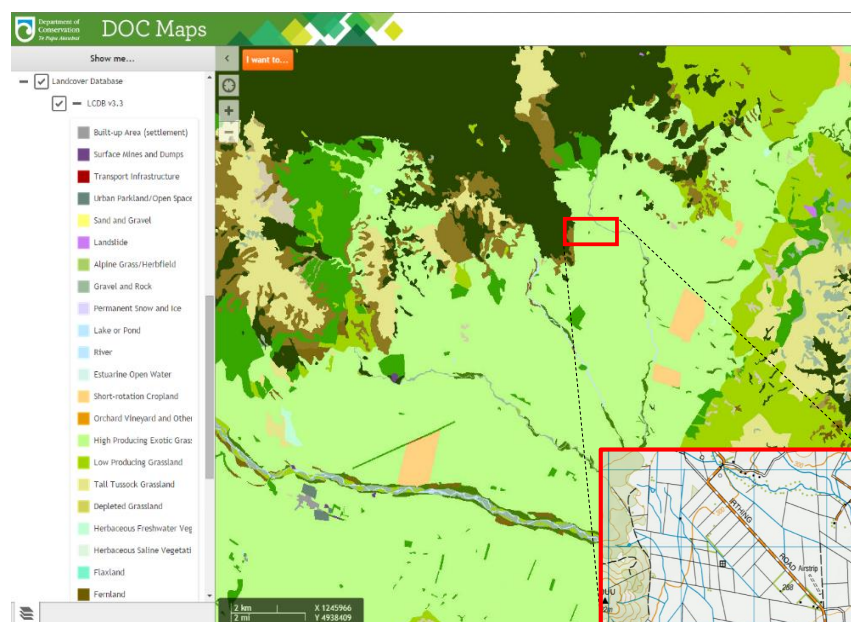


FIGURE 2.3: Vegetation at Irthing Road Field Site (DOC, 2010)

2.3 Socio-economic Condition

One of the reasons that the field site beside Irthing Road was chosen is the previous land use and farming history of this property. Prior to 2013 the land was used as a low

intensity deer farm with minimum density of stock that would have been producing very little animal discharge. The change to wintering dairy cattle was made by Ben Walling in 2014 for obvious financial reasons. The dairy industry in Southland is incredibly strong and growing at an enormous pace. This has raised the demand for free draining pastures on which to graze the dairy cows during the winter months when they are not being milked. There were approximately 1300 dairy cows on the Irthing Road property from early June until the end of August 2014 (Walling, pers. comm., 2014). The cattle were provided with swedes and bailage in a strip grazing format to ensure the food was used to its maximum efficiency (See Figure 2.4 on page 8). This involves confining the cattle to a small area of the paddock until they have eaten the area clear of all feed and then moving the fence slightly to allow them access to slightly more feed (See Figure 2.5 on page 9). There was estimated to be about 1300 kilogrammes of dry feed per square metre of grazing area (Walling, pers. comm., 2014).



FIGURE 2.4: Swedes and Bailage Before Stock Arrival - 27 March 2014 (Photo courtesy of D. C. Nobes)



FIGURE 2.5: Cows Strip Grazing - 07 June 2014 (Photo courtesy of D. C. Nobes)

2.4 Geological History

New Zealand has a relatively young, but incredibly complex and active geological history, and this is also true of Southland. Irthing Stream is situated in an area of intense faulting; there are many faults situated close by including the large Livingstone fault. This has created an area of complex boundaries between the Caples and Maitai terranes with Quaternary deposits infilling valleys (See Figure 2.7 and Appendix A.1).

The Dun Mountain - Maitai terrane is represented to the west of the Irthing Road field area (field area is the red rectangle on Figure 2.7) on the west side of the Livingstone Fault. There are two parts of this terrane in close proximity to Irthing Stream and those are the Greville Formation and the Livingstone Volcanics Group. The Greville Formation is part of the Maitai Group and comprises of thin-bedded sandstone and mudstone. The Greville formation in this area also contains some of the Little Ben Sandstone which is a bedded volcanoclastic sandstone with minor siltstone and breccia. The Livingstone Volcanics Group is undifferentiated volcanics, dikes, microgabbro, and sediments (Turnbull, 2000). The Livingstone Volcanics Group formation represents a portion of Early Permian oceanic crust with the overlaying Maitai Group sediments of the Greville and Little Ben Sandstone formations (Coombs et al., 1976).

The area to the east of the Livingstone Fault, including Irthing Stream, is predominantly Caples terrane with Quaternary deposits infilling the valleys. The Caples terrane becomes more metamorphosed as it gets closer to the Livingstone fault. The undifferentiated volcanoclastic sandstone and siltstone that is typical of the Caples terrane becomes metamorphosed and deformed and this is represented in Figure 2.7 by the unit labelled Yc IIa. This unit is a weakly foliated semischist although it retains its primary appearance and sedimentary texture. The foliation and bedding are both visible and the metamorphic micas are fine grained (Turnbull, 2000). The Irthing Stream valley is primarily the undifferentiated caples terrane sandstone and siltstone with a small area of Upper Peak formation of thin-bedded, graded sandstone and black mudstone.

Caples terrane formed in a depositional setting ranging from trench slope, to trench-slope basins, and possibly trench floor (Carter et al., 1978; Castle, 1978; Turnbull, 1979; Roser et al.). The period of deposition and metamorphism is believed to be between the Early Jurassic and Cretaceous as the Caples-Rakaia terrane was rafted toward the Gondwana margin (Graham and Mortimer, 1992). The tertiary period involved a change in the tectonic setting to strike-slip and the Livingstone fault reactivated with reverse and strike-slip movement (Turnbull, 2000). This then gave way to Quaternary tectonics which involved the Wakatipu area being deformed in response to oblique compression within the Pacific Plate southeast of the Alpine Fault. The faults of the area, including

the Livingstone Fault, are predominantly north to north-east trending with an increasing strike-slip component (Norris, 1979).

A large proportion of the Northern Southland to Wakatipu area was glaciated at intervals throughout the Quaternary and this has developed into extensive areas of fluvioglacial deposits (Turnbull, 2000). The Quaternary deposits in the Irthing Stream area are however a mixture of alluvial terraces and fans from the rivers currently flowing in the area and outwash gravels from the last major glacial advance. The older outwash gravels are believed to be present to the north-west of the field site which rests primarily on the alluvial, locally derived, bouldary, unconsolidated gravel, sand and mud that forms the modern floodplain. An area of undifferentiated, variably weathered gravels sits to the west and south-east of the field site. These are likely to be mixture of outwash terraces and alluvial deposits.

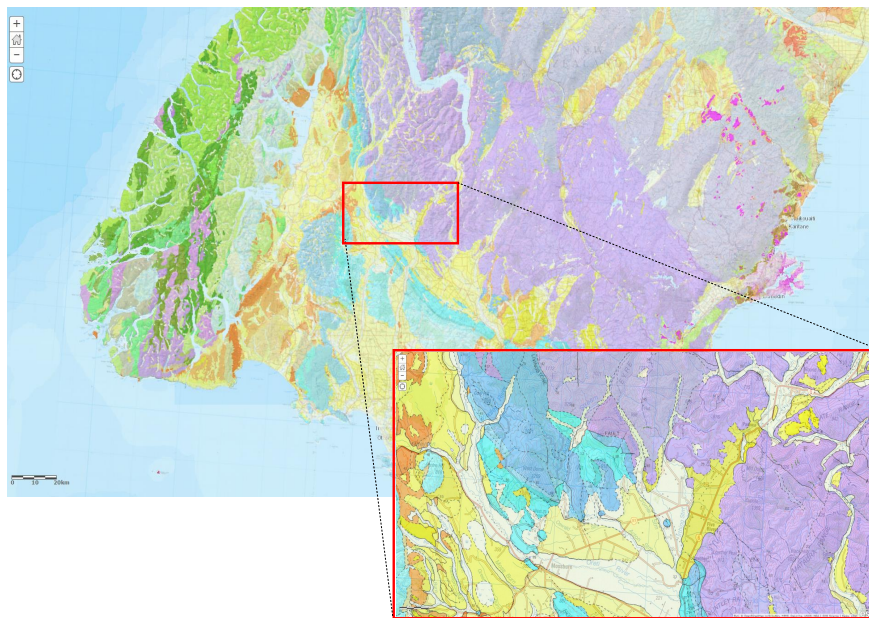


FIGURE 2.6: QMAP Geological Map with topography (ArcGIS et al., 2012; Turnbull, 2000)

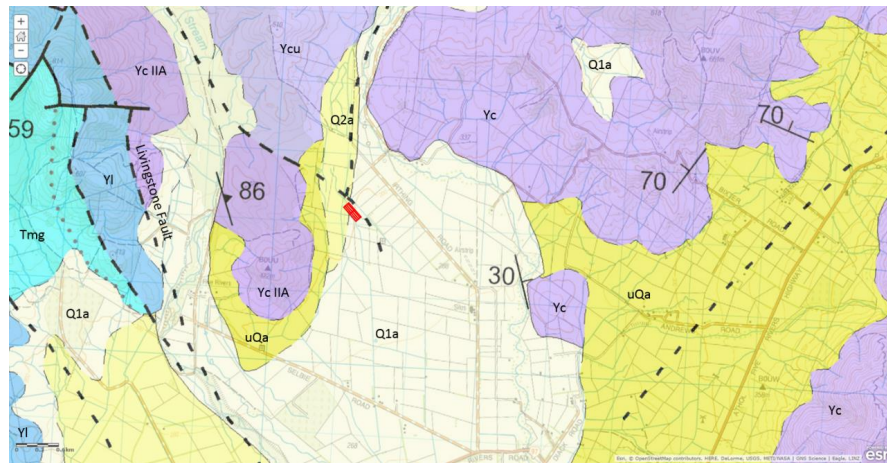


FIGURE 2.7: QMAP Geological Map with topography (ArcGIS et al., 2012; Turnbull, 2000)

2.5 Current Geology and Hydrogeology

The Irthing Stream field site sits upon alluvial terraces and fans which are largely gravelly and bouldery deposits overlain with a thin deposit of Lumsden soils. The subsoil deposits are likely sourced from the Irthing Stream as it moved across the floodplain and are extremely gravelly with large boulders present. The current photos of Irthing Stream show the meandering, slightly braided form that the stream prefers (See Figures 2.11 and 2.12). The boulders in the river are also obvious in these photos and are found in the near surface deposits across the field site (See Figure 2.10).

The Lumsden soils occupy about 2800 hectares of the floodplains near the major streams and rivers in northern and central Southland (Environment-Southland, 2002). The Lumsden soils at this location are a very thin layer of poor sorted gravelly deposits with variable amounts of sand and silt (See Figures 2.8 and 2.9). The clay content of Lumsden soils is usually between 25 and 35 percent (Environment-Southland, 2002). The gravelly sediments are underlain by a basal fine-grained layer, which acts as a confining layer and slows water infiltration slightly. The majority of the field site was always well drained and relatively dry, even during periods of heavy rain. The paddock containing the dairy cattle often had a mud layer approximately 20 centimetres thick during heavy rain events, however within 48 hours this would begin to dry out and the surface water would drain into the subsurface.

The lack of augers being used to collect lithology data is obviously disappointing. It was however deemed unfair to auger holes in a paddock on a working farm because of the impact it could have on the livestock. This does leave uncertainties in the lithology of the area; however it is easy for future auger boreholes to be dug on the site if permission was granted and it was deemed necessary to ground truth the geophysical results. This data could provide some interesting conclusions upon the interaction between the grain sizes infilling historic channels, and the conductivity results.



FIGURE 2.8: Close up photo of Irthing field site - Gravelly Soil



FIGURE 2.9: Close up photo of Irthing field site - Soil



FIGURE 2.10: Close up photo of Irthing field site - Large boulder



FIGURE 2.11: Irthing Stream emerging from Irthing Valley upstream of the field site



FIGURE 2.12: Irthing Stream flowing in Irthing Valley

Chapter 3

Literature Review

3.1 Introduction to Shallow Groundwater Contamination

Groundwater systems are protected by the covering layers or protective layers above them. The surface water percolates down through the protective layers and during this process contaminant degradation occurs by mechanical, physiochemical, and microbiological processes (Kirsch, 2009). The best protection is given by a thick protective layer with low hydraulic conductivity that leads to high residence time of percolating water and hence allows removal of contaminants before they reach the groundwater system.

The danger occurs when this barrier is either not sufficient or has its integrity breached by a natural or manmade occurrence. This is how contaminants from agriculture gain access to shallow groundwater systems that have very little protective layering. The most common issue in agriculture is the addition of large volumes of animal waste onto an area that has a high hydraulic conductivity which allows rapid transport of the contaminants into the shallow groundwater system.

The treatment of animal waste from farming represents a relevant problem around the world from both an environmental and economic point of view. This varies from using animal waste as a fertilizer to high density farming practices inputting large amounts of effluent into the soil, and surface and groundwater systems.

The high nutrient content within animal waste is a great fertiliser and the application of animal waste to land saves farmers millions of dollars per year. The damage to the environment however of applying too much effluent in vulnerable areas is severe and the understanding of this aspect is only beginning (Garnier et al., 1998). Areas such as Chiana River Valley in central Italy and Arkansas in the United States are facing

increasing problems with correct management of high intensity farming over shallow unconfined aquifers that are being found to exceed the legal nitrate limits.

Using models to understand the best times to distribute effluent with relation to climate and soil patterns is being tested in Arkansas to try and combat the issue of poultry litter disposal (Garnier et al., 1998). The use of a GLEAMS (Ground Loading Effects of Agricultural Management Systems) model in Chiana River Valley has also allowed effluent disposal limits to be based upon soil type and aquifer recharge sources to lower the input of nitrogen to the shallow groundwater (Garnier et al., 1998).

Gaining as much information on the groundwater conditions and contamination sources as possible is the crucial first step towards implementing long lasting and successful models to manage contaminants.

3.2 Geophysics in Agriculture

Geophysics was first used in agriculture in the 1930's and 1940's when there was some research into using resistivity methods to monitor soil moisture content (Edlefsen and Anderson, 1941; Kirkham and Taylor, 1949; McCorkle, 1931). Larger scale applications of geophysics in agriculture however did not start until the 1960's and 1970's with the use of resistivity methods to access soil salinity. The 1970's and 1980's also saw the beginning of ground penetrating radar (GPR) being applied to soil survey maps for the USDA (U.S. Department of Agriculture) (Allred, 2012). The 1990's brought with them a huge increase in the use of apparent electrical conductivity mapping using techniques such as resistivity and electromagnetic induction (EMI). These techniques are widely used to evaluate spatial variations in soil properties (Allred, 2012).

Geophysics is now becoming more established and accepted in the agricultural industry with particular techniques such as electromagnetic induction, resistivity, and ground penetrating radar leading the way for more development around further techniques and their applications.

Electromagnetic induction methods measure the electrical conductivity (or resistivity) for a bulk volume of soil below the surface using a ground conductivity meter and electric wire coils. The main advantage of electromagnetic induction is that the process of induction does not require direct contact with the ground, as opposed to electrical resistivity methods which require electrodes to be planted into the ground surface (Reynolds, 2011).

Electrical resistivity methods have also enjoyed a steady increase in popularity since the 1970's, partly due to the increases in computing power for processing and analysing. The resistivity methods also measure electrical resistivity (or conductivity) for a bulk volume of soil below the ground surface.

Ground penetrating radar is the third geophysical technique which has seen substantial application in agriculture since the 1970's. The partial reflection of electromagnetic radio energy (radar) from features below the surface and the depth of penetration can be used to gain insight into below-ground conditions as well as to provide information on the position and character of subsurface features (Allred et al., 2008).

Outlined below are some of the current agricultural applications of electrical resistivity, EMI and GPR methods (Allred et al., 2008):

- Using GPR to create soil suitability and soil water content maps.
- Tree and root biomass evaluations using GPR.
- Monitoring of soil nutrient levels using EMI and resistivity after the application of fertilizers and effluents.
- Determination of clay-pan depth using EMI and resistivity.
- Identification of subsurface flow pathways and groundwater surveys.
- Estimation of herbicide partition coefficients in soil.
- Identification and assessment of subsurface utilities or waste on farmland.
- Assessments of effluent storage ponds and effluent disposal facilities and their integrity.
- Mapping of subsurface flood deposits on farmland near rivers.
- Soil drainage class mapping using resistivity methods.
- Soil salinity assessments, mapping of contaminated land and the delineation of spatial changes in soil properties using EMI and resistivity methods.
- Using GPR to update the USDA and NRCS (Natural Resource Conservation Service) large scale soil surveys.

Although resistivity, EMI, and GPR are all well established in the agricultural community it is obvious that more uses will be discovered for these techniques and also that other geophysical techniques will find applications in agriculture. Geophysical methods such as magnetometry, self-potential, seismic, and gamma-ray spectrometry may

all find commercial agricultural application in the near future. There is currently soil compaction mapping and measurement of soil water potential, being carried out using seismic surveying. Gamma-ray spectrometry can be applied to clay content determination while self-potential has been used alongside EMI and resistivity to detect leaks from effluent storage facilities and treatment lagoons (Allred, 2012).

The agricultural ecosystem will always be a challenge for geophysical methods because of the substantial spatial and temporal variability. The soils electrical conductivity is a function of temperature and water content while the soils dielectric constant is a function of water content (Allred, 2012). Both of these variables can operate on a temporal scale of hours which can create enormous variability for geophysical methods. The subsurface also displays complex horizontal and vertical changes which are always challenging for geophysical surveys to accurately record and interpret.

3.3 Geophysics to Monitor Shallow Groundwater Contamination from Agriculture

Electromagnetic induction is widely used in agriculture and is also common place in hydrogeology. For this reason it is one of the most powerful tools to monitor shallow groundwater contamination from agriculture.

EMI has been used to monitor contaminants in groundwater, salt water intrusion, leachate plumes, landfill and contaminated ground mapping, and changes in subsurface texture (Reynolds, 2011).

The ability to identify between metallic and non-metallic anomalies is important for groundwater applications. Highly conductive responses in the quadrature reading that are not then seen by the in-phase reading are most likely not metallic and are therefore of interest when looking into shallow groundwater (Reynolds, 2011). The EMI will respond to preferential flow paths and changes within the system which is important for shallow groundwater monitoring. The issue with this being the level of contaminants required to generate a change in the EMI apparent conductivity is unknown and variable depending upon site conditions.

The application of electrical resistivity surveys in agricultural and shallow groundwater examples has been tested extensively and some important factors need to be considered when using this technique.

Firstly there are clear indications that resistivity can be used effectively to assess soil texture (% sand, % silt, % clay), organic matter, salinity, bulk density, electrical conductivity, herbicide partition coefficients, clay-pore depth, and most importantly for shallow groundwater contamination to monitor soil nutrient build up and identify and map leachate plumes from landfills (Allred et al., 2008).

The difficulty of using resistivity to identify agricultural groundwater contamination is the need to have electrodes in contact with the ground surface and the cost effectiveness of using resistivity in a commercial application. Resistivity is widely used to monitor containment waste repositories because a leak detection system can be installed and monitored remotely, however agricultural contamination of groundwater is far more variable and spatially harder to identify (Reynolds, 2011).

Ground penetrating radar plays a varying role in monitoring groundwater contamination. The ability for GPR to identify preferential flow paths using radar attenuation is important because that can allow accurate mapping of the subsurface and also increased accuracy for invasive testing such as boreholes testing (Allred et al., 2008).

GPR can also identify and map leachate plumes using the tendency for the radar signal to be attenuated severely by the highly conductive contaminants in the plume (Reynolds, 2011). The areas of attenuated signal in the radargram are opaque and easily identifiable. GPR can also be used to determine the changes in pollution levels by taking repeated surveys along the same line to detect changes as a function of time (Reynolds, 2011). This approach can also be used to test the effectiveness of remediation because as the contamination lessens, the radar signal will attenuate less, penetrate deeper and provide transparent areas on radargrams where there was previously an opaque area. This technique however is not as effective as direct conductivity measurements because the radar is sensitive to even moderate conductivity levels (Reynolds, 2011).

GPR can also be applied to the mapping of groundwater tables which in itself is important for understanding shallow groundwater contamination. The groundwater table will often be easily identifiable in radargrams as a horizontal reflective layer with a large amplitude (Reynolds, 2011).

The best approach for using geophysics to monitor shallow groundwater contamination from agriculture is to employ multiple geophysical techniques and combine this with ground truthing if possible. The spatial and temporal variability within an agricultural setting can create challenges around accurate data interpretation. There are also many possible complications from contaminant types, contaminant levels, groundwater movement, subsurface conditions, and textures.

Chapter 4

Methodology

4.1 Introduction

The investigation and monitoring of the field site at Irthing Road was to determine whether geophysics could be used to successfully monitor leachate from wintering dairy cows on free draining, gravelly soils. The investigation had multiple aspects including whether the leachate levels were high enough to register a visible response in the geophysical results, and how could the results be best interpreted to be of use to all of the interested parties.

The investigation was carried out using EM31, DUAL-EM, 100MHz and 200MHz GPR, and water sampling. The site was selected by representatives of Environment Southland because of their superior knowledge of the Southland geology and hydrogeology. This chapter outlines the steps taken throughout the year to design the monitoring programme and then to gather the data required to produce clear and concise results. Figure 4.1 shows the dates for all of the research trips that were conducted as part of the project. The information is collated and summarised in the following two chapters along with recommendations into future testing and thoughts on the viability and potential of the monitoring programme used.

Fieldwork Plan	
Trip Number	Date
1	25/03/14 - 28/03/14
2	06/05/14 - 09/05/14
3	05/06/14 - 07/06/14
4	09/08/14 - 10/08/14
5	26/08/14 - 28/08/14
6	19/10/14 - 21/10/14

FIGURE 4.1: Table showing the dates of the research trips to Southland.

4.2 Research Site Selection

The decision on site selection was largely left to Environment Southland as they had far more experience with the geology and hydrogeology of the area. There were a few primary concerns around site selection that dictated the decision and these included:

- The site had to be on free draining soils with a shallow water table and preferably a short unsaturated zone lag time. Southlands regional geology is dominated by thin alluvial gravel aquifers that overlay a low permeability basement which is perfect for this investigation.
- The area needed to have been previously used for low density farming and have no previous known contamination.
- During the winter of 2014 the site must be hosting wintering cows in a high density grazing format to provide the most opportunity for potential contamination.
- The area is ideally easy to access and run geophysical surveys across. The survey pegs need to be permitted to remain on site for at least eight months.
- The farmer has to provide access and agree that the surveys are allowed to commence on his property.
- The area selected would preferably have similar geology and hydrogeology to other areas throughout Southland and New Zealand.

It quickly becomes obvious that the list of requirements for the site was quite complex with many factors that were difficult to control. Irthing Road was presented as the only option for the research site and has appeared to be perfect for the needs of the project. The stock rotation had to be so specific due to the desire to start with a site that was as unaltered as possible. This was in an effort to accentuate any findings from the stock that were going to be placed upon the site. Having the cows strip grazed across the fence from the research site was perfect because it allowed the geophysics to be run in an area that was largely undisturbed throughout the year; this meant site access and running the equipment was not affected by stock movements.

4.3 Initial Research Site Development

The Irthing road property was presented as the site for this research to be undertaken, however the exact site placement and survey design were flexible. The initial step in this

process was to establish the groundwater flow direction, the location of the wintering cattle, and the best site for operating geophysical equipment.

The shallow groundwater in the immediate vicinity of the wintering cattle is travelling from north to south and is shown in Figure 4.2 on page 26 as a black arrow. This was established by interviewing the landowner, Ben Walling who had dug multiple holes in and around the field site and had encountered the shallow ground water. This flow direction was towards the large Oreti River to the south and also coincided with the general south to south-west surface water flow trends. The implication of this shallow groundwater flow direction was that the geophysical surveying would have to be conducted to the south of the wintering cattle as to allow the shallow groundwater to flow beneath the contaminant source before it reached the survey area. The location of the wintering cattle is indicated by the large green box in Figure 4.2 on page 26.

The survey area chosen is shown in Figure 4.2 as a rectangle of red survey lines to the south of the wintering cattle. It is obvious from this plan that the shallow ground water is travelling beneath the wintering area for the cattle and then underneath the survey area. Figures 4.3 and 4.4 show a more detailed plan of the survey lines and how they are arranged and labelled. The idea of having five parallel lines is that this will allow the possibility of monitoring changes across the field area and it will also allow a better understanding of the subsurface preferential flow paths. In both of these figures it is possible to see what appears to be the remains of water channels travelling from north to south through the survey area which no longer appear visible on the survey site (Images date from 21/01/2013). The evidence of these has been removed by the agricultural activity happening in the area. There do however appear to be possible changes in vegetation growth visible on the surface which could potentially relate to these historic channels (Shown in Figure 4.5 on page 27). This is likely to be caused by a different material infilling the channel and possibly increased access to shallow groundwater which may be flowing along preferential flow paths within the old channel system. The other option is that the infilling has a slightly higher clay percentage than the surrounding area and this is causing water to pond on or near the surface. This gives the grass greater access to water and is indicated by the fact that the grass growth is noticeably increased over the historic channels.

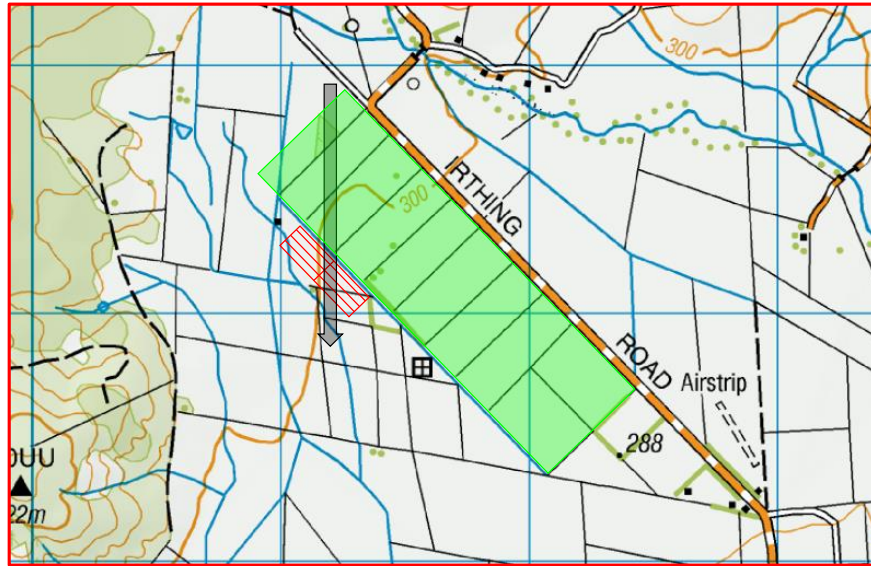


FIGURE 4.2: Topographic map showing Irthing field site line set up. Green box represents the grazing area of wintering cattle, the black arrow is the shallow groundwater flow direction, and the red grid marks the geophysical survey lines.



FIGURE 4.3: Survey line set up showing Irthing Valley. This is a Google Earth image from 21/01/2013 taken at 367 metres elevation.

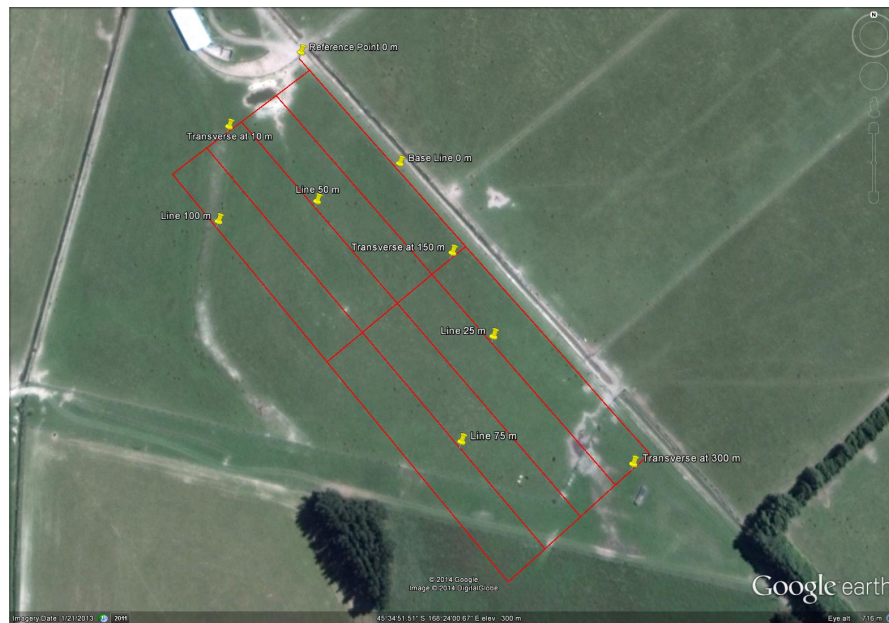


FIGURE 4.4: Survey line layout using Google Earth images taken from 21/01/2013 at 700 metres altitude.



FIGURE 4.5: Photo along survey line 25 taken from the 290 metre mark looking north. This photo appears to show changes in surface vegetation growth that coincides with the location of old channels shown in the Google Earth images of Figure 4.3 and 4.4 which date back to 21/01/2013

4.4 Electromagnetic Methods

Electromagnetic induction techniques were chosen for this project for a variety of reasons. These included:

- Availability of EMI equipment from both the University of Canterbury and Environment Southland.
- The need for Environment Southland to conduct more research using their recently purchased DUAL-EM in an effort to try to find more applications for the device.
- The popularity of EMI products in agriculture means that more farmers are likely to allow EMI surveys to be conducted upon their land. This stems from the fact that they have a basic understanding that the device will not have negative impacts upon their animals or land. This is a form of brand recognition which is important for breaking into an industry that relies heavily on land owners being willing to allow surveys on their properties.
- The ability to be able to run multiple EMI devices was important because it allows cross referencing of data not only with GPR and ground truthing, but also with another EMI device. This can give far more reliable and trustworthy results as anomalies can be cross referenced easily.
- Research has shown that EMI devices can be used to accurately map and record temporal changes in groundwater contaminants, usually stemming from leaking contaminant storage. This project endeavours to use EMI for more sensitive testing.
- When considering future research and commercial application it is obvious that EMI techniques are important to both Environment Southland and Southern Geophysical Ltd. Because of this it was important to include EMI devices in this research.

4.4.1 EM31 Survey

The EM31 survey was conducted using the Geonics Ltd EM31-MK2 device (Shown in Figure 4.6 on page 29). This device is owned by the University of Canterbury and was transported to Southland for the research. The EM31-MK2 is a one-man portable EMI device that has an effective depth of penetration of up to 6 metres using an inter coil spacing of 3.66 metres and an operating frequency of 9.8 KHz (Geonics, 2013).

The initial idea behind the survey set up was to run the EM31 across the preferential flow paths beneath the ground to establish where these flow paths occurred. The subsequent surveys throughout the year were then to record any variations in apparent conductivity along these preferential flow paths associated with leachate input into the shallow groundwater system. The EM31 survey was conducted along all five of the 290 metre long survey lines shown in Figure 4.4 on page 27. The lines began at 10 metres because of the large deer fence at the 0 metre mark which would have caused interference with the geophysics (Shown in the background of Figure 4.6 on page 29). The EM31 was run with the coil orientation parallel to the survey line and then back again with the coil orientation perpendicular to the survey line. This was to ensure that any anomalies were going to be recorded as effectively as possible by one or both of the coil orientations. The tie lines between the five long lines were also scanned with the EM31 at both perpendicular and parallel orientations for completeness.



FIGURE 4.6: David Nobes running EM31

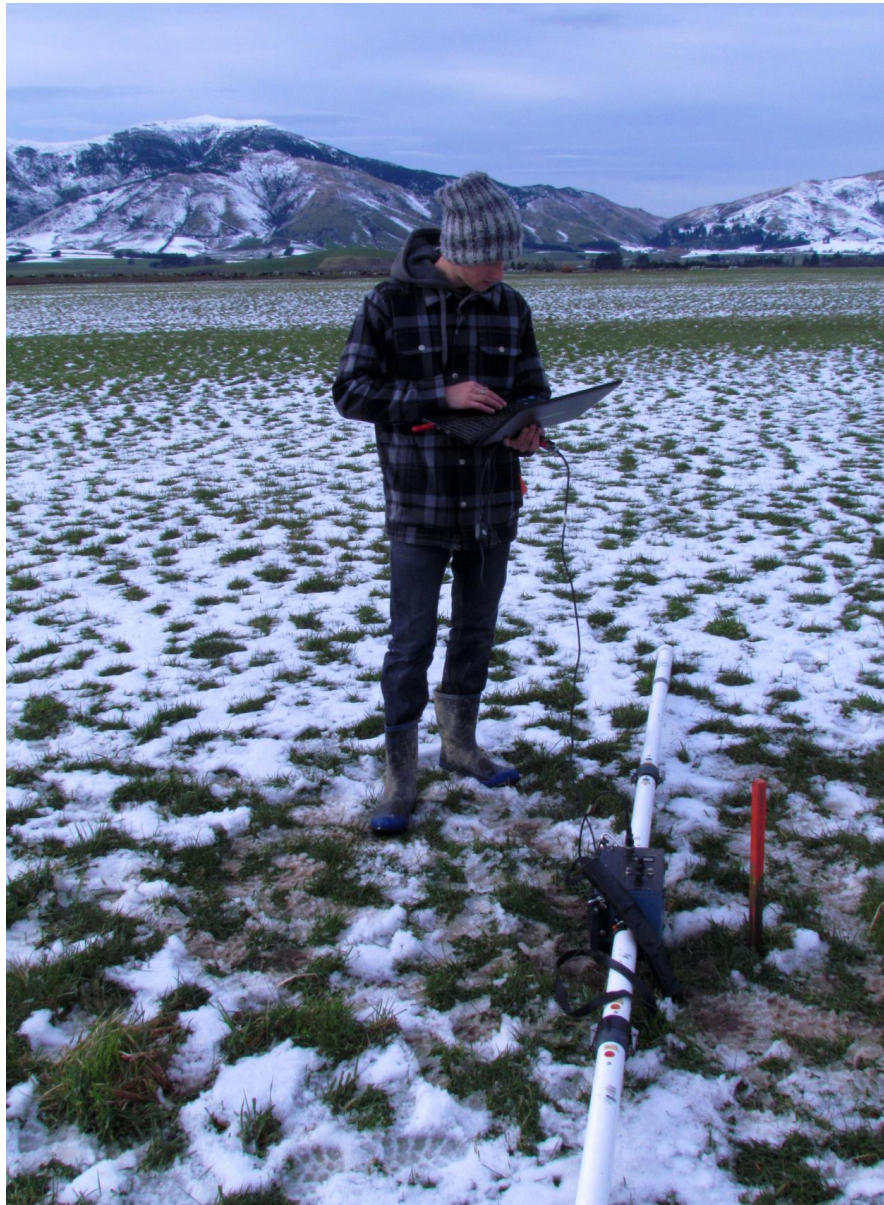


FIGURE 4.7: Matt James running EM31 (Photo courtesy of D. C. Nobes)

4.4.1.1 EM31 Data Processing

The method used to process the EM31 data was very simple because for this application there was no need for complex renderings of the entire subsurface, only apparent conductivities along five lines.

Once the data was collected using the EM31 it was stored upon a field laptop and then transferred into the Conv31pro program where the file type was changed from the raw .R31 to the DAT31W file type .G31 (See Figure 4.8 on page 31).

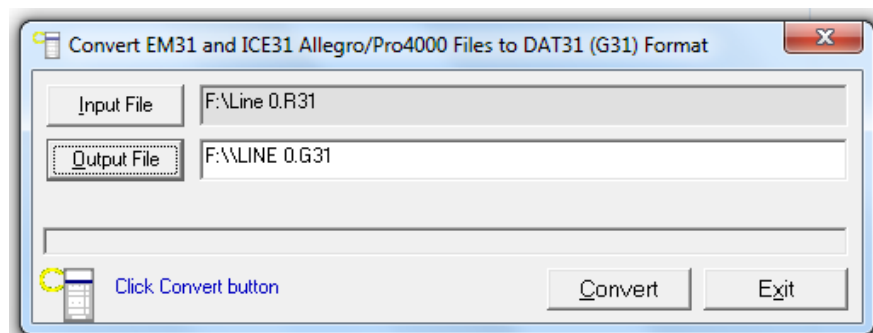


FIGURE 4.8: Changing raw EM31 .R31 format to .G31 format for processing

The new .G31 file was then imported into DAT31W where the data was converted into an XYZ file using a 2D layout (See Figure 4.9 on page 31).

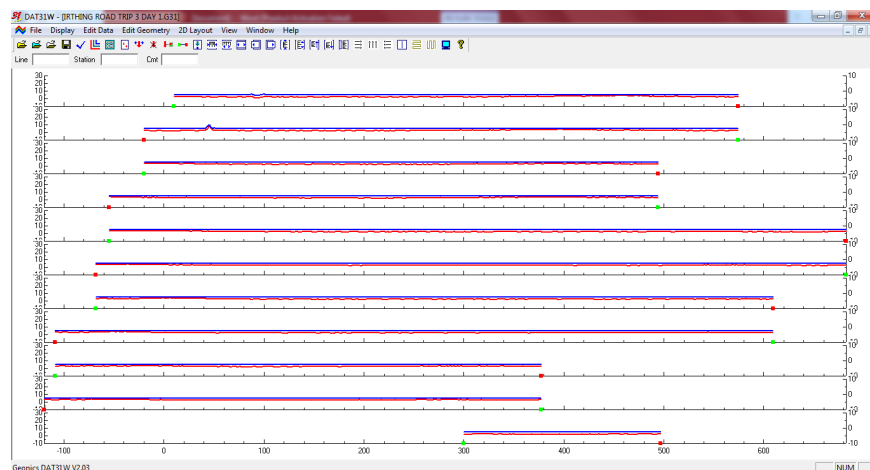


FIGURE 4.9: Changing the .G31 format to XYZ format using DAT31W

This XYZ file could then be imported into Microsoft Excel and divided into each survey line (See Figure 4.10 on page 32).

The apparent conductivity and inphase data for each survey line was then put into Matlab and interpolated over the 290 metre length of the survey line (See Figure 4.11 on page 33). Matlab is an advanced mathematical computation program designed by

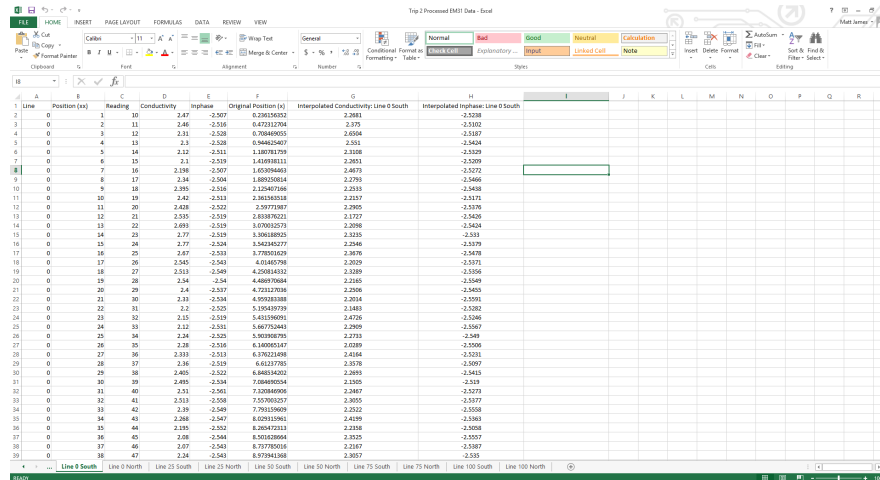


FIGURE 4.10: Processing the XYZ file in Microsoft Excel

MathWorks that was able to do interpolation in one easy step. The interpolation was done to provide one interpolated value per metre of the survey length instead of graphing using the raw data which contained thousands of readings over the 290 metre long line. It is important to note that for this thesis the interpolation was done across 290 values, instead of 291 values. This is a processing error that was identified toward the end of the project and it was decided that the effect was so minimal that the data would not be changed. This error also effected the DUAL-EM interpolation, but as the data was interpolated in a consistent manner across the project it was unnecessary to reprocess the data.

The interpolated values were then put back into the Microsoft Excel document and the data was ready to be graphed and interpreted using Grapher 9 (See Figure 4.12 on page 34). Grapher 9 is made by Golden Software and enables complex graphs to be created quickly and presented in a clear manner. The reason Grapher 9 was chosen for this application was because many of the graphs contained at least five y axis and multiple data groups which needed to be presented in a way as to allow the small variations in the data to be obvious.

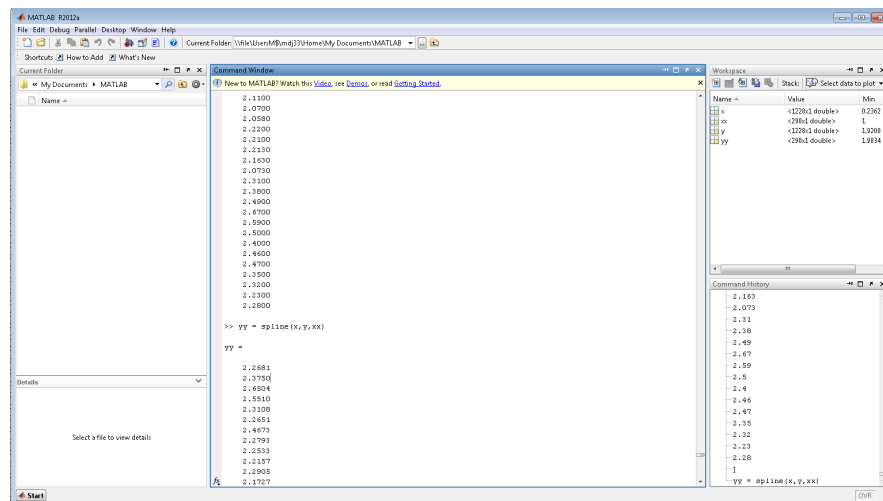


FIGURE 4.11: Interpolating EM31 data using Matlab

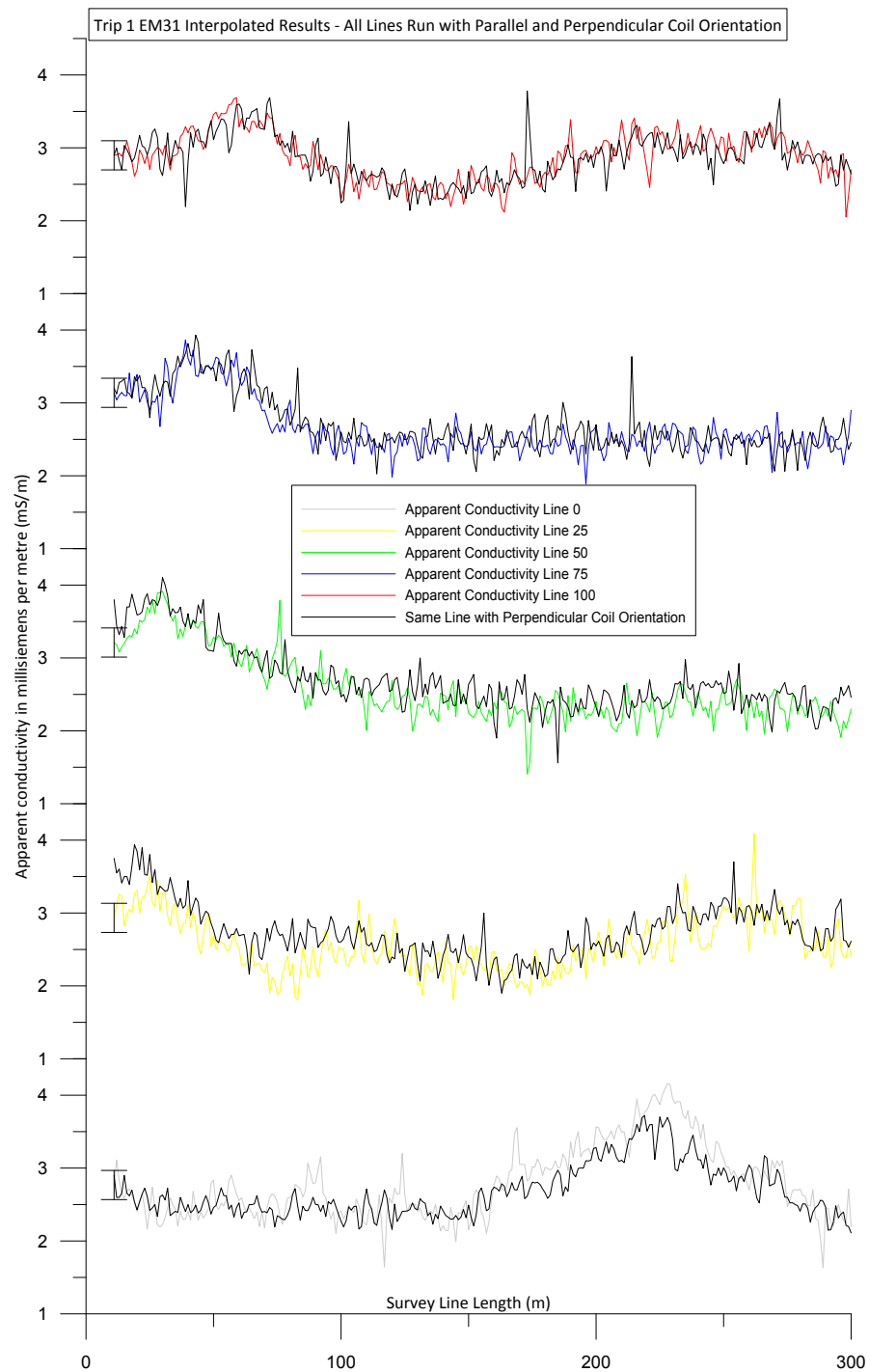


FIGURE 4.12: Using Grapher 9 software to present EM31 data. This example shows the difference between parallel and perpendicular coil orientations along all five of the survey lines. Error bars represent the ± 0.2 mS/m error of the EM31 device.

4.4.2 DUAL-EM Survey

The DUAL-EM surveying was conducted using Environment Southlands DUAL-EM 421s unit and was run by Darren May from Environment Southland. The DUAL-EM 421s is made by Dualem Inc. which is a Canadian company specialising in EMI devices. The DUAL-EM 421s uses both horizontal co-planar (HCP) and perpendicular (PRP) receiver coil orientations with reference to the receiver. HCP or horizontal co-planar refers to the geometry of the transmitter coil in relation to the receiver coil. In this case the transmitter windings are horizontal, as are the receiver coil windings (DualemInc., 2013). In the case of PRP, the transmitter windings are horizontal, but the receiver coil windings are vertical (DualemInc., 2013). The DUAL-EM unit also includes six different coil spacings unlike the EM31 which only has the single 3.67 metre coil spacing. This allows apparent conductivity measurements to be made using 1 metre, 1.1 metre, 2 metre, 2.1 metre, 4 metre and 4.1 metre coil spacings simultaneously. The 1, 2, and 4 metre readings are using the HCP receiver coils while the 1.1, 2.1, and 4.1 metre are made using the PRP receiver coils. The various effective depths of exploration (DOE), coil spacings and configurations are shown in Figure 4.14 on page 36.



FIGURE 4.13: Matt James and Darren May running DUAL-EM (Photo courtesy of A. Langdale)

Rx & Tx Configuration	Rx & Tx Separation (m)	Combined Nomenclature	Effective DOE (m)
HCP	1	HCP1	0 – 1.5
PRP	1.1	PRP1	0 – 0.5
HCP	2	HCP2	0 – 3.0
PRP	2.1	PRP2	0 – 1.0
HCP	4	HCP4	0 – 6.0
PRP	4.1	PRP4	0 – 2.0

FIGURE 4.14: Table showing the Effective Depth of Exploration (DOE) for the various coil spacings and configurations in the DUAL-EM 421s. Sourced from (May, 2014), based upon data from (Triantafilis et al., 2013)

4.4.2.1 DUAL-EM Data Processing

The DUAL-EM data was taken straight from the device as an XYZ file and imported into Microsoft Excel (See Figure 4.15 on page 37) where it was separated into survey lines and run through the same Matlab interpolation as the EM31 data (See Figure 4.11 on page 33).

A	B	C	D	E	F	G	H	I	J	K	L	M	N	O	P	Q	R	S	T	U	V	W	X	Y	Z	AA	AB	AC
1	14085 N	10 E	10.0	-2.1	0.41	113.7	-2.85	-2.7	0.43	42.4	-7.76	-0.2	-0.07	9.3	18.22	1	1	12	1	10.757	284.7	-1	-1.3	4.8	442000	45.58164	168.4016	164.3
2	14086 N	10 E	10.0	9.4	0.22	110.7	-3.09	1.2	0.11	34.8	-7.97	0.7	-0.27	7.2	-17.97	1	1	12	2	10.892	284.7	-1	0.7	26.8	432000	45.58164	168.4016	164.3
3	14087 N	10 E	10.0	12.4	0.19	97.5	-3.01	2.3	0.05	11	-7.84	1	-0.39	6.2	-17.94	1	1	12	3	10.609	284.7	-1	0.9	21.1	432000	45.58164	168.4016	164.3
4	14088 N	10 E	10.0	15.8	0.19	97.4	-3	2.1	0.07	31.3	-7.84	0.7	-0.38	6	-17.99	1	1	12	4	10.686	284.7	-1	0.3	20.4	432000	45.58164	168.4016	164.3
5	14089 N	10 E	10.0	19.2	0.19	97.7	-3	2.3	0.08	31	-7.84	0.9	-0.41	6.1	-17.98	1	1	12	5	10.603	284.7	1	1.3	21.3	432000	45.58164	168.4016	164.3
6	14090 N	10 E	10.0	22.6	0.19	98.4	-3	2.3	0.06	31.5	-7.85	1.1	-0.39	6.1	-17.93	1	1	12	6	10.608	284.7	1	1.3	20.3	432000	45.58164	168.4016	164.3
7	14091 N	10 E	10.0	26.0	0.18	100.8	-3.05	2.4	0.05	32.1	-7.8	1.1	-0.32	6.2	-17.92	1	1	12	7	10.679	284.7	1	1.3	21.9	432000	45.58164	168.4016	164.3
8	14092 N	10 E	10.0	29.4	0.17	100.1	-3.08	2.1	0.04	32	-7.93	0.9	-0.34	6.2	-17.98	1	1	12	8	10.675	284.7	1	-1.9	24.9	432000	45.58164	168.4016	164.3
9	14093 N	10 E	10.0	32.8	0.16	100.5	-3.11	2.1	0.04	32.1	-7.95	0.9	-0.39	6.4	-17.91	1	1	12	9	10.673	284.7	1	2.4	21.8	432000	45.58164	168.4016	164.3
10	14094 N	10 E	10.0	36.2	0.17	100.3	-3.09	2.3	0.04	31.9	-7.93	0.9	-0.35	6.3	-17.98	1	1	12	10	10.671	284.7	1	0.5	22	432000	45.58164	168.4016	164.3
11	14095 N	10 E	10.0	39.6	0.16	100	-3.07	2.1	0.04	31.7	-7.98	0.9	-0.34	6.2	-18.09	1	1	12	11	10.67	284.7	1	1.6	24.8	433000	45.58164	168.4016	164.3
12	14096 N	10 E	10.0	43.0	0.19	100.2	-3.08	2.2	0.07	32	-7.94	0.9	-0.31	6.1	-18.04	1	1	12	12	10.668	284.7	1	0.5	23.2	433000	45.58164	168.4016	164.4
13	14097 N	10 E	10.0	46.4	0.18	100.4	-3.09	2.2	0.06	31.9	-7.96	0.9	-0.31	6.1	-18.02	1	1	12	13	10.666	284.7	1	1.7	21	433000	45.58164	168.4016	164.3
14	14098 N	10 E	10.0	49.8	0.17	99.8	-3.09	2.2	0.06	31.5	-7.98	1	-0.32	6.2	-18.05	1	1	12	14	10.664	284.7	1	-0.4	20.6	433000	45.58164	168.4016	164.4
15	14099 N	10 E	10.0	53.2	0.17	100.4	-3.12	2	0.07	32	-7.96	0.8	-0.35	6.4	-17.95	1	1	12	15	10.662	284.7	1	1	23.9	433000	45.58164	168.4016	164.3
16	14100 N	10 E	10.0	56.6	0.18	101.6	-3.13	2.4	0.07	32.1	-7.95	1	-0.28	5.9	-18.03	1	1	12	16	10.66	284.7	1	0.3	21.4	433000	45.58164	168.4016	164.4
17	14101 N	10 E	10.0	60.0	0.18	101.7	-3.15	2.1	0.05	32.4	-8.01	0.7	-0.3	6.3	-18.06	1	1	12	17	10.659	284.7	1	0.1	21.1	433000	45.58164	168.4016	164.3
18	14102 N	10 E	10.0	63.4	0.16	101.2	-3.18	2.2	0.03	32.3	-7.99	0.9	-0.31	6.4	-18.03	1	1	12	18	10.658	284.7	1	1.5	23.1	433000	45.58164	168.4016	164.5
19	14103 N	10 E	10.0	66.8	0.17	102	-3.18	2.2	0.04	32.7	-8	0.9	-0.32	6.4	-18	1	1	12	19	10.655	284.7	1	0.1	21.1	433000	45.58164	168.4016	164.5
20	14104 N	10 E	10.0	70.2	0.18	102.9	-3.19	2.4	0.07	32.8	-8.03	1	-0.31	6.3	-18.12	1	1	12	20	10.653	284.7	1	0.1	22.1	433000	45.58164	168.4016	164.6
21	14105 N	10 E	10.0	73.6	0.18	103	-3.21	2.3	0.04	32.8	-8.04	1	-0.26	6.7	-18.13	1	1	12	21	10.652	284.7	1	0.2	24.7	440000	45.58164	168.4016	164.6
22	14106 N	10 E	10.0	77.0	0.18	103	-3.21	2.4	0.04	32.8	-8.01	1.1	-0.35	6.6	-17.94	1	1	12	22	10.65	284.7	1	1.1	23.9	440000	45.58164	168.4016	164.7
23	14107 N	10 E	10.0	80.4	0.18	104.7	-3.2	2.1	0.06	32.3	-8.06	0.9	-0.28	6.4	-18.18	1	1	12	23	10.65	284.7	1	1.4	21.7	440000	45.58164	168.4016	164.8
24	14108 N	10 E	10.0	83.8	0.18	103	-3.19	2.4	0.07	32.7	-8.03	1	-0.33	6.7	-18.03	1	1	12	24	10.649	284.7	1	0.7	20.2	440000	45.58164	168.4016	164.9
25	14109 N	10 E	10.0	87.2	0.18	102	-3.16	1.9	0.08	32.3	-8.02	1	-0.33	6.7	-18.03	1	1	12	25	10.645	284.7	1	1.4	20.5	440000	45.58164	168.4016	164.7
26	14110 N	10 E	10.0	90.6	0.19	103	-3.19	2.1	0.04	32.9	-8.03	1.1	-0.33	6.7	-18.07	1	1	12	26	10.643	284.7	1	1.2	24.2	440000	45.58164	168.4016	164.7
27	14111 N	10 E	10.0	94.0	0.18	100.1	-3.13	2.4	0.07	31.7	-8	1	-0.3	6.4	-18.09	1	1	12	27	10.643	284.7	1	1	22.4	440000	45.58164	168.4016	164.7
28	14112 N	10 E	10.0	97.4	0.1	68.9	-2.45	3.8	-0.03	22.1	-7.31	1.6	-0.43	3.7	-17.46	1	1	12	28	10.641	284.7	1	2	11.5	440000	45.58164	168.4016	164.7
29	14113 N	10 E	10.0	100.8	0.08	89.4	-2.3	3.7	-0.09	22.6	-7.35	1.5	-0.45	3.9	-17.46	1	1	12	29	10.639	284.7	1	1.2	18.7	440000	45.58164	168.4016	164.7
30	14114 N	10 E	10.0	104.2	0.07	70.2	-2.33	3.7	-0.12	23	-7.37	1.3	-0.5	3.4	-17.53	1	1	12	30	10.637	284.7	1	1.2	21.2	440000	45.58164	168.4016	164.8
31	14115 N	10 E	10.0	107.6	0.07	70.7	-2.34	3.7	-0.12	23	-7.36	1.4	-0.48	3.9	-17.51	1	1	12	31	10.635	284.7	1	0.5	22	440000	45.58164	168.4016	164.8
32	14116 N	10 E	10.0	111.0	0.06	71.1	-2.35	3.6	-0.11	23	-7.32	1.5	-0.5	4	-17.4	1	1	12	32	10.634	284.7	1	2	24.9	441000	45.58164	168.4016	164.8
33	14117 N	10 E	10.0	114.4	0.06	71.1	-2.36	3.9	-0.13	22.9	-7.36	1.4	-0.45	4.1	-17.53	1	1	12	33	10.633	284.7	1	-1.5	20.6	442000	45.58164	168.4016	164.5
34	14118 N	10 E	10.0	117.8	0.05	71.7	-2.39	4.1	-0.13	23.3	-7.37	1.4	-0.44	4.4	-17.41	1	1	12	34	10.631	284.7	1	0	22.9	443000	45.58164	168.4016	164.6
35	14119 N	10 E	10.0	121.2	0.05	71.3	-2.39	4.1	-0.12	23.3	-7.34	1.7	-0.46	4.3	-17.29	1	1	12	35	10.629	284.7	1	0.6	21.5	444000	45.58164	168.4016	164.6
36	14120 N	10 E	10.0	124.6	0.05	71.7	-2.39	4.2	-0.14	23.5	-7.38	1.6	-0.51	4.2	-17.43	1	1	12	36	10.628	284.7	1	1	21.1	445000	45.58164	168.4016	164.1
37	14121 N	10 E	10.0	128.0	0.04	71.8	-2.41	3.8	-0.15	23.5	-7.36	1.5	-0.48	4.4	-17.31	1	1	12	37	10.626	284.7	1	1	21.2	446000	45.58164	168.4016	164.2
38	14122 N	10 E	10.0	131.4	0.05	67.8	-2.32	3.6	-0.14	22.3	-7.34	1.4	-0.48	3.9	-17.41	1	1	12	38	10.626	284.7	1	0.7	22.7	447000	45.58164	168.4016	164.3

FIGURE 4.15: Raw XYZ data from the DUAL-EM after it has been imported into Microsoft Excel.

4.5 Ground Penetrating Radar

The GPR survey was undertaken using Canterbury Universities' Sensors & Software pulseEKKO GPR system. This system contains both 100 MHz and 200 MHz unshielded antennas connected to the pulseEKKO receiver and transmitter. The system is mounted upon a sled (See Figure 4.16 on page 38) and then towed by either a human or vehicle. The unshielded system is vulnerable to large metallic objects and electrical fields so towing with a vehicle requires a long rope to ensure adequate separation between the device and the vehicle (see Figure 4.17 on page 39).



FIGURE 4.16: Sled with 100MHz antennas attached.



FIGURE 4.17: Running 100MHz GPR (Photo courtesy of A. Langdale).



FIGURE 4.18: Running 200MHz GPR past metal objects can cause interference in the data.

4.5.1 GPR Data Processing

GPR data processing is quite labour intensive and required a lot of time because of the large number of GPR lines. The first step was to remove the data from the laptop that was connected to the GPR and create a new project within the pulseEKKO EKKO View Deluxe software package. The data was then imported into the project in a raw state (See Figure 4.19 on page 42).

The next stage started with analysis of the traces within each file to delete the bad traces and fix the trace comments (See Figure 4.20 on page 42). The importance of this is to remove bad data and then have the traces arranged correctly so they may be rubber banded to the correct length of the survey line (See Figure 4.21 on page 43). Rubber banding is a process of interpolating the GPR traces to a standard trace spacing, using regularly spaced fiducial markers for references. The number of traces was always greater than the number required for optimal trace spacing for best-practice imaging of the subsurface (Reynolds, 2011). For example, the 100MHz GPR lines were often collected at around 1 trace per 8 centimetres and then rubber banded to 1 trace per 10 centimetres. The rubber banding is followed by migration based upon the velocity of the sub surface which in this case was calculated using a CMP to be 0.09 m/ns (See Figure 4.23 on page 44). The CMP analysis was conducted using a range of velocities between 0.03 m/s and 0.15 m/s. The colour scale is then inverted to show the concentration of velocities around 0.9 m/s clearly in black (See Figure 4.22).

The final stage of processing involves adding the topography file which was collected using GPS and adding this onto the GPR file (See Figure 4.24 on page 44). This is followed by adjusting the gain settings within EKKO View Deluxe as to best display the data accurately (See Figure 4.25 on page 45). The SEC gains were used because using auto gains was causing the program to invent data by simply increasing the gains beyond a feasible value.

The final product for one of the GPR lines is then completed (See Figure 4.26 on page 45). These radargrams are then imported into Microsoft Excel and overlain with EMI data to create multi technique displays (See Figure 4.28 on page 47).

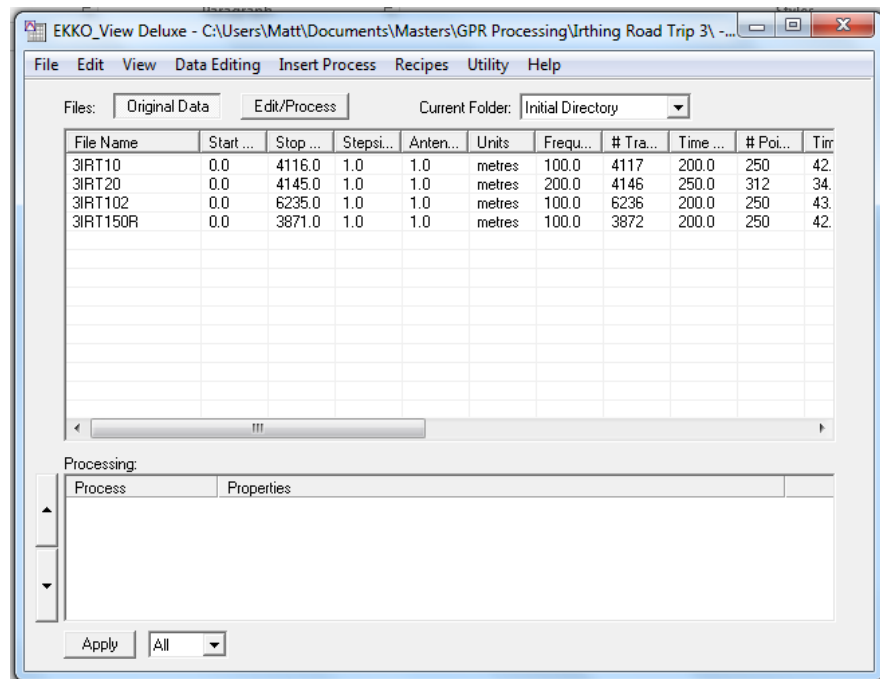


FIGURE 4.19: Importing raw GPR data into EKKO View Deluxe.

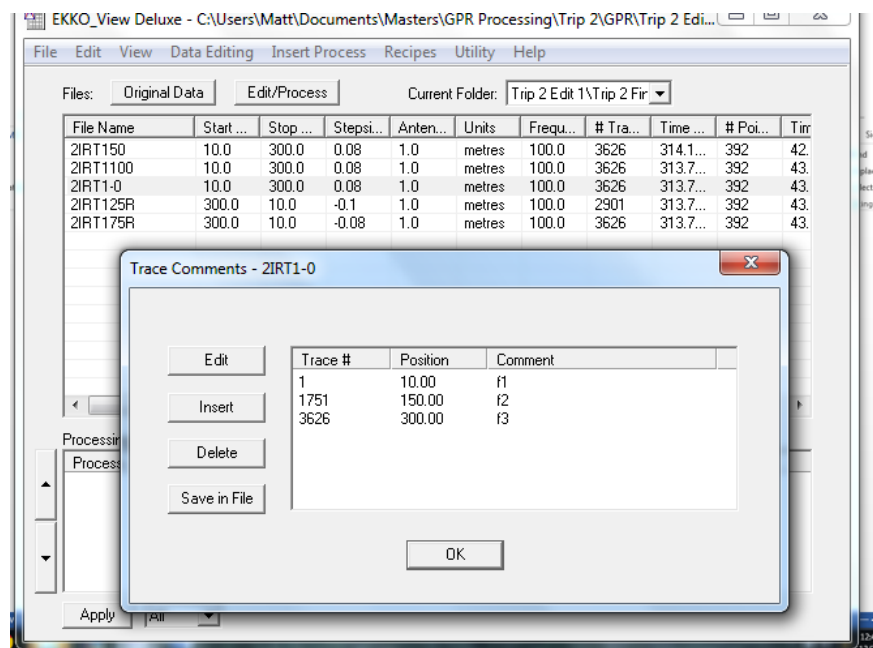


FIGURE 4.20: Editing GPR trace data within EKKO View Deluxe.

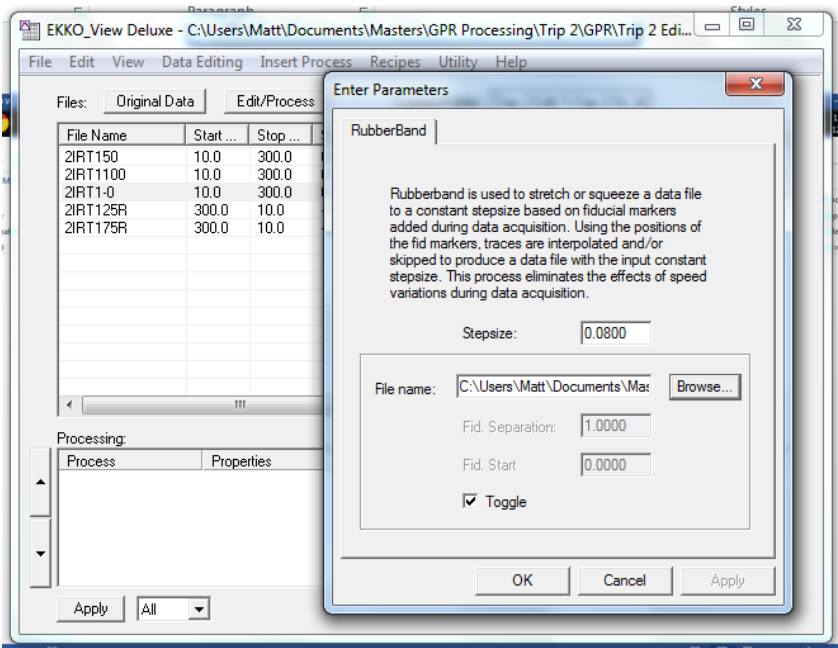


FIGURE 4.21: Rubberbanding GPR data using EKKO View Deluxe.

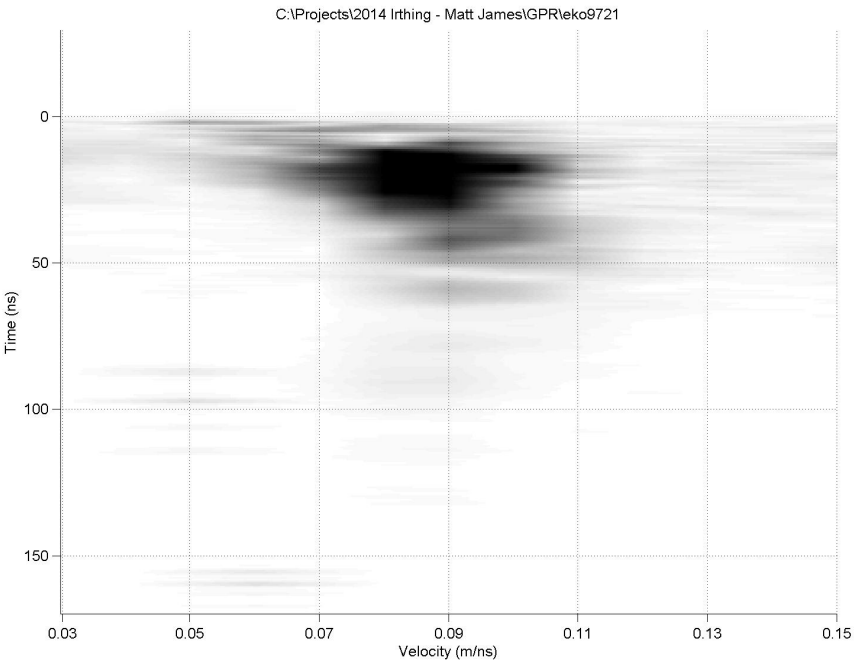


FIGURE 4.22: CMP Analysis showing the sub surface velocity of 0.9 m/s.

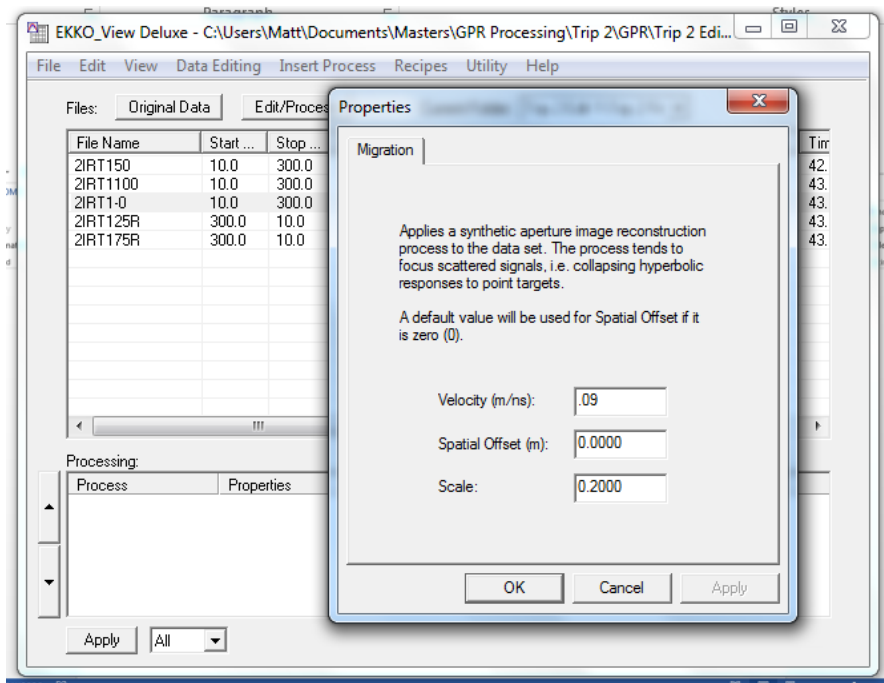


FIGURE 4.23: Migrating GPR data using EKKO View Deluxe.

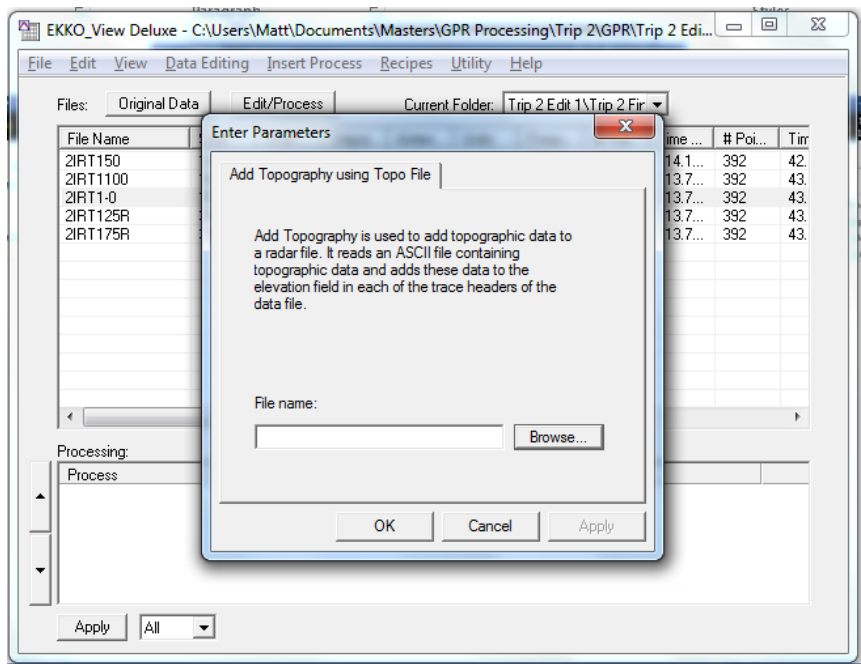


FIGURE 4.24: Adding topography to GPR data using EKKO View Deluxe.

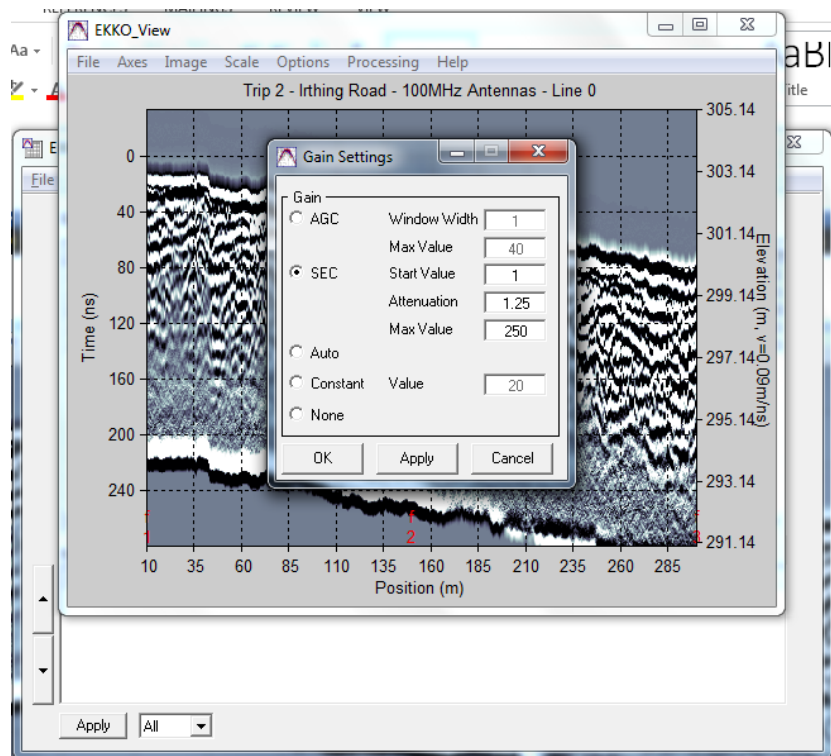


FIGURE 4.25: Adjusting gains using EKKO View Deluxe.

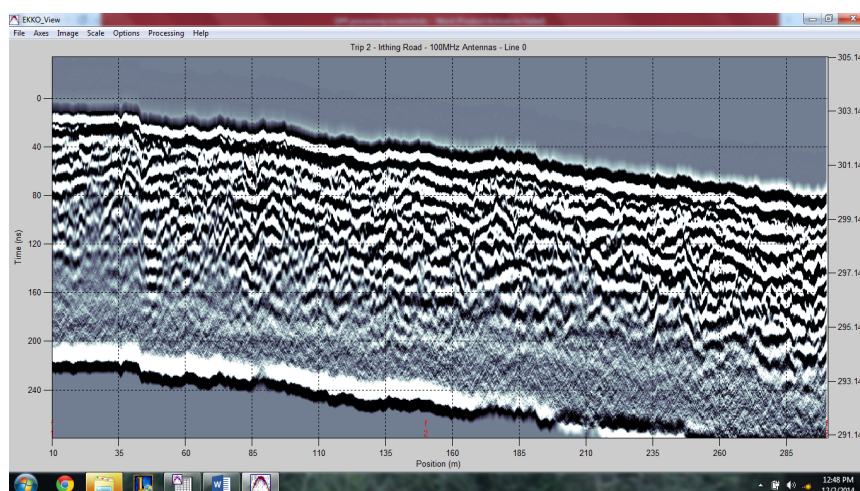


FIGURE 4.26: Final radargram output.

4.6 Groundwater Sampling

The groundwater sampling program faced multiple difficulties throughout the project and was only completed about two months after the cattle had left the grazing area. The initial plan was to implement staged water sampling throughout the duration of the geophysical testing, however due to issues with gaining access to the groundwater, Environment Southland made the decision to cease water sampling in mid July 2014. This decision was reviewed in October 2014 and the decision was made that if the land owner, Ben Walling, was prepared to dig two holes down to the shallow ground water then Environment Southland would be able to conduct the sampling. The location of the holes had to be within the survey area because of the need to avoid interrupting the farm operations. This meant that no sampling could be done directly into the area where the cattle had been grazing during the winter. The location of the water sampling pits were determined using the results of the EMI and GPR surveying that had been undertaken to date. The data indicated that there were two channels of increased apparent conductivity through the field site. These areas also coincided with noticeable changes in the surface vegetation (Visible in the photos on Figure 4.27, page 47) and also possibly with what appear to have previously been water channels. The pit locations that were chosen are possibly the areas with the fine grained sediment and the areas between the pits could have been the main water transport zones. This is a possible error in the choice of groundwater sampling location. The two sampling pits were dug using a 20 ton digger and were situated on the 100 metre and 25 metre lines of the survey grid (See Figure 4.27 on page 47). There were also soil water samples taken from the paddock that contained the wintering cows and the research site. The entirety of this sampling was done on the 25th of November 2014, after the cattle had been removed. This creates uncertainty around the usefulness of the results, especially the soil water samples as the grazing paddock had been ploughed and fertilised.

4.7 Combination of Techniques

Using a combination of different geophysical and non-geophysical techniques is the best method for gaining an accurate understanding of a survey area and the processes that are at work in the area. The methodology that was decided upon for this field investigation was to collect data from two different EMI sources, EM31 and DUAL-EM, and then combine that with GPR (both 100 MHz and 200MHz), and water sampling. This combination of techniques produced figures such as radargrams with EMI apparent conductivities displayed above the image which allow the comparison of two or three different techniques in one figure (See Figure 4.28 on page 47). The strength of this

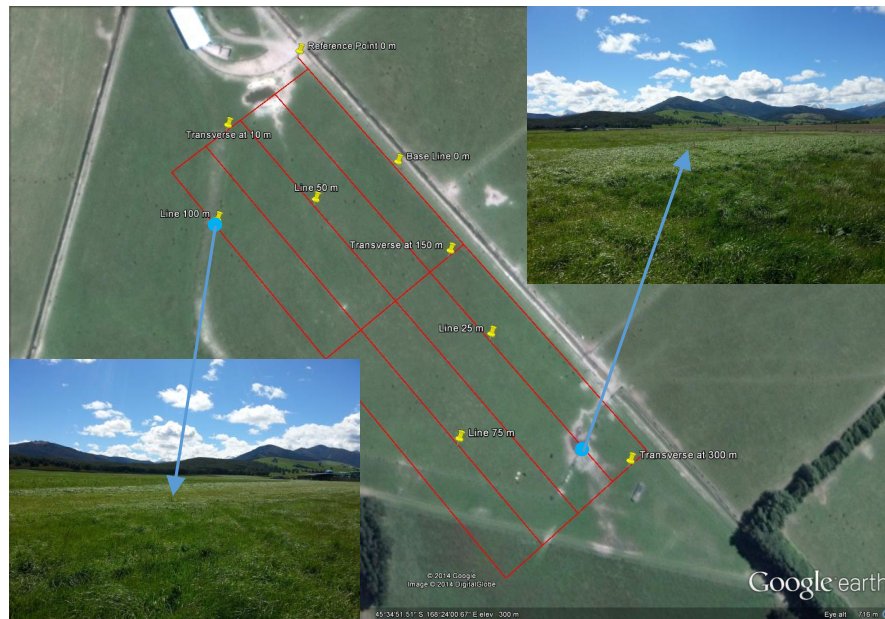


FIGURE 4.27: Locations of groundwater sampling pits with photos showing possible changes in surface vegetation across the field area.

revolves around having different techniques to support and assist each other in producing accurate, meaningful data.

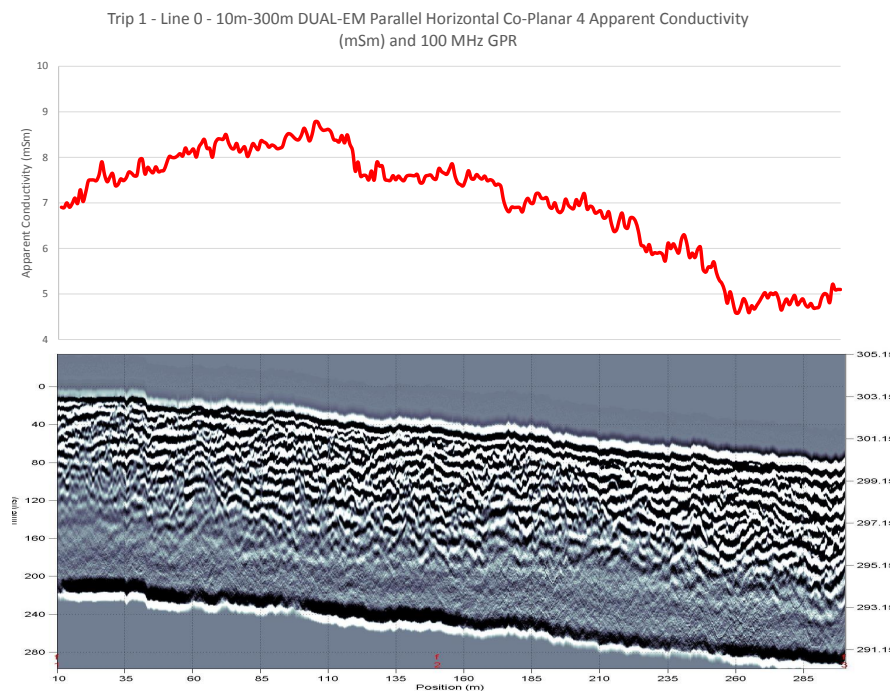


FIGURE 4.28: GPR radargram with a 100MHz EM31 apparent conductivity overlay.

Chapter 5

Results and Interpretation

5.1 EM-31 Results

5.1.1 EM-31 Base Level Initial Results

The EM31 was run on every trip to Southland and was seen as a very reliable source of consistent information. This was due to the confidence in the data that was collected by the EM31. The device had proved that it was consistent and well calibrated on many previous applications so it was relied on to provide information about both the field site and the accuracy of the DUAL-EM, which hadn't seen the same level of use.

The key factor that was identified in the first two trips was that the EM31 results were almost identical between the two trips and also between the two orientations of the coils. Figure 5.1 shows all of the orientations for all of the lines over both trips. This shows how well all the results match each other and means that the base level readings are highly likely to be accurate and trustworthy. Figure 5.2 and 5.3 show a clearer picture of both trips EM31 data and again show the great correlation between the readings taken at different device orientations on both trips. The comparison between the parallel coil orientation results from both trips is shown in Figure 5.4. The results shown in this figure show the correlation even more clearly and also show that the only difference may be a slight increase in conductivity along the 25 metre and 50 metre line during trip 2.

There are areas of increased apparent conductivity visible in the EM31 data and these could relate to shallow groundwater preferential flow paths, a higher conductivity material such as clay which could be preventing surface water drainage, or a combination of both. The shape of the blue, high conductivity points in Figure 5.5 does suggest that the high conductivity areas are historic flow paths. These are likely to have been infilled

with a fine grained material that has given higher conductivity readings and prevented percolation and drainage of surface water, thus also increasing the apparent conductivity. The shape of the high conductivity points at the north end of the site (shown by the blue areas with a red arrow through them in Figure 5.5 on page 54) correlate well with the groundwater flow direction of the site and also with the historic channel and surface vegetation changes which were commented upon in the initial research site development section of chapter 4. The green oval in the centre of Figure 5.5 represents an area that is of relatively low conductivity and does not appear to have any conductive medium beneath it whether that be water or clays. This could easily contain gravels and less fine grained sediments would give it a lower apparent conductivity, but higher hydraulic conductivity. This could lead to the central low conductivity zone being the area of preferential groundwater flow. The south end of Figure 5.5 appears to be more complex than the north end. This is because the high conductivity area shown here appears to vanish along line 50 and 75. The explanation to this may lie in the increased conductivity of the 25 and 50 lines that was identified previously in Figure 5.4. When a comparison is made between Figure 5.5 and Figure 5.6 it is more obvious that the high points do move very slightly. By applying a broader approach to the behaviour of the high conductivity area at the south end of the site it is possible to narrow the three arrows that represented possible subsurface behaviour in Figure 5.5 down to the two similar arrows shown in Figure 5.6. This is done by analysing both the trips results and observing the movement of the apparent conductivity at the southern end. It appears most likely that there is a mixture of depth and flow path orientation effecting the results. The path of higher apparent conductivity is likely to make a slight turn similar to the light blue arrow in Figure 5.6 and also perhaps have a slight decrease in the amount of fine grained sediments and pore water beneath the 50, 75, and 100 metre lines.

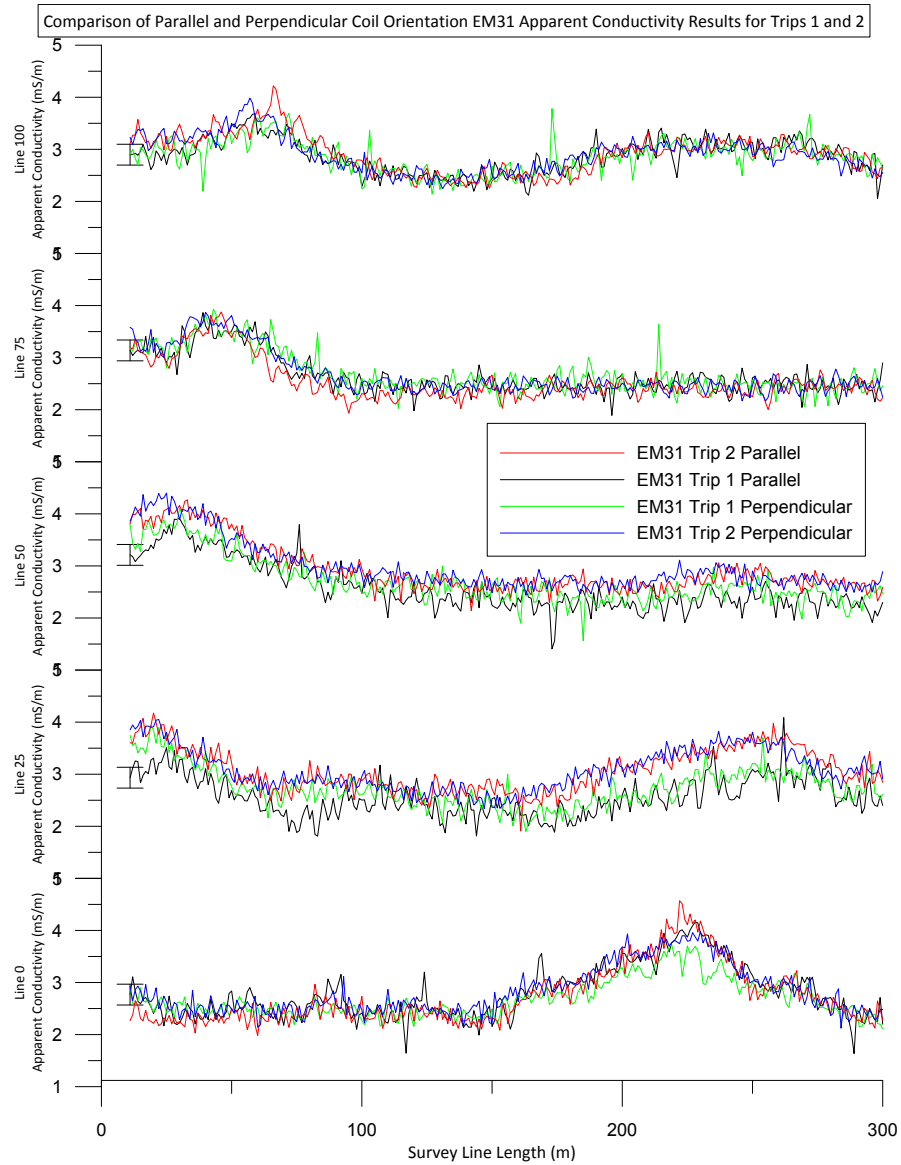


FIGURE 5.1: Comparison of EM31 apparent conductivities recorded with both parallel and perpendicular coil orientation. The results include data from trip 1 and 2. Error bars represent the $\pm 0.2 \text{ mS/m}$ error of the EM31 device.

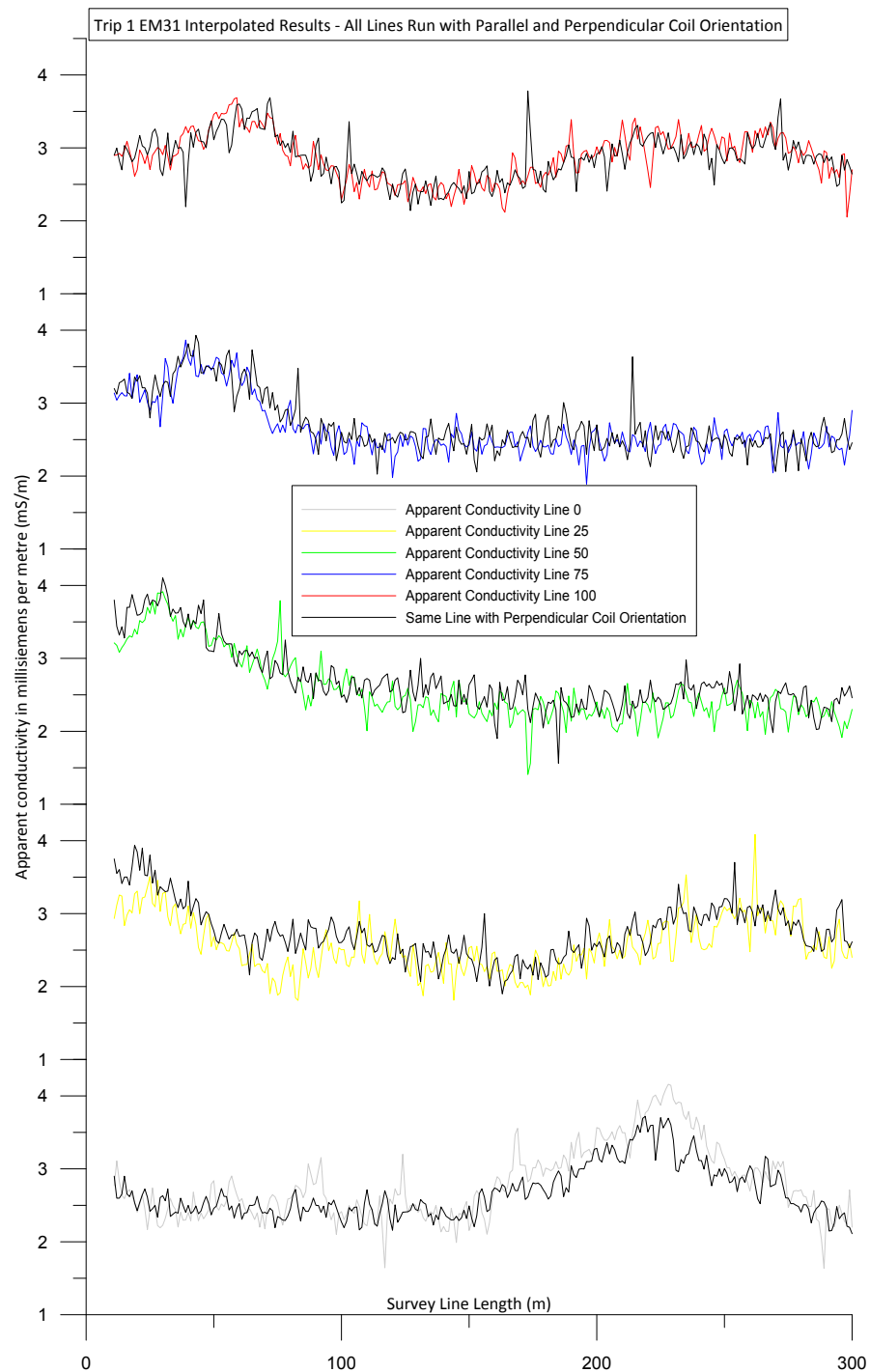


FIGURE 5.2: Comparison of EM31 apparent conductivities recorded during trip 1 with both parallel and perpendicular coil orientation.

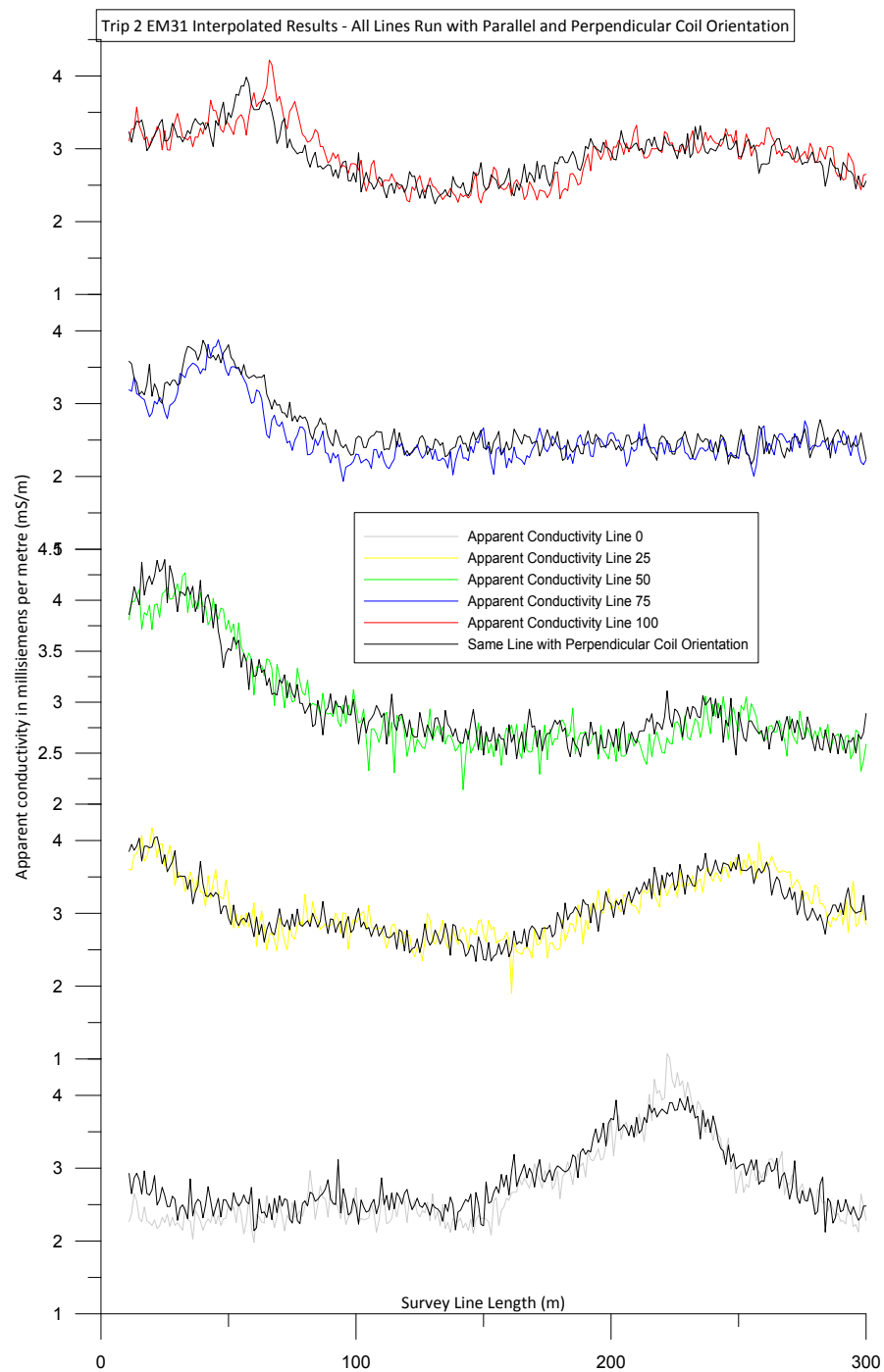


FIGURE 5.3: Comparison of EM31 apparent conductivities recorded during trip 2 with both parallel and perpendicular coil orientation.

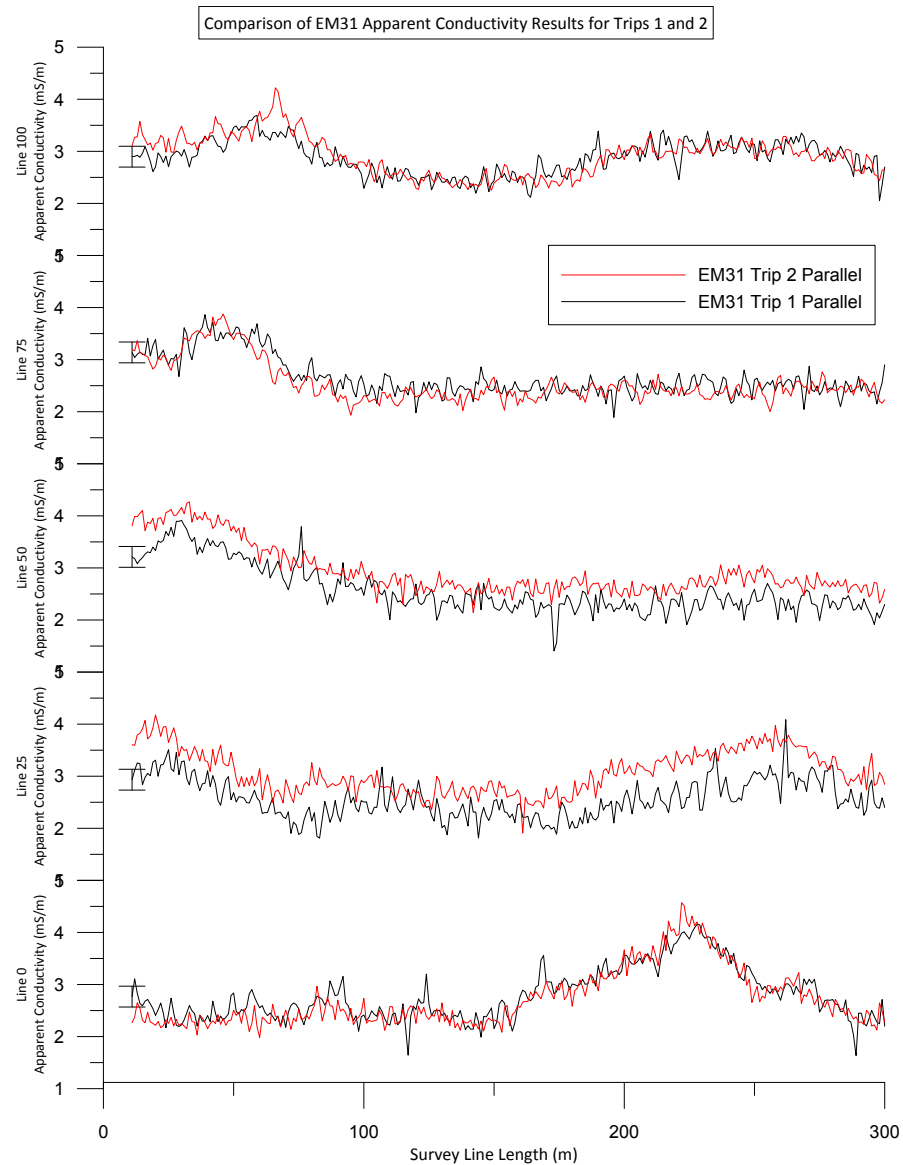


FIGURE 5.4: Comparison of EM31 apparent conductivities recorded during trips 1 and 2 using a parallel coil orientation. Error bars represent the ± 0.2 mS/m error of the EM31 device.



FIGURE 5.5: Google Earth image with an overlay of the trip 1 EM31 data collected using parallel coil orientation. The blue areas identify high apparent conductivity areas. The arrows represent possible infilled historic flow paths and the green oval marks the central low conductivity zone.



FIGURE 5.6: Google Earth image with an overlay of the trip 2 EM31 data collected using parallel coil orientation. The blue areas identify high apparent conductivity areas. The arrows represent possible infilled historic flow paths and the green oval marks the central low conductivity zone.

5.1.2 EM-31 Temporal Changes

Temporal changes in the geophysical results across the field area are important to the project because they are to be used to identify the potential of these geophysical methods to identify shallow ground water contamination. After analysing all of the EM31 data as a whole (See Figure 5.7) it became obvious that the changes, if there were any, were small and would require more precise graphing. Figure 5.7 shows all of the EM31 data that was collected using a parallel coil orientation and it is obvious that precise observations on the subtle changes in the data cannot be ascertained using this figure. This is also true of Figure 5.8 which shows the EM31 data recorded using a perpendicular coil orientation. The only possible trend visible in this figure is a possible increase in conductivity from the trip 3 data.

The next stage of temporal analysis is to look closely at the individual lines and see how they changed over the course of the survey. Figure 5.9 shows a composite plot of all the EM31 data that was collected along line 0 throughout the year at both a parallel and perpendicular coil orientation (Note: Composite plots are labelled as Summation plots in the figures due to the Grapher software that was used. It is also important to note that Grapher does not allow the addition of error bars on composite/summation plots. The EM31 device error on the composite plots of each trip is ± 0.4 mS/m. The EM31 device error on the composite plots of two trips combined is ± 0.8 mS/m.). The use of composite plotting came about because of the difficulty comparing so many data sets with only small differences. Composite plotting allows the information from ten data sets (each line run at parallel and perpendicular coil orientations over five trips) to be presented in a way that shows small variations between trips. The composite plot of line 0 (Figure 5.9) has two aspects to it. The first being the five lower plots that are a summation of the parallel and perpendicular results taken from each trip. This group of data sets allows interpretation of changes between specific trips. The second part of Figure 5.9 revolves around the upper three lines which are composite plots of the parallel and perpendicular data from two trips combined into one line. This is done to show the overall changes in a clearer manner. For example it is obvious that the composite plots of the apparent conductivity data from trips 3 and 5, and 5 and 6, are greater than that of trips 1 and 2. This is relatively clear when seen in the upper composite plots however it is more difficult to identify in the lower composite plots because of the larger number of data sets plotted. The composite plots are an effort to ensure clarity of the results.

To summarise the results of line 0 shown in Figure 5.9, it appears that the apparent conductivity increased slightly after the base level trips, 1 and 2. This change is only minor and appears at most to be an increase of 0.5 to 1.0 mS/m. This is larger than the instrument error of plus or minus 0.2 mS/m so does suggest some external influence.

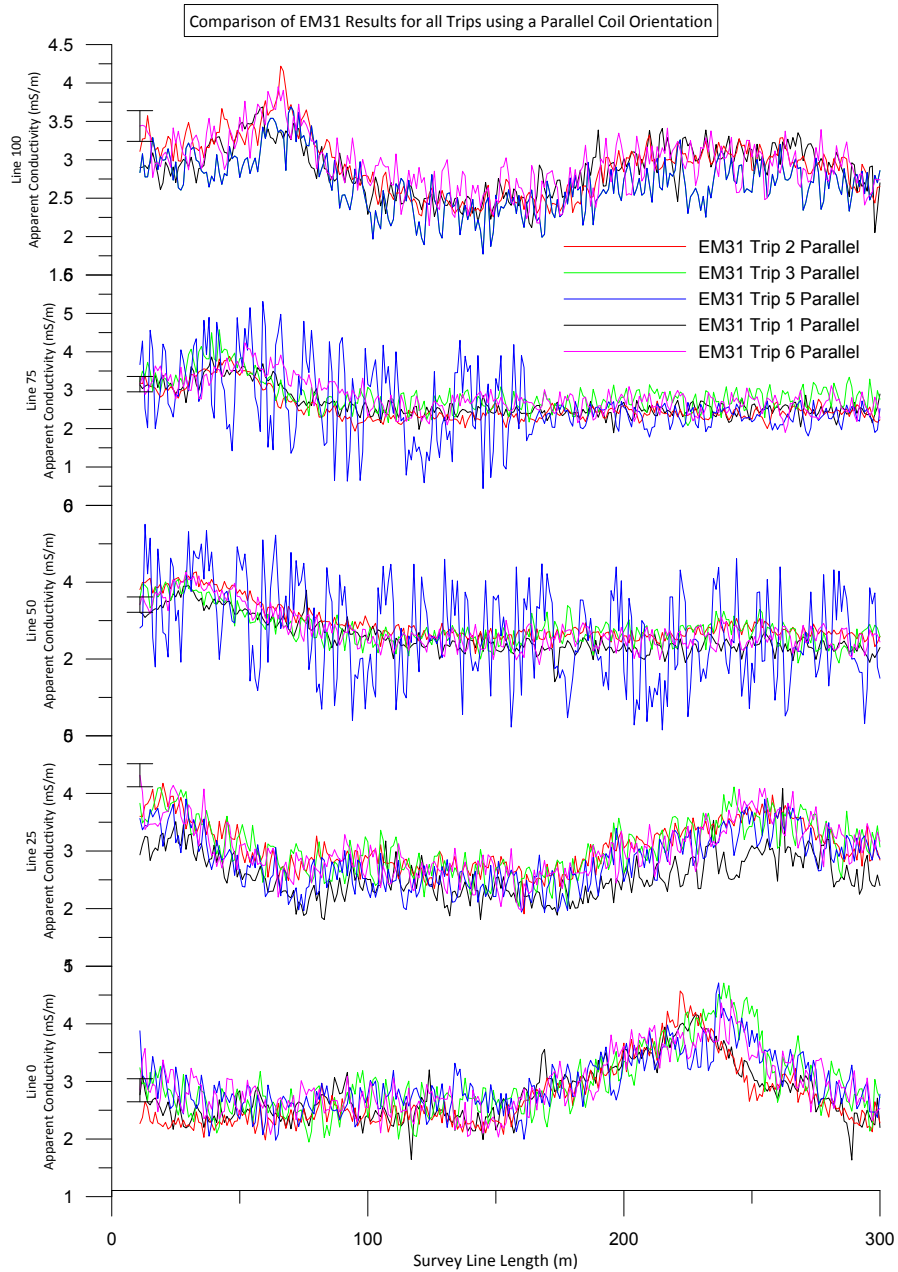


FIGURE 5.7: EM31 data recorded over five trips using a parallel coil orientation. All lines are shown and data from different trips is distinguished using different colours. Error bars represent the ± 0.2 mS/m error of the EM31 device.

The composite plot of the data collected along line 25 is shown in Figure 5.10. There are two major points to identify within this figure. The first being the minor increase in apparent conductivity that appears to be present between the data from trips 1 and 2, and the later trips. It appears initially as though the data is showing the same relationship as was observed in the line 0 data however the second point that needs to be addressed here confuses this explanation.

The second point involves the consistent difference in conductivities recorded between

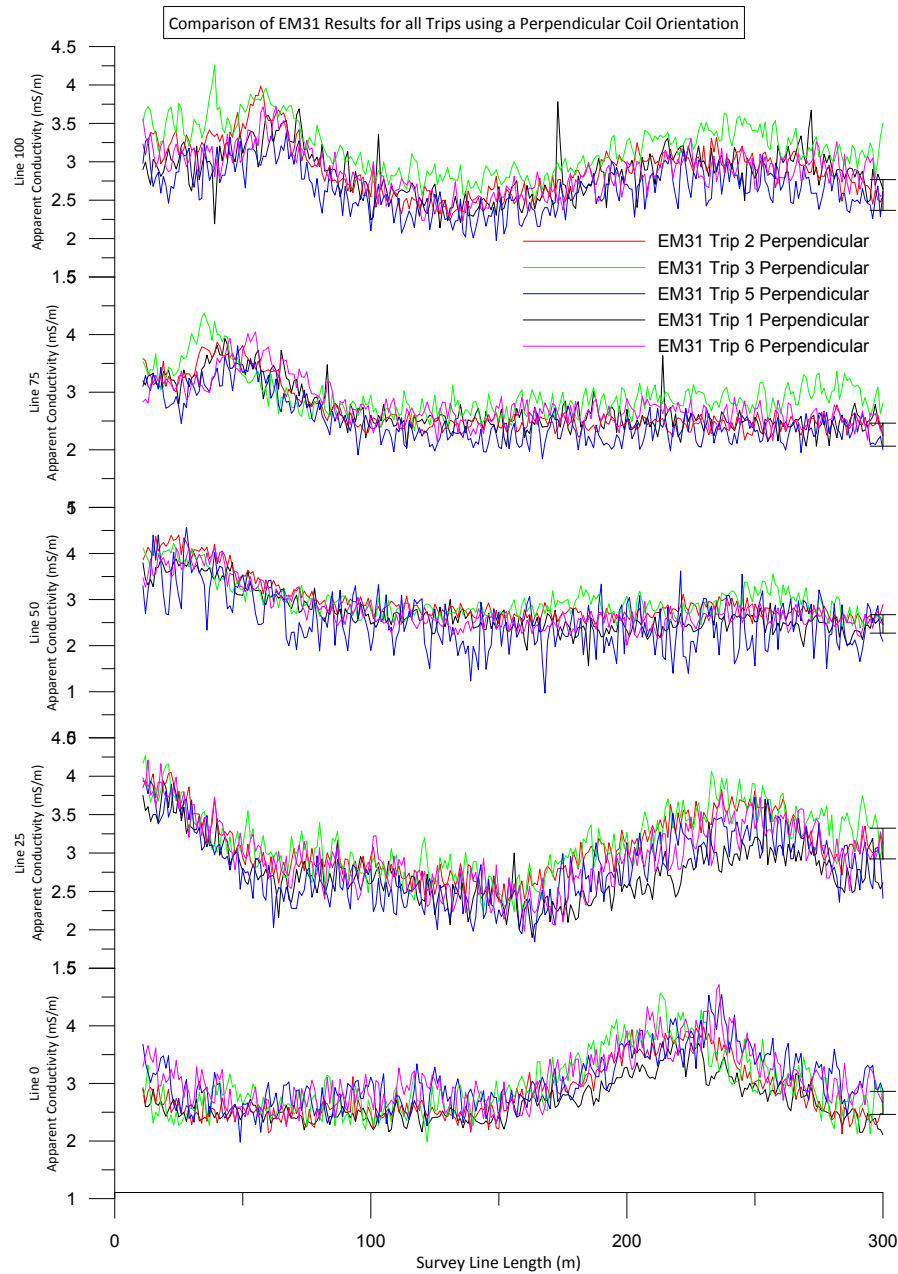


FIGURE 5.8: EM31 data recorded over five trips using a perpendicular coil orientation. All lines are shown and data from different trips is distinguished using different colours. Error bars represent the ± 0.2 mS/m error of the EM31 device.

trip 1 and 2. These were both base level trips that were intended to identify the normal conductivity present beneath the field site. Trip 2 however appears to have consistently higher apparent conductivity results than trip 1 and this raises questions as to what is truly influencing the conductivity results (See trip 1 composite plot vs. trip 2 composite plot in Figure 5.10). As there were no cattle grazing near the site during trip 2 it appears that the increase in conductivity is most likely to have been caused by the extremely wet conditions that were encountered on that trip. This raises further questions around how sensitive the shallow groundwater is to climate and how quickly the effects from

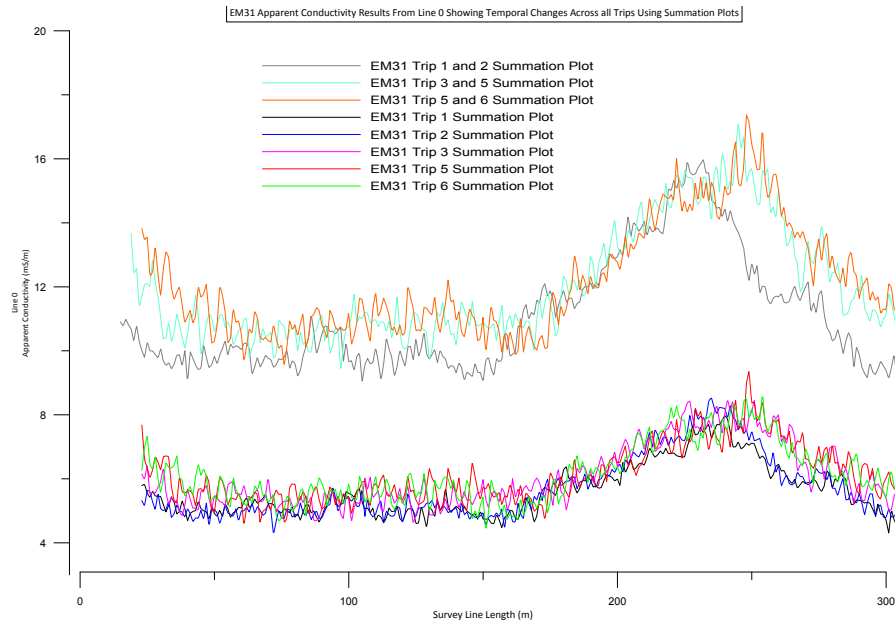


FIGURE 5.9: EM31 data recorded over five trips using a parallel coil and perpendicular coil orientations along line 0. This data has then been turned into composite plots to compare trends between trips.

heavy rain are seen in the geophysical data.

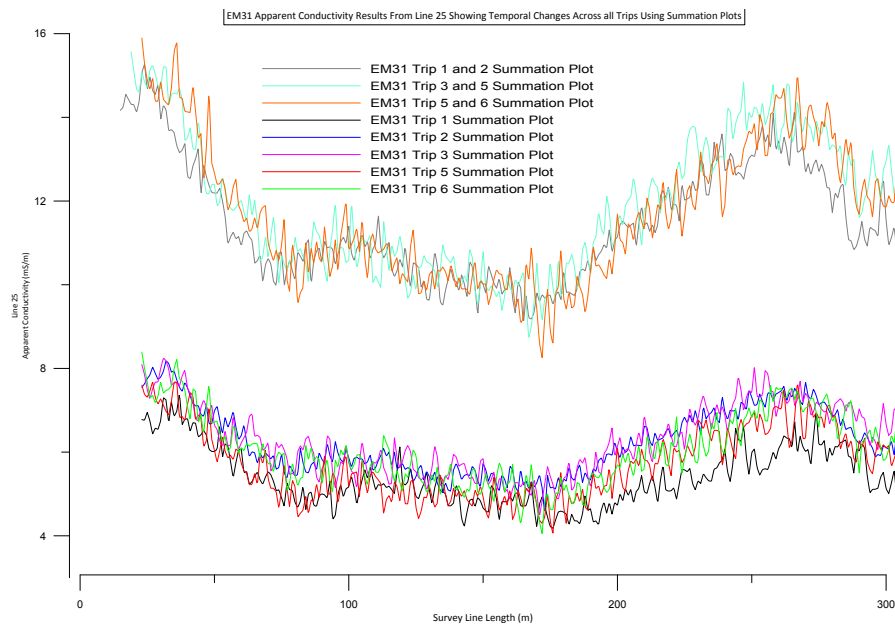


FIGURE 5.10: EM31 data recorded over five trips using a parallel coil and perpendicular coil orientations along line 25. This data has then been turned into composite plots to compare trends between trips.

The first point to be raised when looking at the composite plot of line 50 (See Figure 5.11) is that the data from trip 5 has been removed. This is because of the extreme variation that was picked up during the testing and is visible in Figures 5.7 and 5.8. The issue with this data is only recorded upon line 50 and 75 and is believed to have been

instrument or user fault, most likely caused by low batteries in the device. The inclusion of this noisy data had such a negative effect upon the composite plots of line 50 (Figure 5.11) and line 75 (Figure 5.12) that the decision was made to remove the data.

The composite plot of line 50 shows a slight increase in the apparent conductivity from trips 3 and 6 between the 150 to 300 metre marks. The plot also shows the consistent difference in apparent conductivities between trips 1 and 2 which was also identified in line 25. This difference is shown by a consistent 0.25 to 0.75 mS/m increase in the trip 2 readings when plotted against the trip 1 values. This difference is again in excess of the plus or minus 0.2 mS/m error that the EM31 device allows.

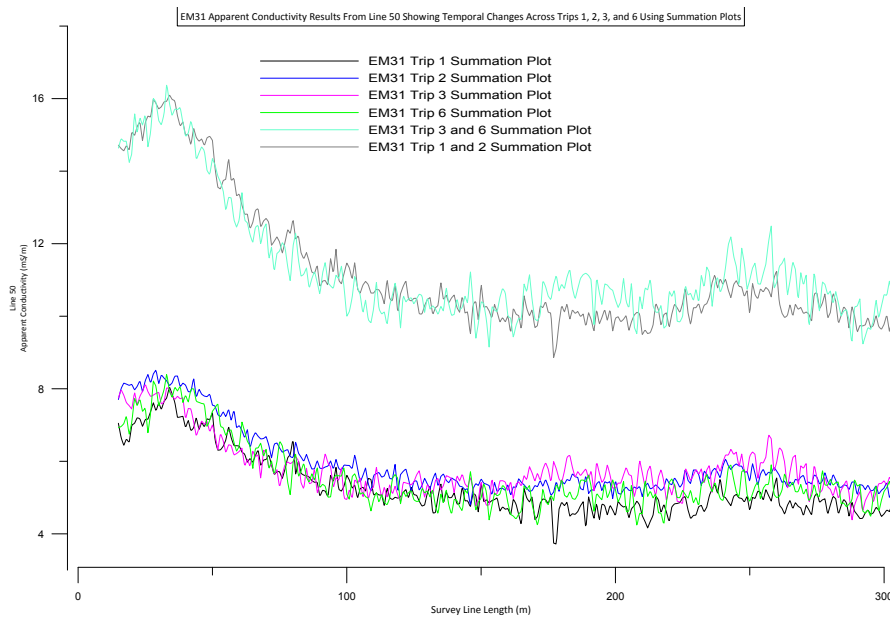


FIGURE 5.11: EM31 data recorded over five trips using a parallel coil and perpendicular coil orientations along line 50. This data has then been turned into composite plots to compare trends between trips.

The composite plot of line 75 shows a consistent increase in the apparent conductivities recorded in trips 3 and 6 (See Figure 5.12). The trip 3 and 6 apparent conductivity values appear to be a relatively consistent 0.25 to 0.50 mS/m above the trip 1 and 2 values. Another important point is that the difference in conductivities between trip 1 and 2 data that was identified in line 25 and 50 seems to have disappeared.

The line 100 composite plot (Figure 5.13) appears to show that the apparent conductivities changed very little throughout the trips. It is apparent however when looking at the trip 3 composite plot that it is consistently higher across the length of the line. This difference is only slight and again may be climate influenced as the conditions were extremely wet during trip 3.

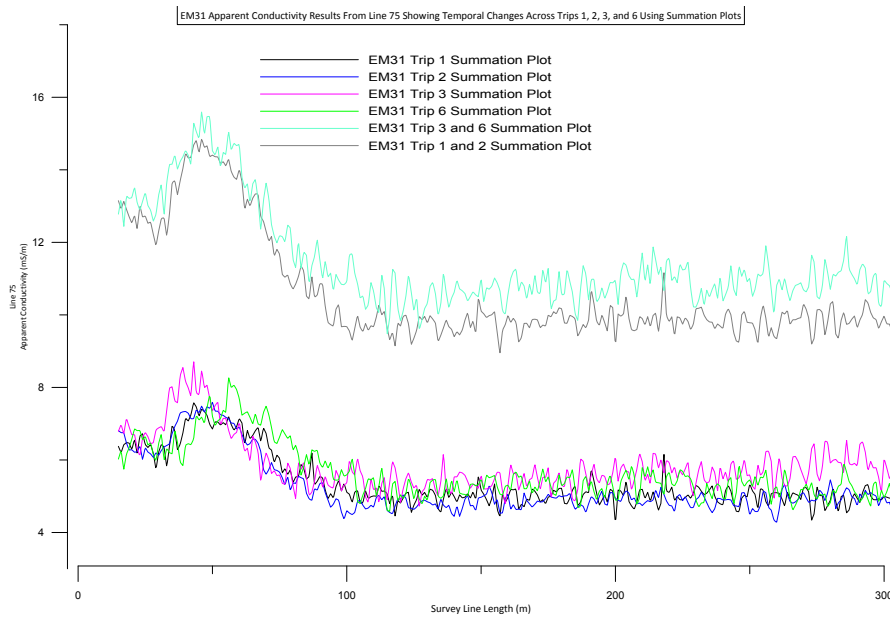


FIGURE 5.12: EM31 data recorded over five trips using a parallel coil and perpendicular coil orientations along line 75. This data has then been turned into composite plots to compare trends between trips.

The trip 5 data set also appears to show lower apparent conductivity readings along the length of line 100 (See the red line in Figure 5.13). Again the argument could be made that this is climate controlled because of the dry weather prior too, and during the data collection phase of trip 5.

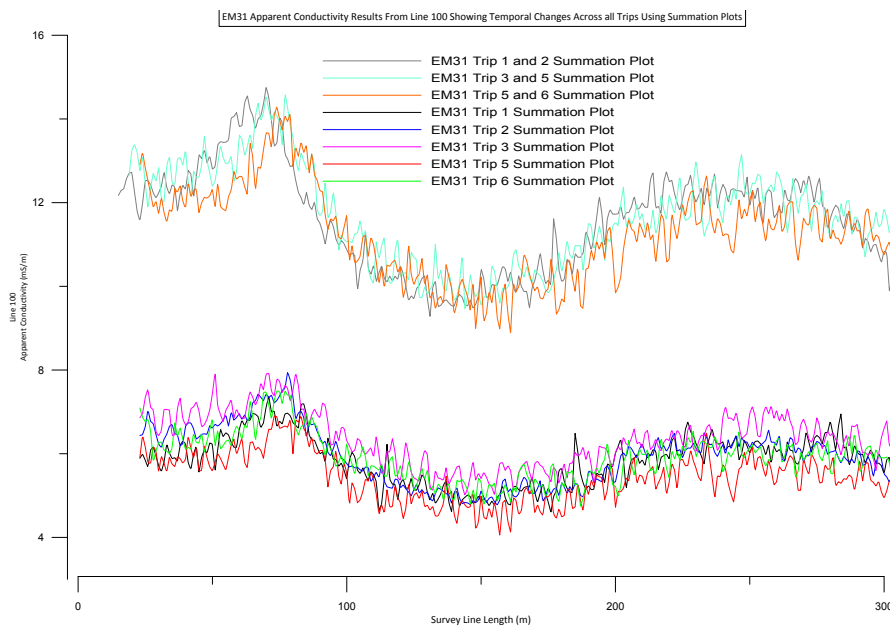


FIGURE 5.13: EM31 data recorded over five trips using a parallel coil and perpendicular coil orientations along line 100. This data has then been turned into composite plots to compare trends between trips.

5.2 DUAL-EM Results

5.2.1 DUAL-EM Base Level Initial Results

The DUAL-EM was run across the Irthing Road field site on both of the first two trips to Southland to establish base level readings. The results were mixed and raised some initial concerns about the use of the DUAL-EM and how accurate and consistent the results were.

The first limitation that became obvious through using the DUAL-EM was that the horizontal co-planar 1 (HCP1) coil separation was too sensitive and unpredictable for this application. The 1 metre coil separation used to obtain the HCP1 data meant that the DOE (Depth of Exploration) was at maximum 1.5 metres, and this made the data highly sensitive. The results of the HCP1 surveying from trips 1 and 2 are shown in Figures 5.14 and 5.15. When analysing this data it is obvious that the HCP1 results are not going to be useful for this project and the decision was made to concentrate primarily upon the HCP2 and HCP4 data which achieves a greater DOE (3 and 6 metres respectively).

The horizontal co-planar 2 (HCP2) data was also collected on both trips and is shown in Figure 5.16. Because of the greater depth of exploration (three metres) due to the two metre coil spacing this data is often more reliable and less sensitive to interference than the HCP1 data. However the HCP2 is still relatively shallow for this survey and the data shows many examples of unusual readings in Figure 5.16. These include the trip 1 parallel coil orientation readings from line 0 which start negative and then increase dramatically and also the trip 2 parallel coil orientation results for line 100 which decrease while all the other results on that line increase. It is also concerning that many of the HCP2 readings are negative and that very few of them show any correlation to the EM31 data. The negative readings are not valid apparent conductivity readings and suggest that the data may be unreliable and incorrect.

There are some HCP2 data that does appear to match the EM31 data however. The trip 2 data along line 0 appears to show the same higher conductivity zone just after the 200 metre mark that is shown in the EM31 data in Figure 5.3 on page 52. The trip 2 data along line 50 also seems reliable. The trip 1 data along line 100 follows the same highs and lows as the EM31 data in Figure 5.3, however the actual readings are negative which suggests that the device is only picking up a trend, rather than recording reliable data.

Horizontal co-planar 4 (HCP4) is the major interest for this project because it has the largest coil spacing at 4 metres, which gives it an impressive DOE of up to 6 metres.

This is slightly deeper than the EM31 and should be giving similar results to the EM31. The HCP4 data is the best indication of not only the subsurface conditions but also how well calibrated and reliable the DUAL-EM device truly is and how viable its application could potentially be for shallow groundwater monitoring.

The HCP4 results shown in Figure 5.17 on page 66 show a far more reliable data set than either of the HCP1 or HCP2 graphs. This is to be expected because of the greater DOE making the HCP4 less susceptible to interference as it is testing a larger volume of the subsurface.

The first point to notice is that the line 0 data is following the same pattern as the EM31 data with a high point around the 225 metre mark. There is however quite a large range in the conductivity measurements with an average of 6 mS/m difference between the high and low readings from different runs. This is in contrast to the EM31 which had a very low variation between the readings of less than 1 mS/m (See Figure 5.1 on page 50). There is also a negative start to the trip 2 perpendicular data although it appears to correct itself at around the 40 metre mark.

The 50 metre line appears to follow the EM31 data quite closely and has far less range within the values than the 0 and 100 metre lines. This suggests that the data is fairly accurate and trustworthy.

The 100 metre line again has the issue around the trip 2 parallel reading being a reverse of the other data. Because this matches the HCP1 and HCP2 data for this run it is assumed to be bad data from that particular run or that a mistake has been made during the processing of the data for that line. The remaining data strongly correlates with the EM31 data trend. The trip 1 data is closely spaced and correlates very closely so is deemed to be accurate data. The trip 2 perpendicular data follows the trend well but does seem to be too low so apparent conductivity values from this line should be treated with caution.

Overall the HCP4 data was definitely the most reliable and accurate data when compared with the EM31 however the first two trips do not give enough data to really comment on the viability and reliability of the DUAL-EM device for monitoring shallow groundwater. The data from subsequent trips will be important when assessing the value of the DUAL-EM to this project and others like it.

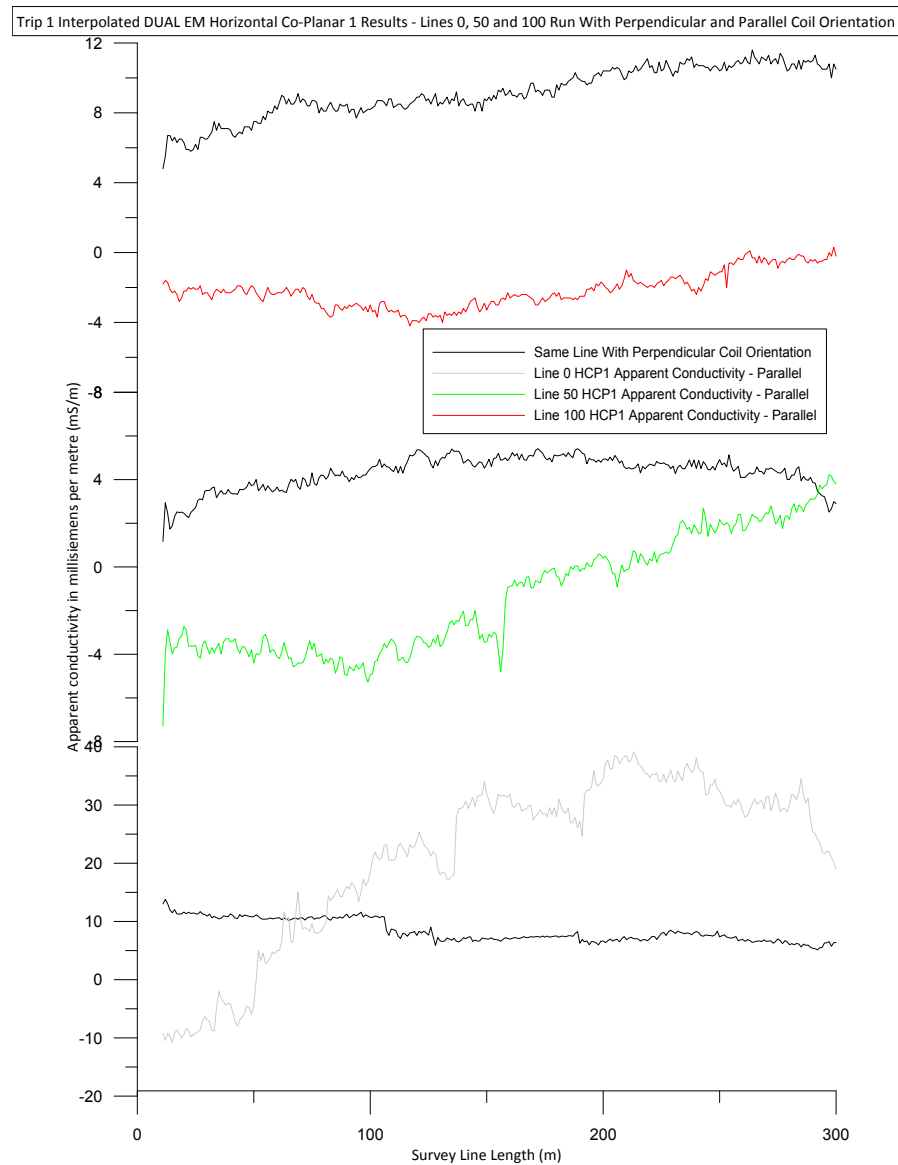


FIGURE 5.14: DUAL-EM horizontal co-planar 1 apparent conductivity from trip 1. Both parallel and perpendicular coil orientations are shown for the 1 metre coil spacing.

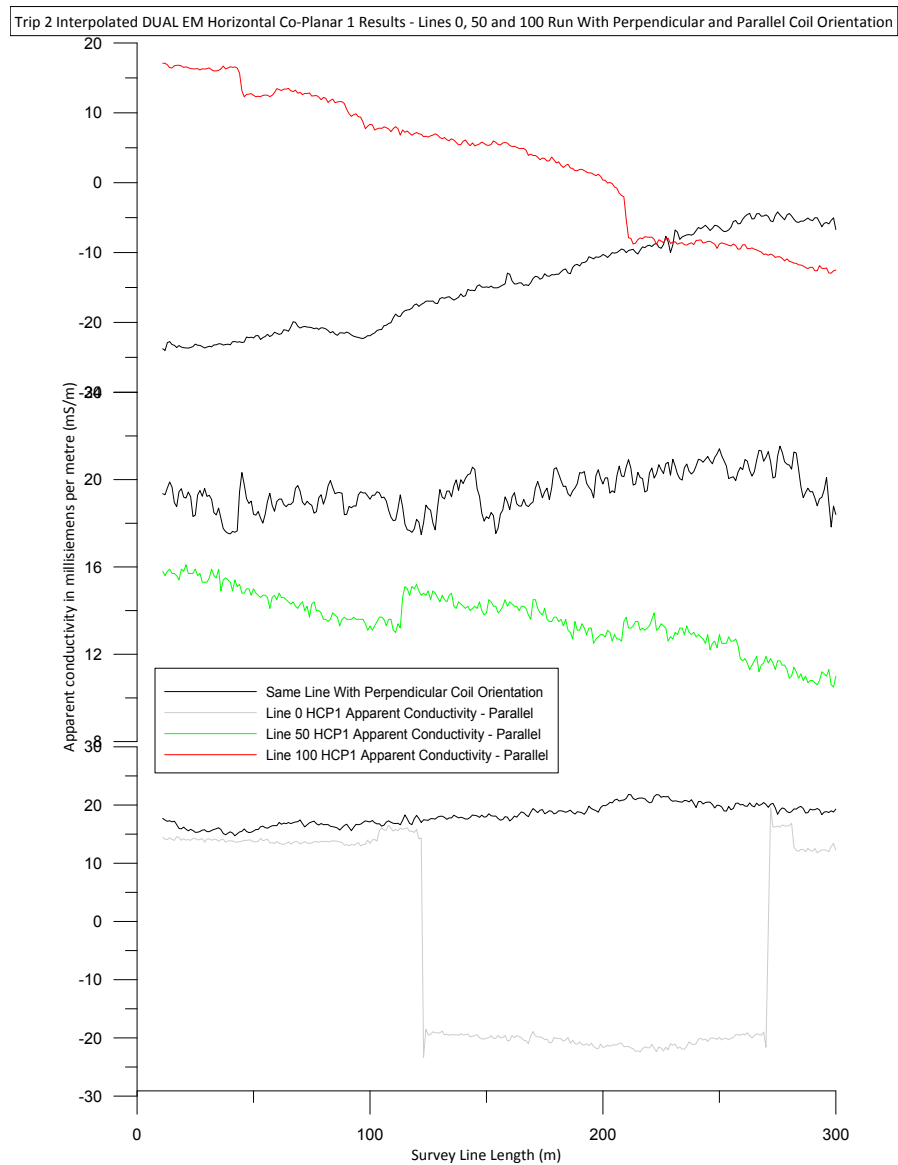


FIGURE 5.15: DUAL-EM horizontal co-planar 1 apparent conductivity from trip 2. Both parallel and perpendicular coil orientations are shown for the 1 metre coil spacing.

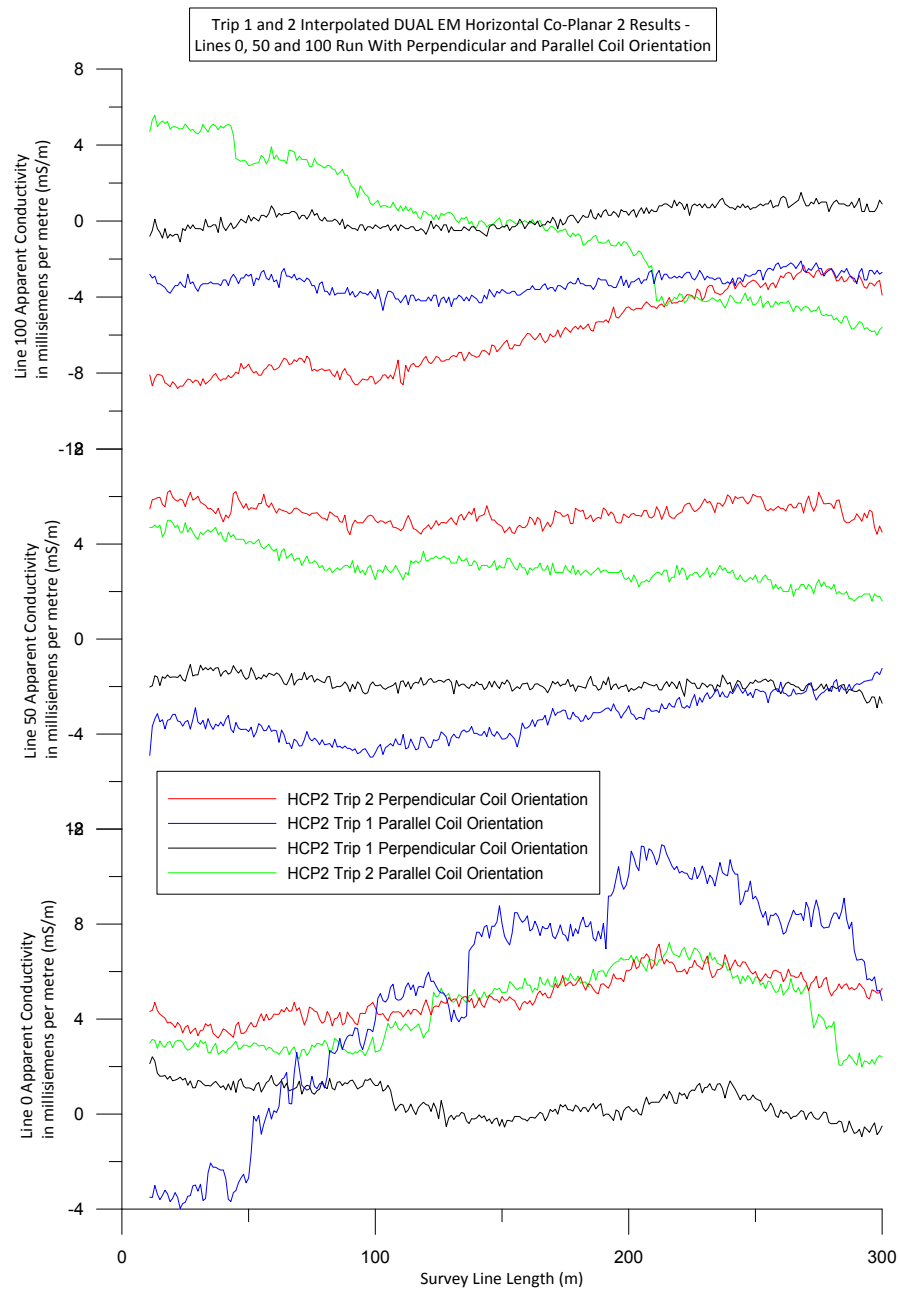


FIGURE 5.16: Comparison of DUAL-EM horizontal co-planar 2 apparent conductivity results from trips 1 and 2. This figure shows data from both coil orientations across three lines using a 2 metre coil spacing.

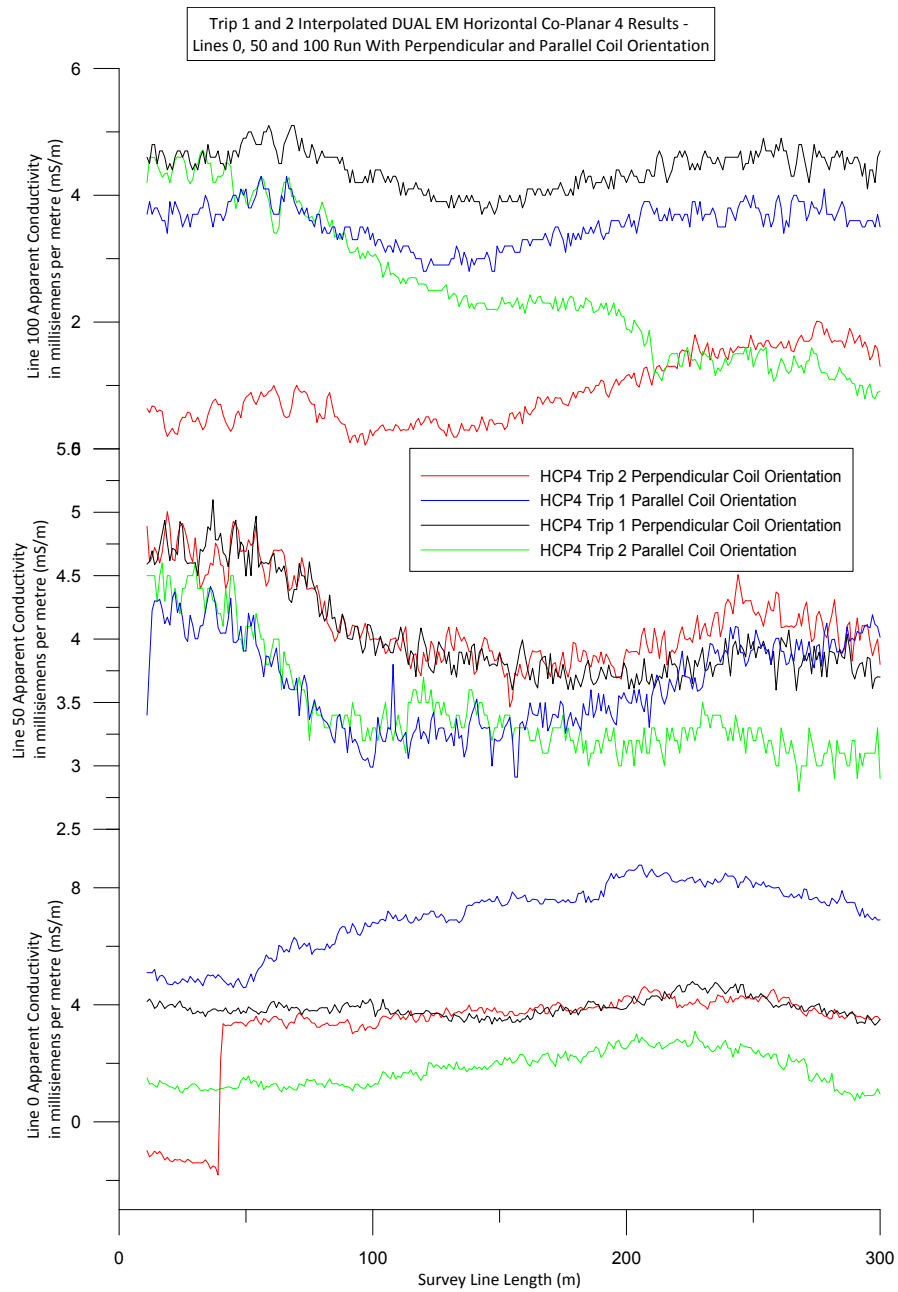


FIGURE 5.17: Comparison of DUAL-EM horizontal co-planar 4 apparent conductivity results from trips 1 and 2. This figure shows data from both coil orientations across three lines using a 4 metre coil spacing.

5.2.2 DUAL-EM Temporal Changes

Analysis of the temporal changes that are happening in the DUAL-EM data is important when drawing conclusions on the usefulness of the technique for this application. The initial stage of this analysis involved the creation of a graph which shows all of the results from every line obtained using a parallel coil orientation (See Figure 5.18 on page 67). The first obvious point to raise when looking at Figure 5.18 is the variation in the data when compared to the EM31 data shown in Figure 5.1 on page 50. The DUAL-EM data has a far greater spread and trip 5 and 6 data all appears to have large negative and positive spikes. Trends within the data are also far less obvious than in the EM31 results which in itself raises questions as to the accuracy and usefulness of the DUAL-EM data.

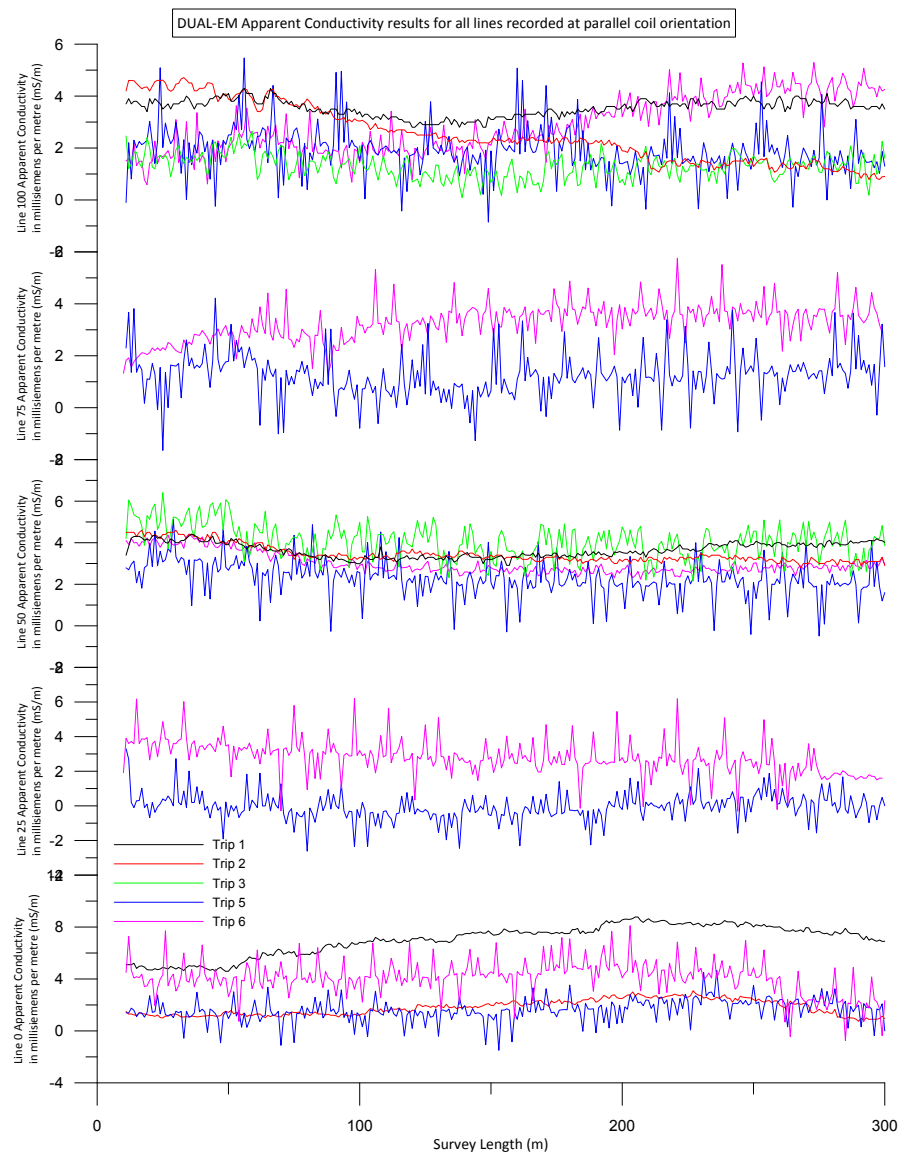


FIGURE 5.18: Comparison of DUAL-EM horizontal co-planar 4 apparent conductivity results across all of the lines from all of the research trips.

Due to the lack of obvious temporal changes and trends within Figure 5.18 it became necessary to create composite plots along the lines with the most data in an effort to ascertain some information from the results. The composite plot for line 0 is shown in Figure 5.19 and contains composite plots of the data collected from trips 1, 2, 5 and 6. One of the most important aspects of the composite plots are the added EM31 reference composite plots which have been included. The decision to add EM31 data to the DUAL-EM plots was an effort to show how the DUAL-EM data was comparing to another technique. The reference plots add vital information on how accurate the DUAL-EM apparent conductivities are, and also on whether the DUAL-EM is picking up the sub surface trends that have been identified using the EM31. The reference plot can also serve to show possible errors in the DUAL-EM data.

The key points from the DUAL-EM line 0 data are that the DUAL-EM results do follow the EM31 composite plot trend and the DUAL-EM data apparent conductivity readings are similar to the EM31 results. Both of these points are important for showing the reliability of the DUAL-EM method in this application. There is an obvious issue in the 0 to 50 metre section of the trip 1 data which is likely to be either user or instrument error. The other issue with the data is that the trip 5 and 6 composite plot shows many high and low spikes, and while the data does follow the correct trend, the spikes are a concern for reliably detecting small differences in apparent conductivity.

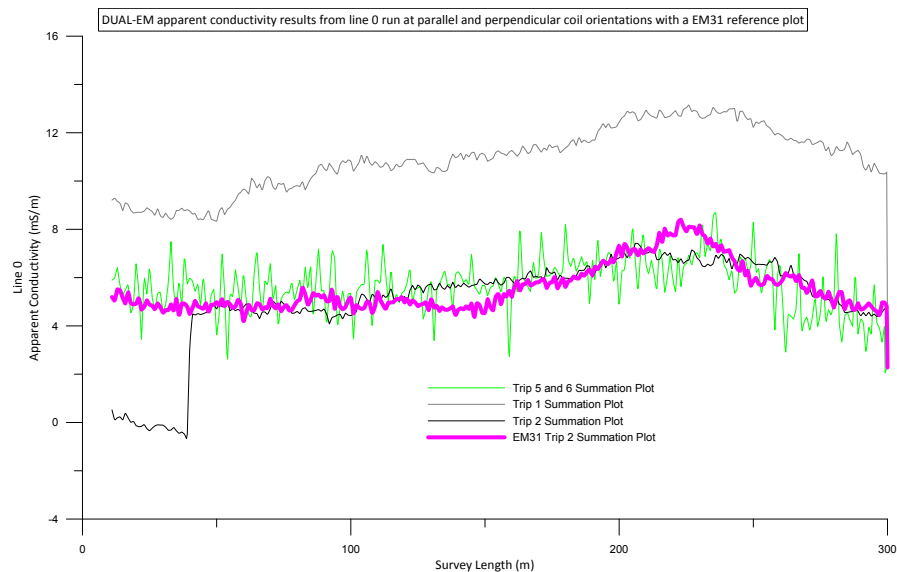


FIGURE 5.19: composite plot showing the DUAL-EM horizontal co-planar results from trips 1, 2, 5, and 6 along line 0. This data is recorded using a 4 metre coil separation. There is also a composite plot of the EM31 data along line 0 from trip 2. This EM31 plot is intended to be used as a reference to compare techniques.

The composite plot of the line 50 DUAL-EM data is shown in Figure 5.20 on page 69. The data does appear to show the overall trends quite well however there is again the issue with data spikes in the trip 3, 5, and 6 data sets. The DUAL-EM apparent

conductivity data from the first two trips does appear to be an average of 1.5 - 2 mS/m higher than the DUAL-EM data from trips 5 and 6 and the EM31 data from trip 2.

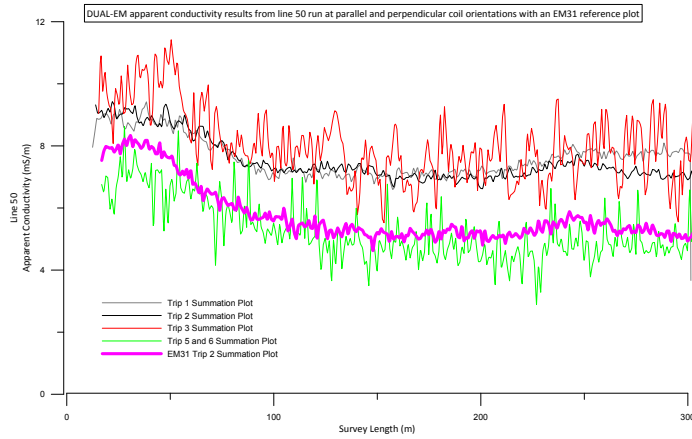


FIGURE 5.20: composite plot showing the DUAL-EM horizontal co-planar results from trips 1, 2, 3, 5, and 6 along line 50. This data is recorded using a 4 metre coil separation. There is also a composite plot of the EM31 data along line 50 from trip 2. This EM31 plot is intended to be used as a reference to compare techniques.

The DUAL-EM data from line 100 (See Figure 5.21) appears to show trip 1 and 2 data closely matching the EM31 trend. The data from trips 3, 5, and 6 however appear to be only roughly corresponding with these trends and again suffering from high variation. The trip 1 DUAL-EM data again appears to be about 0.75 to 1.5 mS/m than the EM31 results and this has been the case across all three lines. The trends between the lines however appear to match almost perfectly.

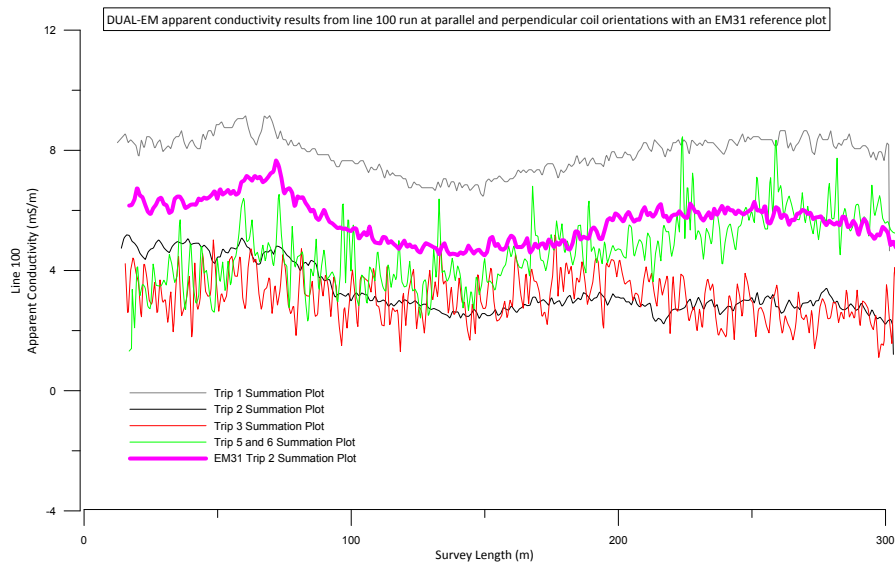


FIGURE 5.21: composite plot showing the DUAL-EM horizontal co-planar results from trips 1, 2, 3, 5, and 6 along line 100. This data is recorded using a 4 metre coil separation. There is also a composite plot of the EM31 data along line 100 from trip 2. This EM31 plot is intended to be used as a reference to compare techniques.

In summary, the DUAL-EM data all seems to be achieving apparent conductivities which are comparable to the EM31 results as expected. The trends shown in the DUAL-EM trip 1 and 2 data appear to closely match the EM31 data trends which is also good for reliability. The issues revolve around the data from trips 3, 5, and 6 which tend to have extreme variability and spikes along the length of the lines. This is also combined with a more random trend which does not appear to match with either the earlier DUAL-EM data or the EM31 data.

5.2.3 The use of DUAL-EM as a stand alone method

The DUAL-EM device is a highly valued part of this research and the potential for this device to be used in future work on shallow groundwater is very high. There are however major issues that need to be addressed before the device can be applied to any shallow groundwater project with confidence. The results were at times so random, unpredictable, and dissimilar to the EM31 that the DUAL-EM data became unusable and this is a real problem for Environment Southland. There were however times when the DUAL-EM data looked to be accurate and worked well alongside the EM31. The issue really was consistency with the device and the data it produced.

The DUAL-EM device worked brilliantly along some of the lines and provided great data that correlated perfectly with the EM31. Figure 5.51 shows the DUAL-EM data following the EM31 data perfectly and correlating well with the GPR radargram. Figure 5.48 also shows the DUAL-EM parallel and perpendicular data correlating well with the EM31 and GPR. The DUAL-EM device undoubtedly has the ability to identify the high and low conductivity areas around preferential flow paths or subsurface lithological changes, and even potentially to accurately identify small changes in conductivity within a shallow groundwater system.

There are however many examples throughout this research of the DUAL-EM returning unsatisfactory results. An issue that kept appearing throughout multiple surveys was the DUAL-EM data containing large positive and negative spikes (shown in Figure 5.22 by the green line). This led to having to average the DUAL-EM data along the line in an effort to show the trends within the data (shown in Figure 5.46 by the red line). This issue still often provided usable data and the data would often match the trends within the EM31 data which allowed it to be used to make interpretations. The main issues are that the spikes within the data mean that the results have to be treated with caution. The cause of this issue is unknown; however low battery levels could be a contributing factor.

Possibly the largest issue with the DUAL-EM data revolved around the device returning negative values and values that did not match the trends of the other devices. Figures 5.14, 5.15, 5.16, and 5.17 all show dramatic variation in the data with negative spikes and data trends that directly conflict with each other. The examples shown create many issues with reliability within the DUAL-EM data as a whole.

To summarise the experience of working with the DUAL-EM, it is apparent that the device has enormous potential, however the issues around reliability and consistency within the results mean that currently the DUAL-EM is not fit for shallow groundwater geophysics. Groundwater geophysics relies on consistent sampling to detect very slight

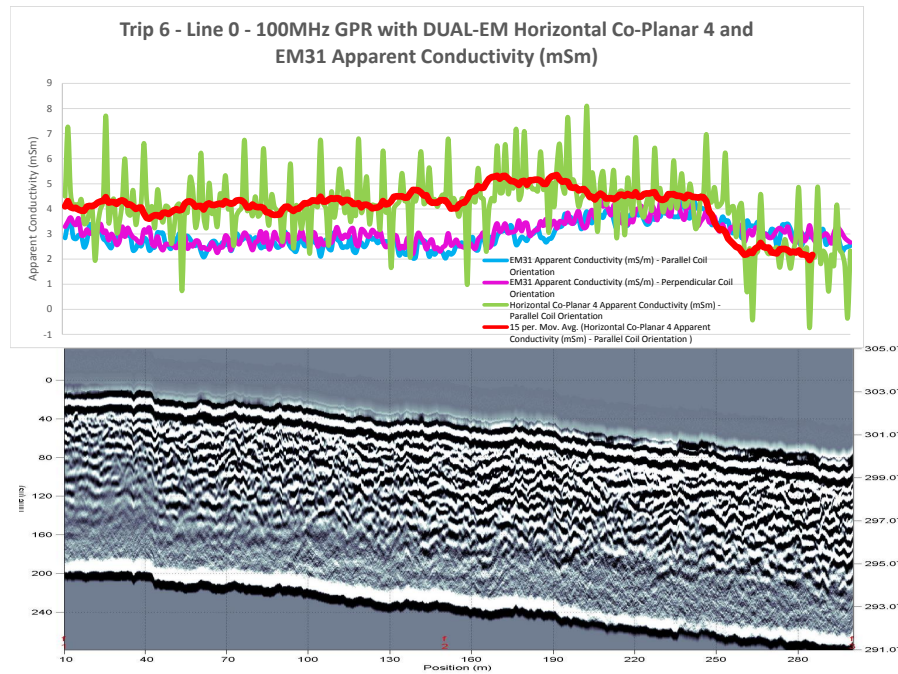


FIGURE 5.22: 100MHz radargram along line 0 from trip 6. This is then overlain with the line 50 EM31 and DUAL-EM data from trip 6.

changes within a system and currently, the DUAL-EM cannot provide that. The DUAL-EM does appear however to be calibrated correctly because there are multiple examples throughout this research of the device working brilliantly. The issues may revolve around set up of the device, operation, or data processing. The chance of a data processing error during this project is very low due to the same simple technique being used in both the EM31 and DUAL-EM data processing. The fact that the EM31 data is so consistent and exact and yet the DUAL-EM is so unpredictable implies that processing of the data was not the issue in this case.

Once Environment Southlands DUAL-EM device is working consistently it would be fit as a stand alone method to at least identify preferential flow paths. Whether the DUAL-EM technology can detect shallow groundwater contamination would depend upon many factors as in the case of this research. The best application of the DUAL-EM device may be as a tool to identify the changes in conductivity which could potentially correlate to the preferential flow paths of the shallow groundwater. This could then be combined with highly targeted water sampling to gain a good understanding of contaminant flow.

5.3 GPR Results

5.3.1 GPR Base Level Initial Results

The first two trips to the field site in Southland involved use of both the 100 MHz and 200 MHz ground penetrating radar systems. These trips were intended to record the base level readings for the area prior to any interference from wintering cattle.

The first research trip involved the use of both the 100 MHz and 200 MHz GPR systems. The second trip only used the 100 MHz GPR system because there was no evidence that the 200 MHz was providing anything extra to the survey and an effort to speed up the surveying was needed. The systems were run along the five major survey lines in an effort to identify the possible preferential flow paths beneath the research site.

Line 0 begins with about 60 metres of relatively poor radar penetration depth using both the 100 MHz and 200 MHz antennas (See Figures 5.24 and 5.23 on pages 75 and 74). When viewing the 100 MHz radargrams from both the first and second trip it is obvious that the radar waves appear to have struggled to gain depth past 4 metres (Figures 5.24 and 75). This suggests that the signal is being attenuated by a conductive medium, most likely fine grained sediments which are also impeding water percolation and drainage.

The depth of exploration (DOE) also drops from about 6 - 7 metres between the 70 metre and 165 metre positions to 3 - 4 metres between the 165 metre and 245 metre marks (shown in Figure 5.25 on page 76). The 200 MHz GPR also recorded this drop in DOE between 165 and 245 metres very clearly (Shown in Figure 5.23 on page 74). The penetration between the 250 metre mark and the end at 300 metres is again quite deep at around the 6 - 7 metre mark (Shown in Figure 5.25 on page 76).

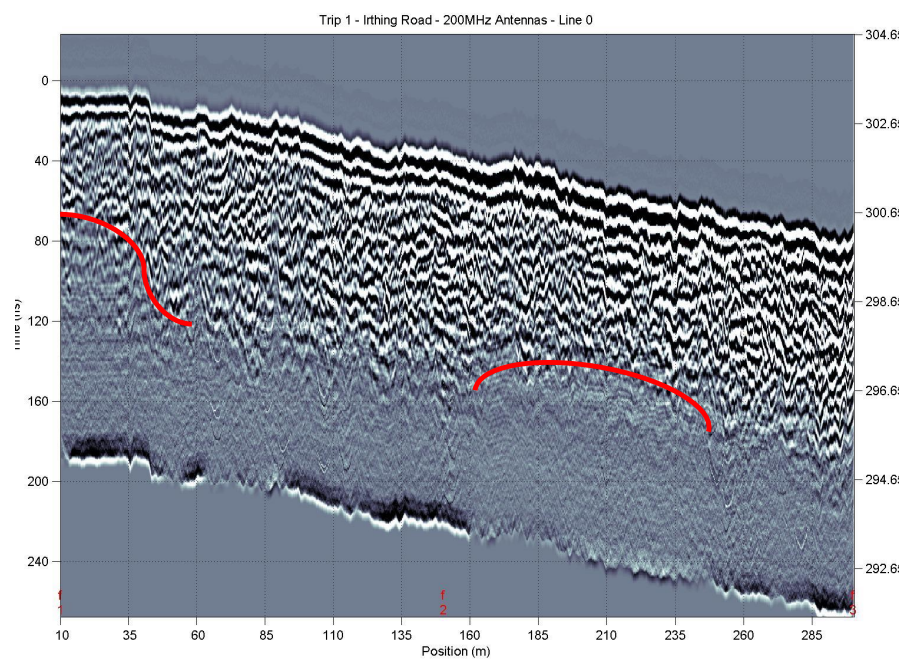


FIGURE 5.23: Radargram showing the 200 MHz results from Trip 1, Line 0.

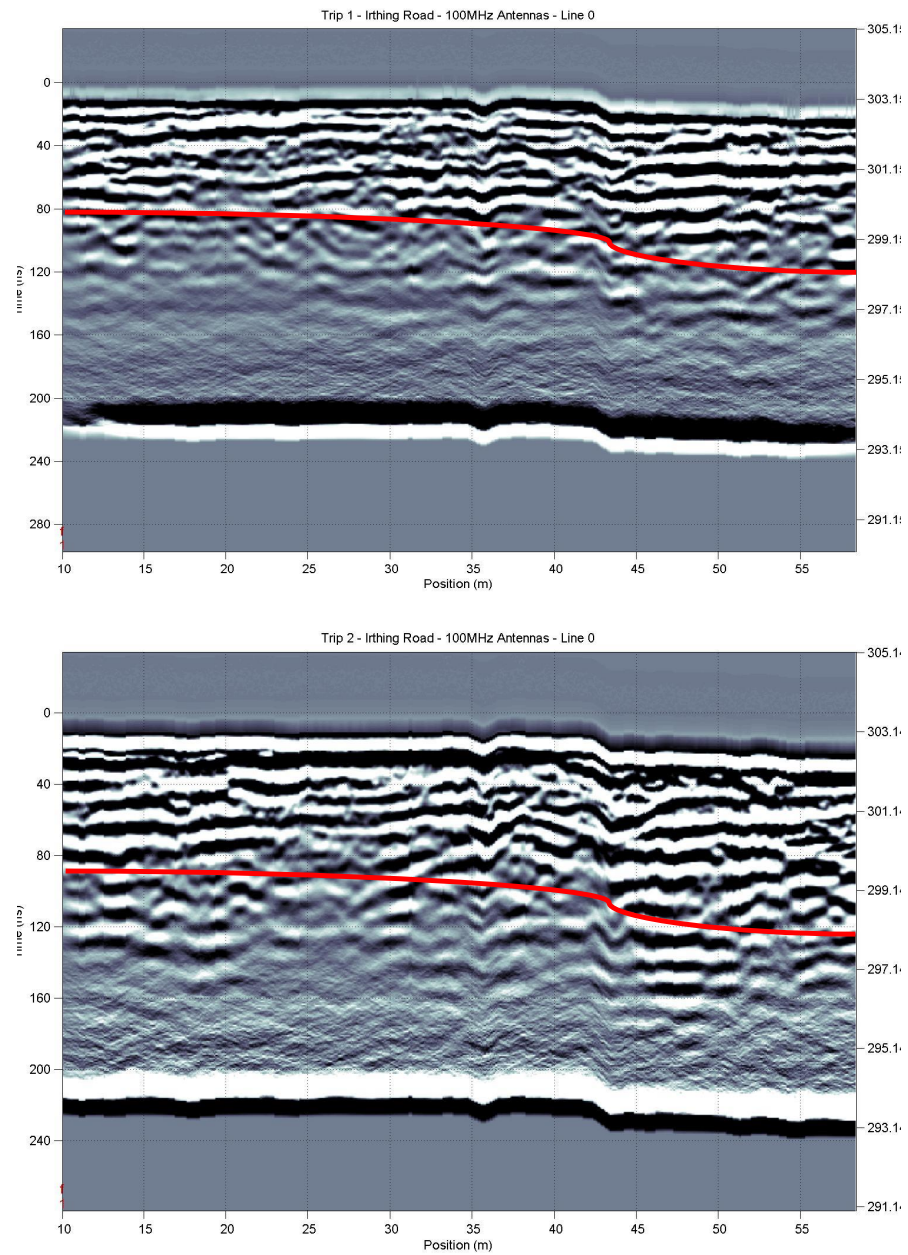


FIGURE 5.24: Comparison of 100 MHz GPR radargrams from trip 1 and 2 along line 0 between the 10 metre and 60 metre marks.

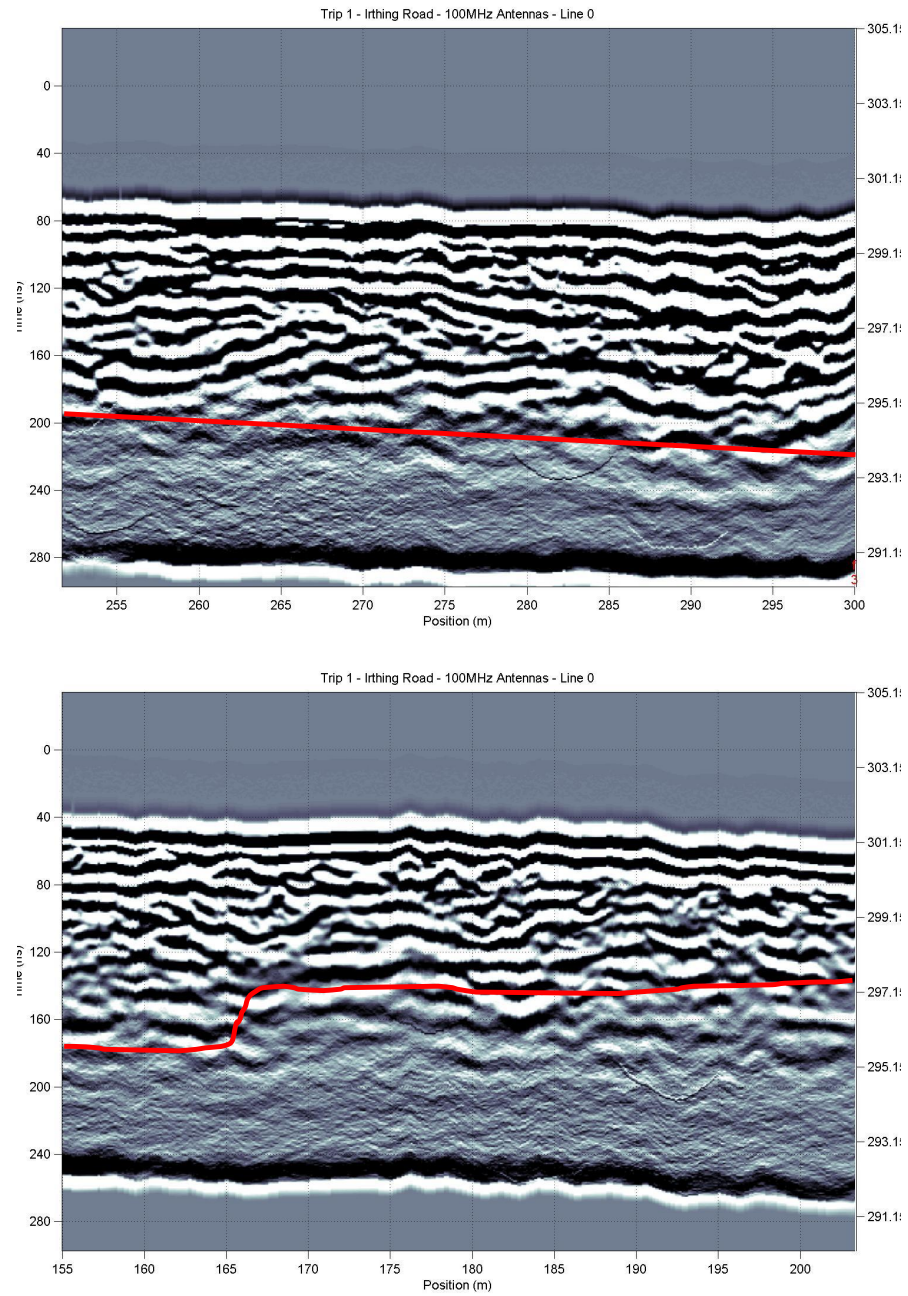


FIGURE 5.25: 100MHz radargram from trip 1 showing the difference in DOE between the 165 - 245 metre mark and the 250 - 300 metre mark.

Line 25 differs from line 0 by a large amount considering the relatively small distance between the lines. The depths of exploration between the 10 metre and 150 metre marks are grading from extremely shallow near the 10 metre mark (DOE of below 3 metres shown in Figure 5.26 on page 78) to about 4.5 metres towards the 150 metre mark (shown in Figure 5.27 on page 79). From 150 metres onwards the DOE appears to be a relatively uniform 6+ metres. The survey results between trip 1 and 2 also appear to be very similar as shown by the comparison between radargrams in Figure 5.26.

Line 50 again shows clearly a poor DOE at the 10 metre mark with increasing penetration further along the line (shown in Figure 5.28 on page 79). The consistently poor DOE for the first 75 metres suggests a conductive medium, such as clay rich sediment infilling a historic channel, beneath the surface which is attenuating the radar waves. Figure 5.29 shows how little penetration is achieved using the 200 MHz antennas. The radargram using the 100 MHz antennas during trip 2 (Figure 5.29) also shows the lack of penetration and matches closely with the 200 MHz image to show that the techniques are effectively agreeing with one another.

Line 75 again shows the poor DOE starting at the 10 metre mark. However in Figure 5.30 the interruption of the radar waves appears to extend to the 190 metre mark. This is shown by the blurring of the reflections in the radargram. Compared to the previous lines this appears to show that the conductive medium is spread further across the survey area at this point and this is causing interruption to the DOE. This also infers that the conductive area is curving as it travels through the edge of the survey area and that it appears to be present at different depths along the survey line. The conductive material is only 3 metres below the surface near the 10 metre mark and then grades down to 4 – 5 metres depth by the time it is recorded at the 180 metre mark.

Line 100 appears to show the conductive medium split into two channels on both the 100 MHz and 200 MHz radargrams (See Figure 5.31). The first is between the 10 and 100 metre marks, this is followed by 60 metres of deeper, clearer radar signal before the reflections again blur and the DOE reduces to 4 metres between the 175 and 270 metre marks (See Figure 5.32 on page 83).

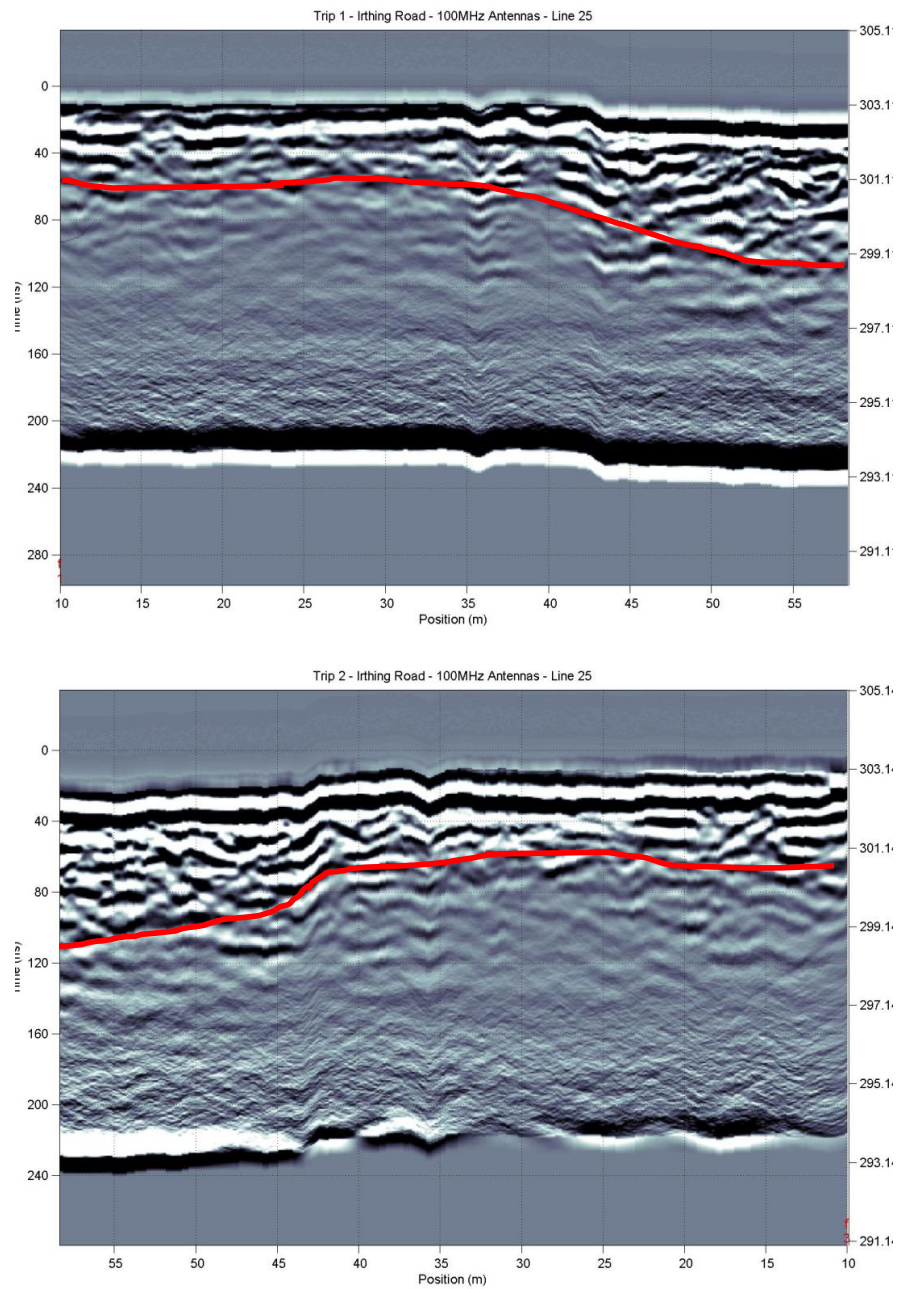


FIGURE 5.26: 100MHz radargram from trip 1 showing the difference in DOE between the 165 - 245 metre mark and the 250 - 300 metre mark.

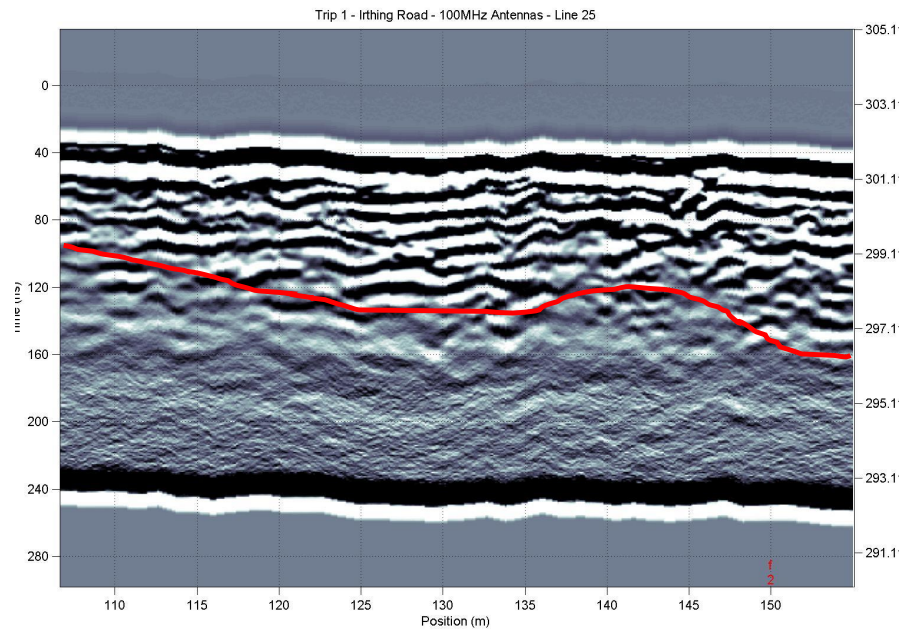


FIGURE 5.27: 100MHz radargram from trip 1 showing the point at 150 metres when the DOE appears to plateau and continue at a relatively uniform 6 metres depth.

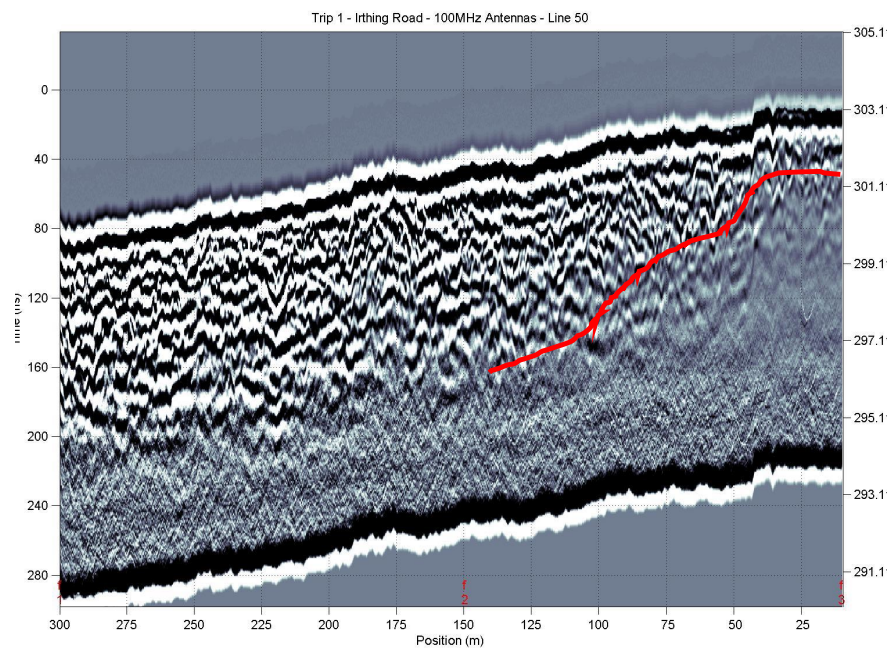


FIGURE 5.28: 100MHz radargram from trip 1 showing the increasing depth of penetration along the 50 metre line as the radar travels away from the 10 metre mark.

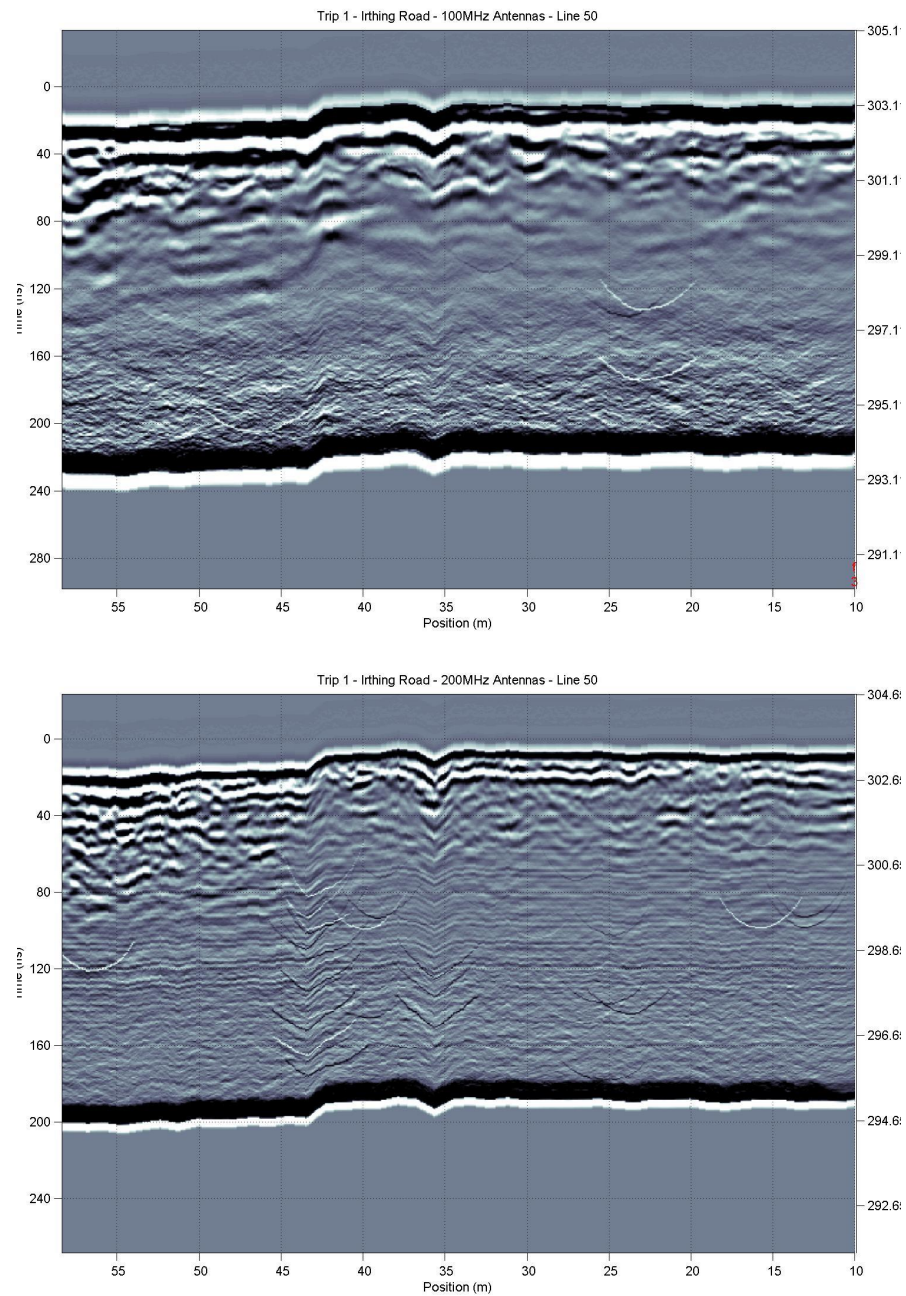


FIGURE 5.29: 100 MHz and 200 MHz radargrams from trip 1 showing the extremely poor DOE near the 10 metre mark on the 50 metre line. These two radargrams also show how well the two frequencies compare with one another.

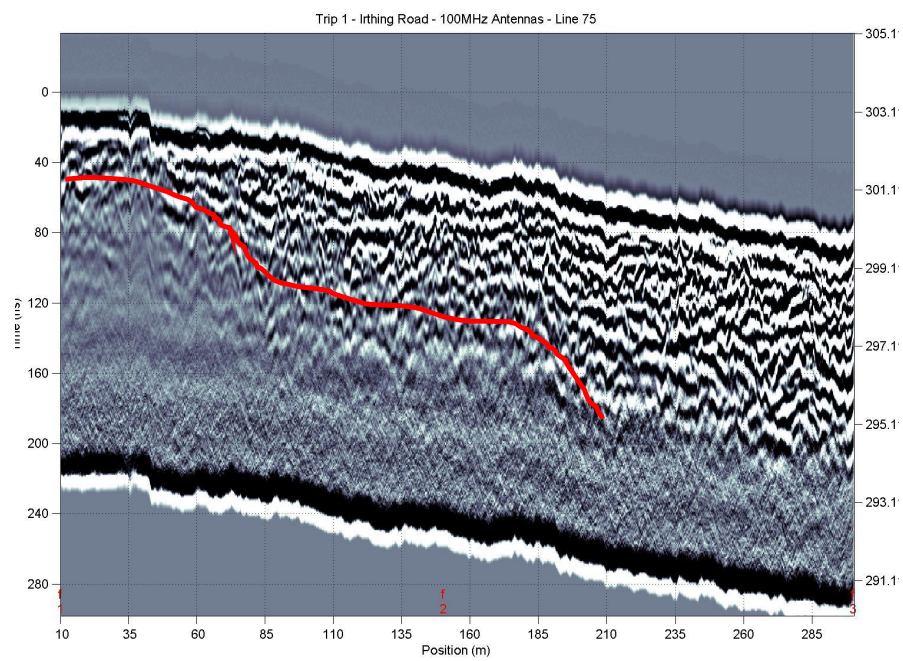


FIGURE 5.30: 100 MHz radargram from the 75 metre line showing the DOE slowly increasing from the 10 metre mark until the 190 metre mark.

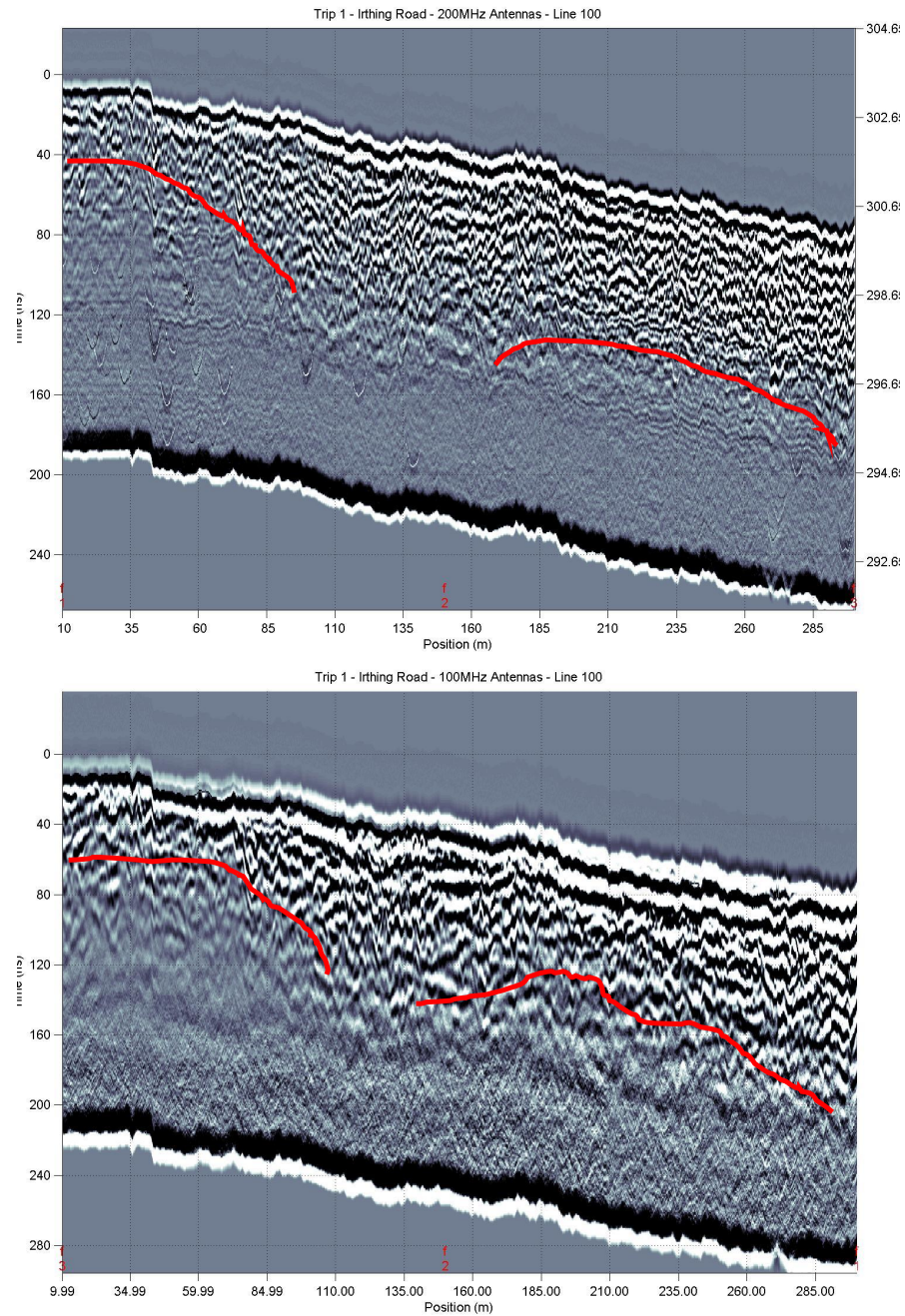


FIGURE 5.31: Comparison between the 100 MHz and 200 MHz radargrams showing the areas of lower radar penetration.

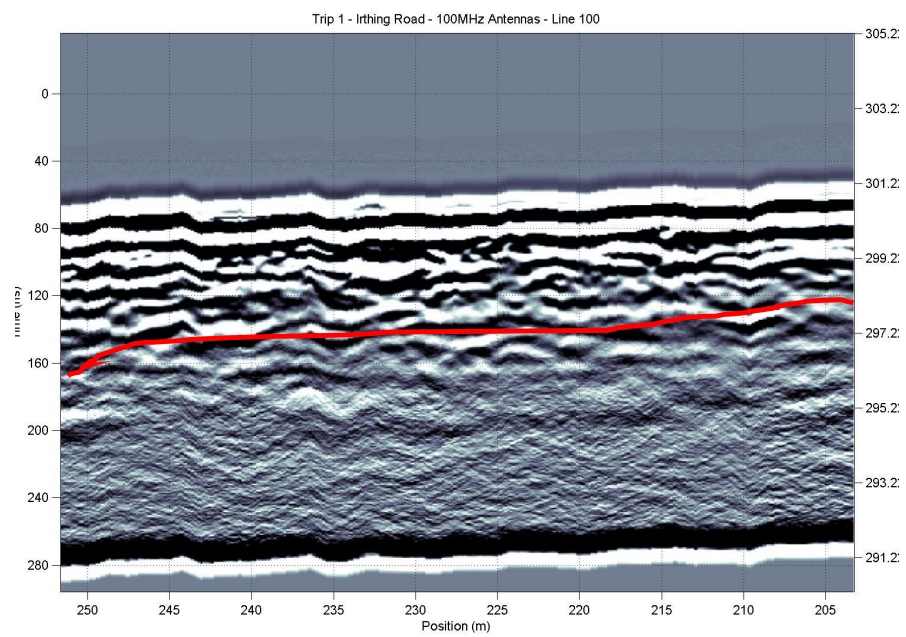


FIGURE 5.32: 100 MHz radargram showing the poor DOE towards the end of the 100 metre line.

5.3.2 GPR Temporal Changes

Temporal changes within the GPR data that was recorded at the Irthing Road field site are not to be expected unless large changes in conductivities and groundwater flow were to occur. The reason for this being that the preferential flow paths that have already been identified beneath the site using the GPR are unlikely to change noticeably in size or orientation. The GPR data however can give great data on flow path locations and be used to verify the EM data sets. The GPR data has been presented for each line and shows the entire collection of data for that line, followed by any special areas of interest.

The data for line 0 is shown by the collection of the five radargrams recorded on each of the five trips to the site (See Figure 5.33 on page 86). There appears to be two areas of interest in these radargrams. The first is the area near the beginning of the line, or the 0 metre mark. The second is at about the 200 metre mark (Identified using red lines in the radargrams). Both of these areas show a reduction in the penetration of the radar waves which suggests an area of higher conductivity. The conductive medium near to the 0 metre mark appears to be shallower, however a comparison with EM data would possibly show which area is producing a higher conductivity reading.

Figure 5.34 on page 87 shows two other radargrams that were recorded during trip three. The purpose of these was too identify whether towing the GPR with a 4WD vehicle was a viable option to increase the speed and ease of data collection. The outcome may seem surprising because the vehicle towed data appears too be just as good, if not slightly clearer and slightly deeper penetrating. This could be attributed with the slower and more steady pace that was achievable when using the low gears of the towing vehicle. From trip 3 onwards, the decision was made to use truck towed GPR because of the increase in productivity and no apparent negative impact upon data quality.

The radargrams recorded along line 25 are shown in Figure 5.35 on page 88. It is obvious from the radargrams that there appears to be a similar trend as was identified in line 0. This consists of a lower depth of penetration of the radar waves near the 0 metre mark and also around the 250 metre mark (Shown using a red line in Figure 5.35. Figure 5.36 shows a section of the line 25 radargrams. This section shows the area between 250 and 300 metres where the penetration of the radar waves appear to change over the course of 10 to 20 metres. This indicates the edge of the higher conductivity zone that was identified around the 250 metre mark (Marked using red lines in Figure 5.36).

Line 50 appears too show again an area of high conductivity around the 0 metre mark and also a possible zone at around the 250 metre mark (marked using a red line). Both of these are shown in Figure 5.37 on page 90. Figure 5.38 also shows the 0 to 50 metre

section of the radargrams in greater detail. This figure shows how much the radar is struggling to penetrate to any significant depth in this area and suggests that something in the sub surface is attenuating the radar waves. This is likely to be a layer of fine grained sediment infilling a historic channel. This, combined with large volumes of water within the near surface, would attenuate the radar waves significantly, leading to a very poor DOE.

Figure 5.39 on page 92 shows the radargrams taken along line 75. There again appears to be areas of poor penetration near the 0 metre mark and also farther along the line (marked by a red line). The variation in radar penetration is shown in Figure 5.40 by the red arrows. The arrows are all on the identical point within the radargram however the reflections shown at the bottom of the arrow differ dramatically. It appears that the first and last radargrams taken on trip 1 and 6 have the poorest penetration in this area.

Line 100 shows two large areas of poor radar penetration (identified with a red line in Figure 5.41 on page 94). The trip 1 data shows this possibly the most clearly, although the areas are obvious throughout the GPR images. These areas are highly likely to correlate with high EM readings and each area is about 100 metres across which could correlate to large historic channels.

Finally it is worth looking through at the areas of greater penetration as there are obvious buried channel features throughout the profiles. These take the shape of channel banks dipping down or in some cases a historic channel bed has been recorded. A very clear example is in Figure 5.33, where on the trip 5 radargram at the 185 metre mark there is a large downward trending reflection.

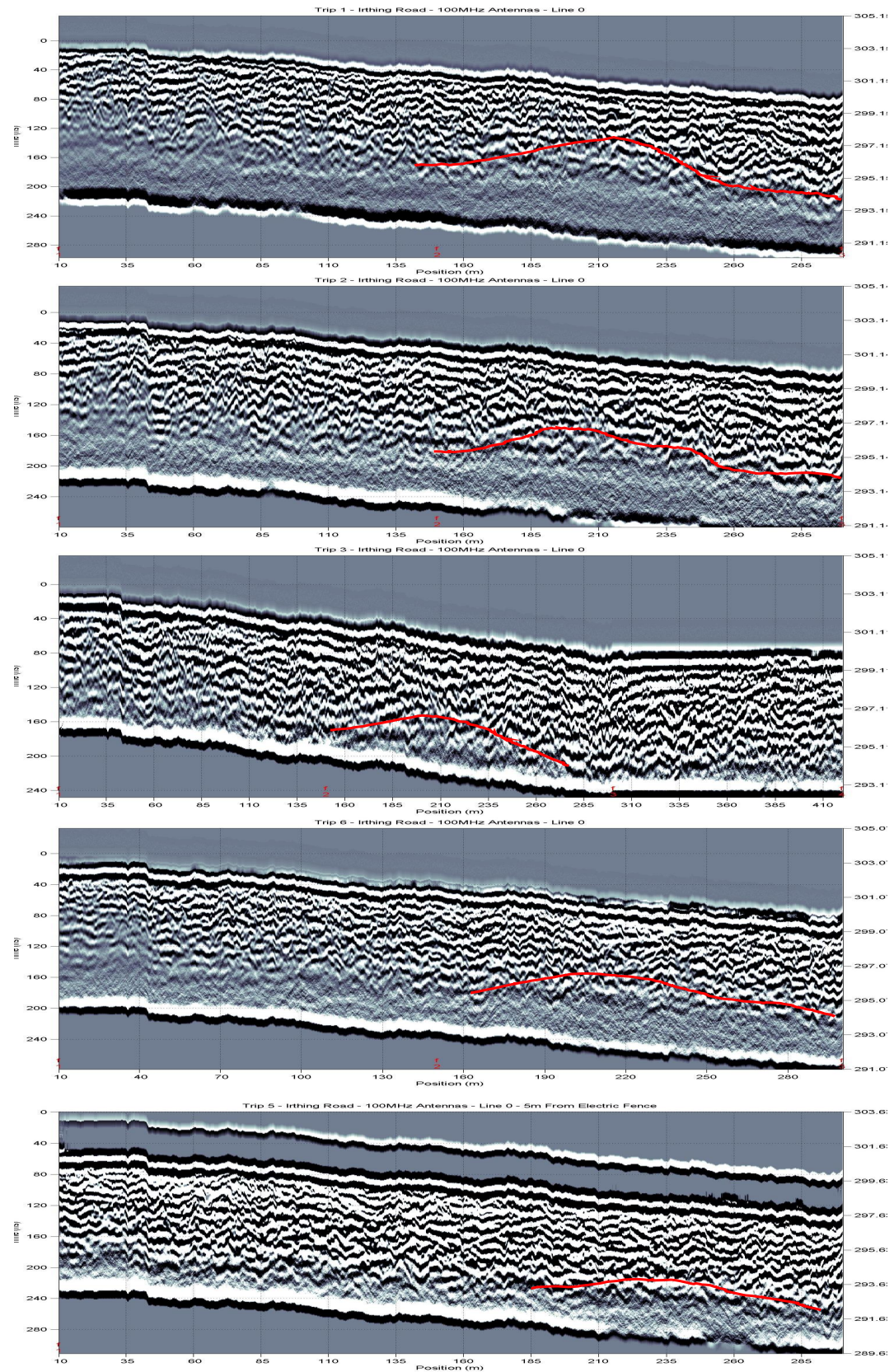


FIGURE 5.33: A collection of all of the 100 MHz radargrams that were recorded along line 0.

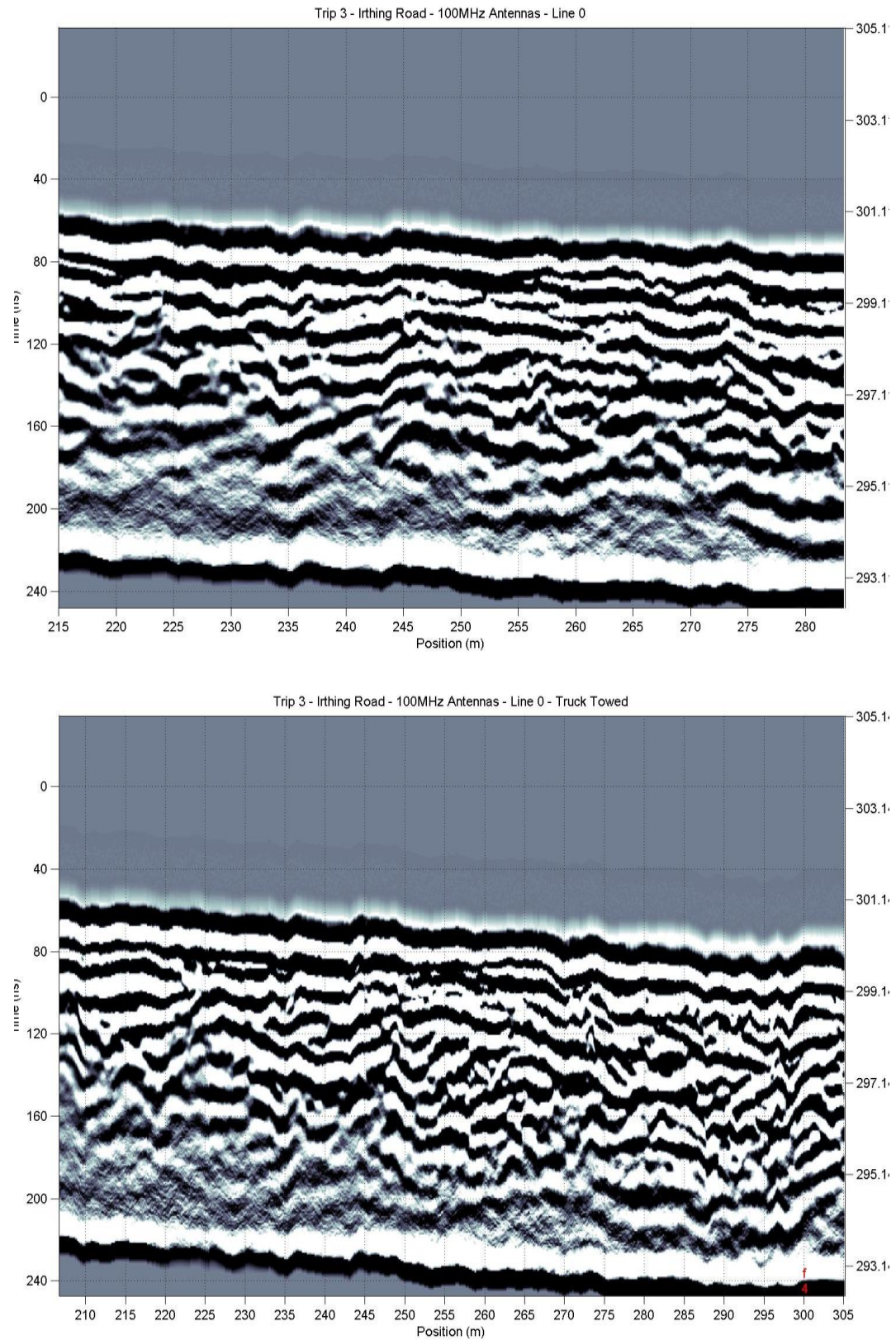


FIGURE 5.34: Comparison between two 100 MHz radargrams recorded along line 0. The first is towed by hand, the second is towed using a Toyota Hilux 4WD vehicle.

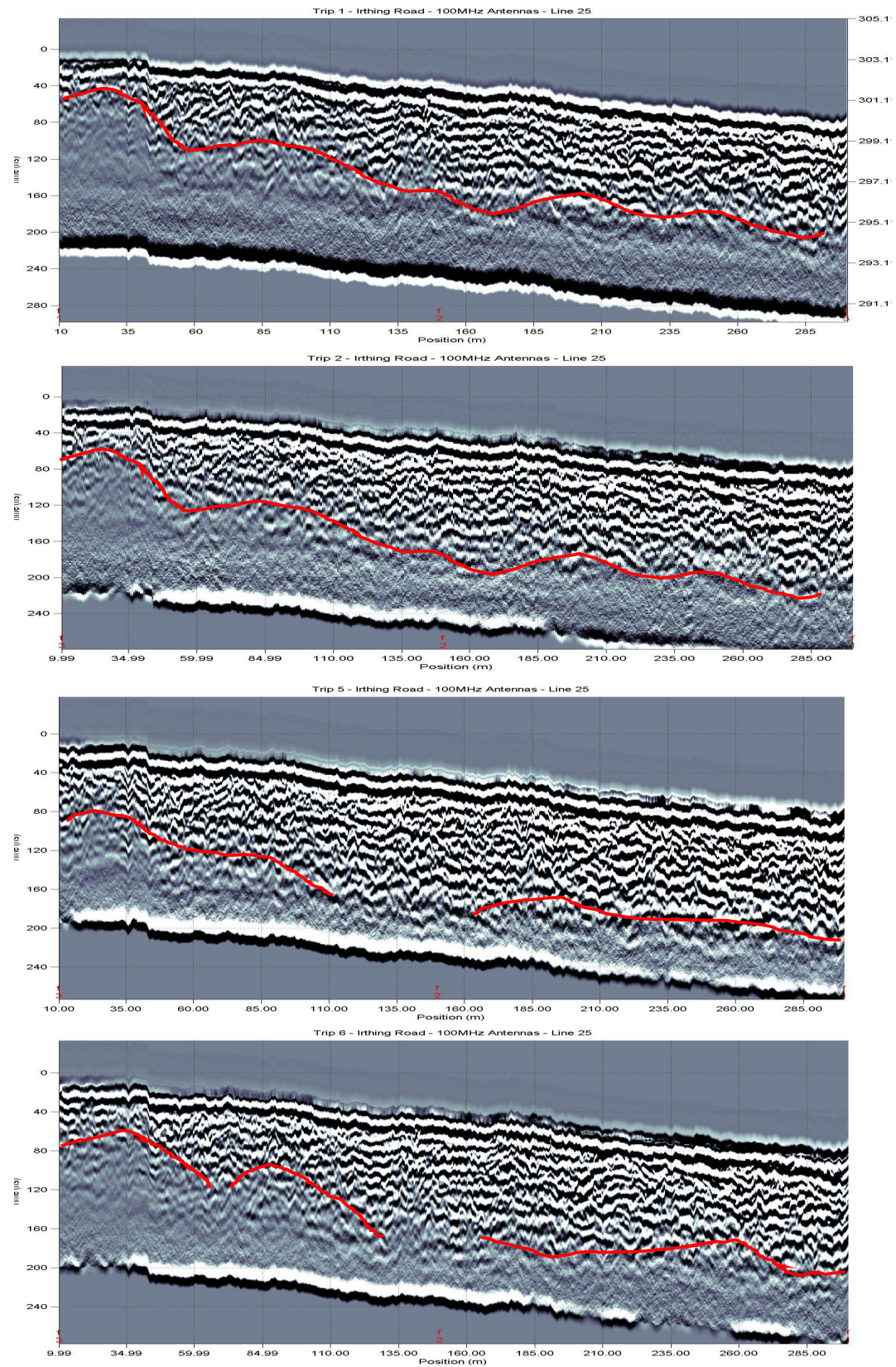


FIGURE 5.35: A collection of all of the 100 MHz radargrams that were recorded along line 25.

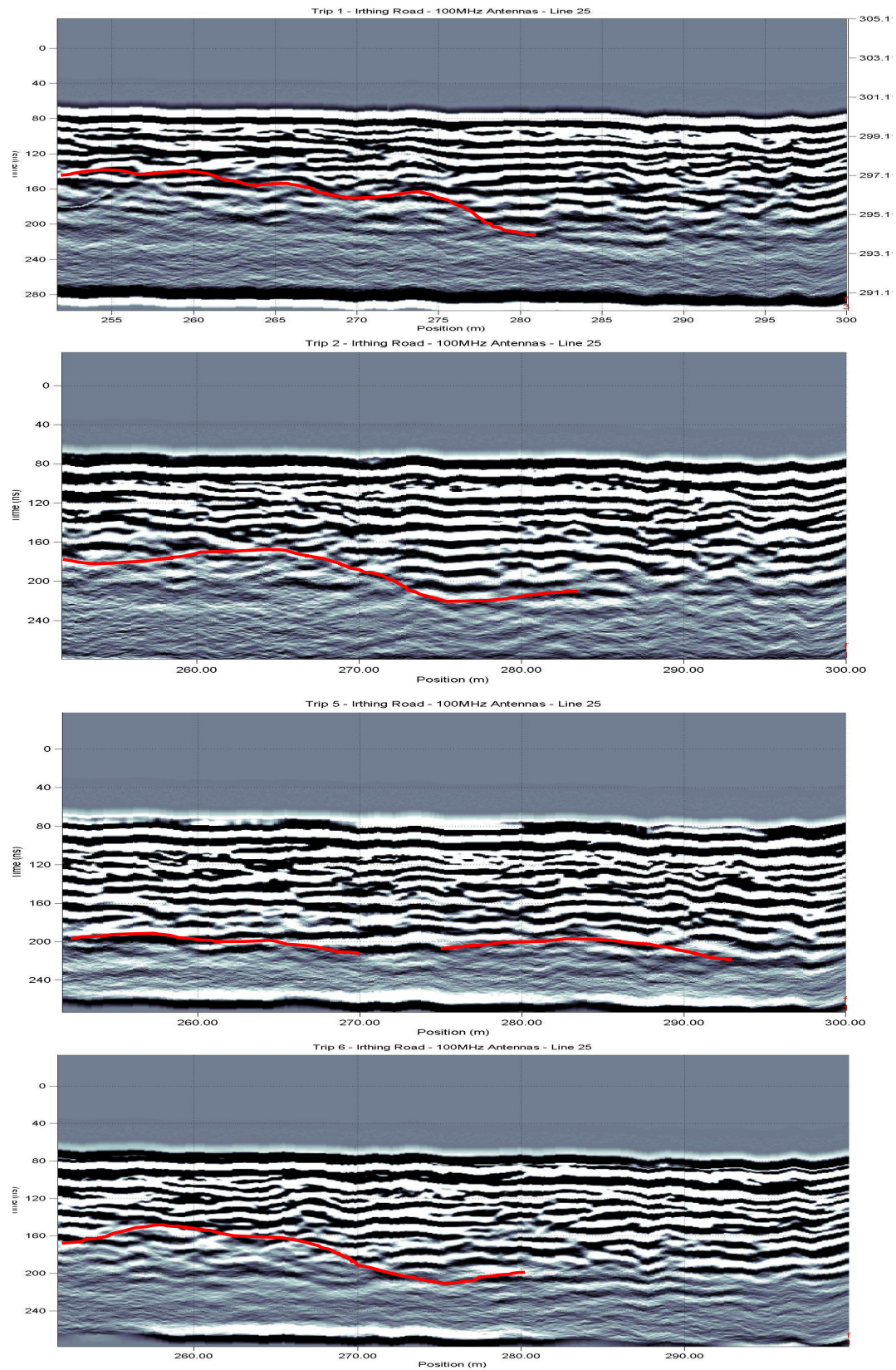


FIGURE 5.36: A collection of 100 MHz radargram sections from line 25. These sections focus on the area between 250 and 300 metres along the GPR line.

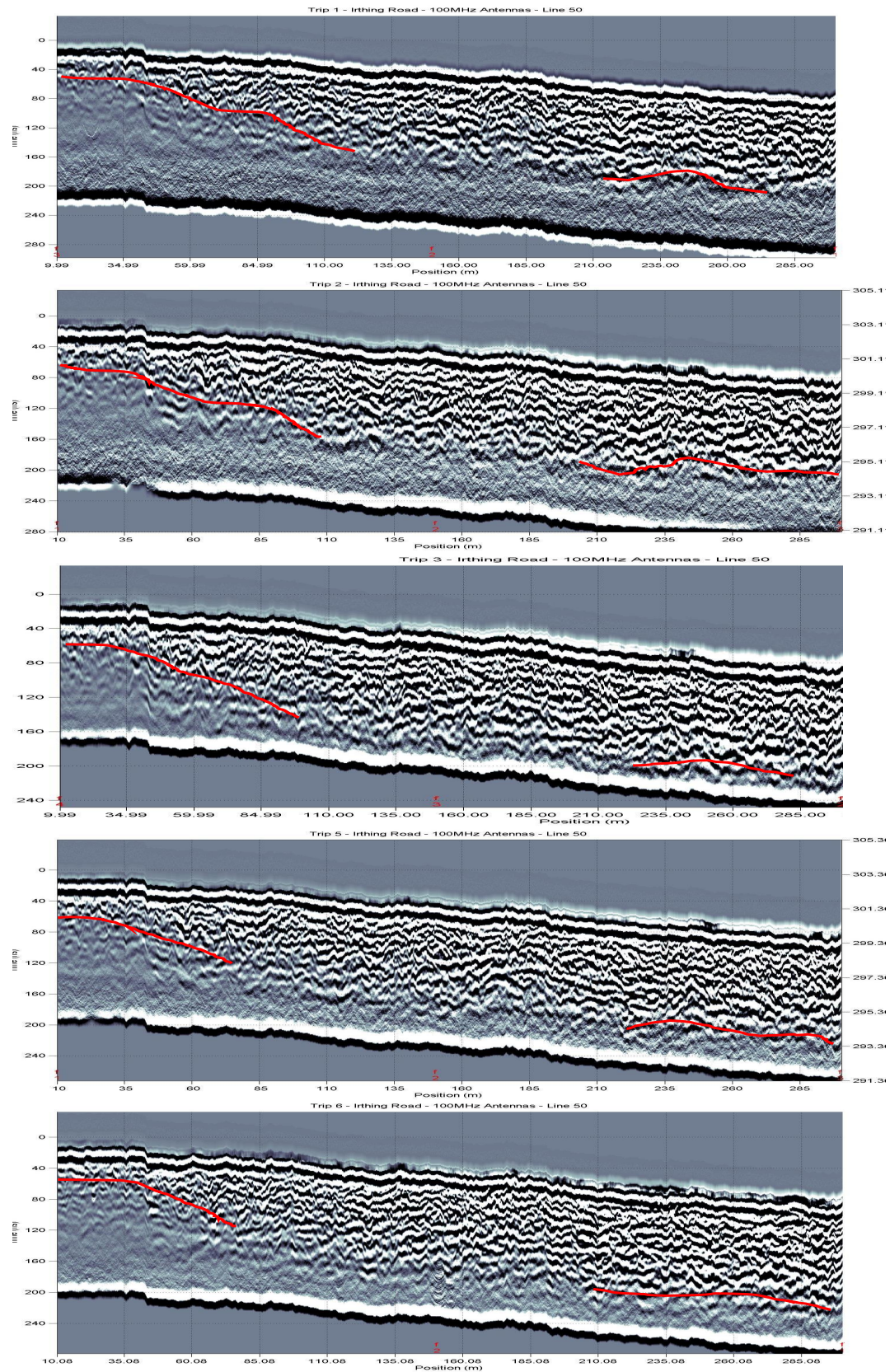


FIGURE 5.37: A collection of all of the 100 MHz radargrams that were recorded along line 50.

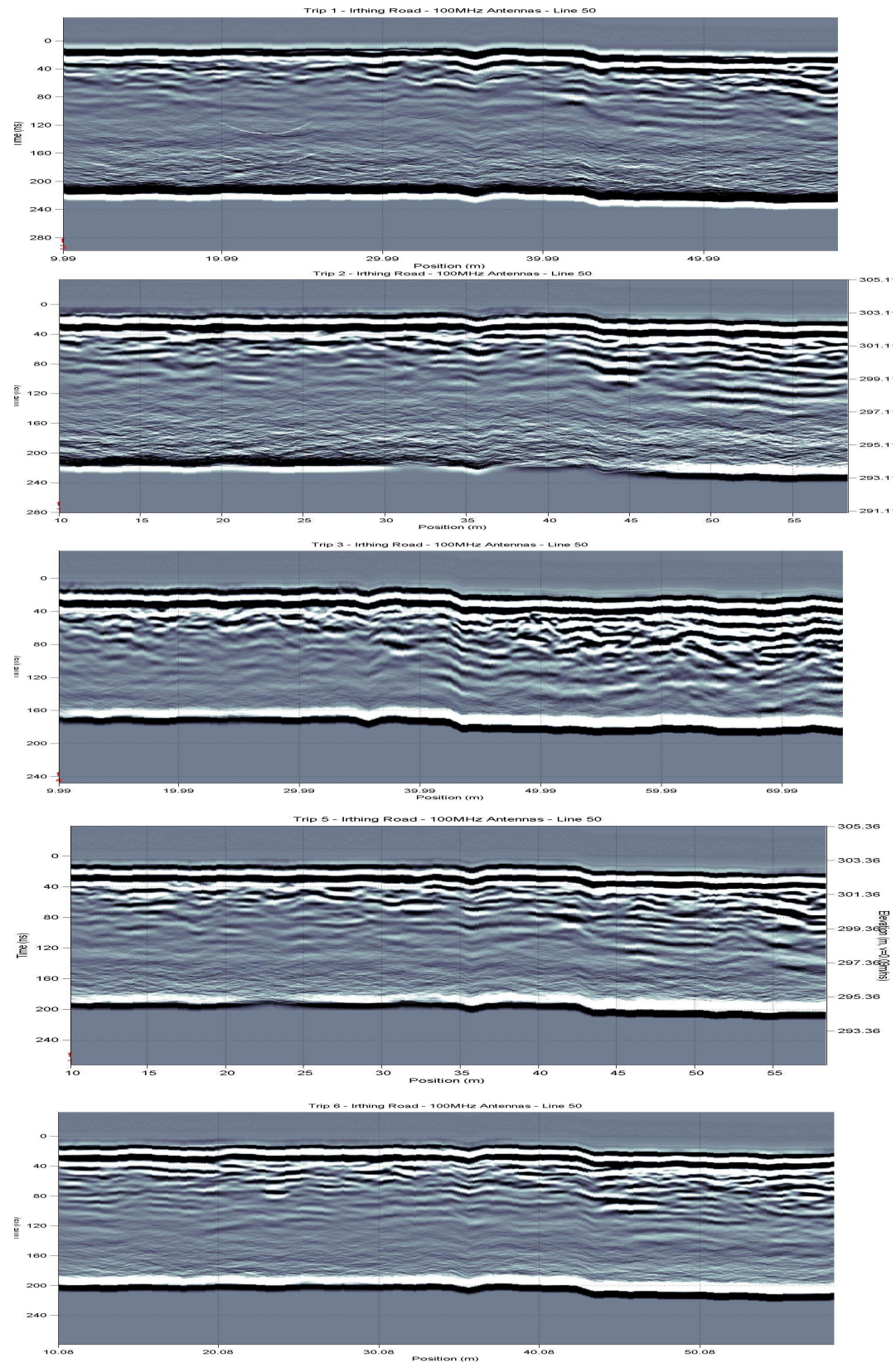


FIGURE 5.38: A collection of 100 MHz radargram sections from line 50. These sections focus on the area between 0 and 50 metres along the GPR line.

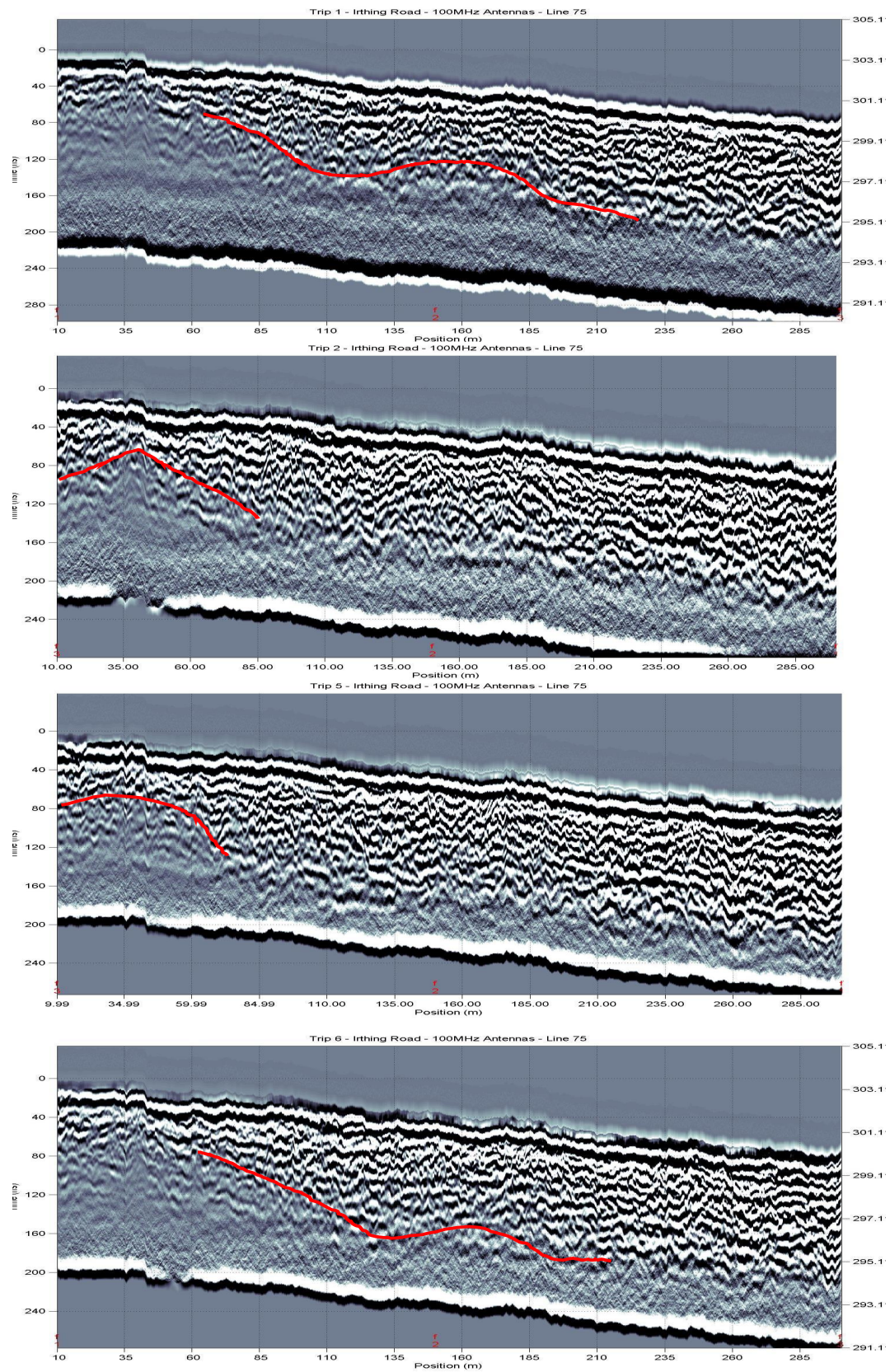


FIGURE 5.39: A collection of all of the 100 MHz radargrams that were recorded along line 75.

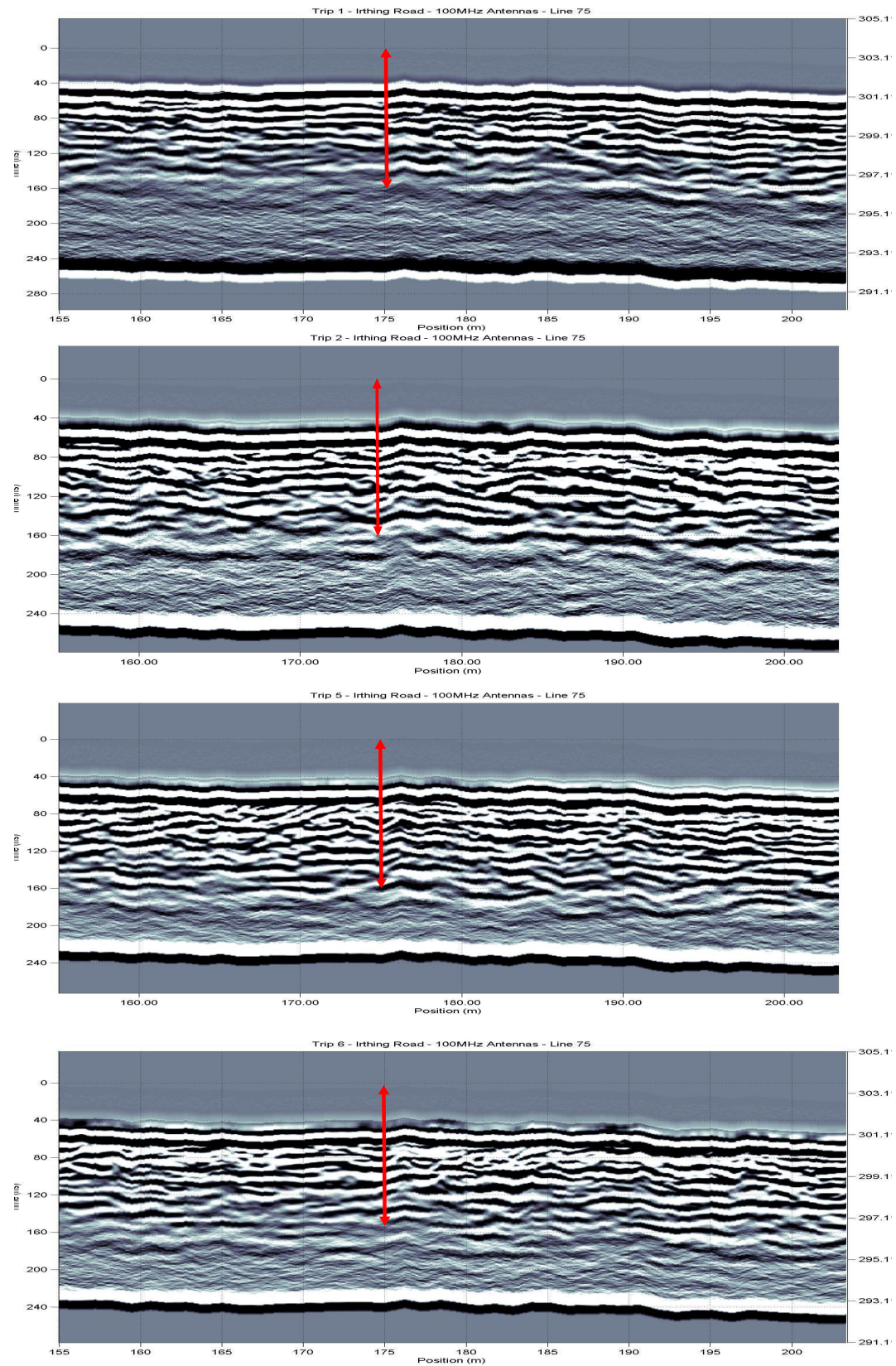


FIGURE 5.40: A collection of 100 MHz radargram sections from line 75. These sections focus on the area between 150 and 200 metres along the GPR line.

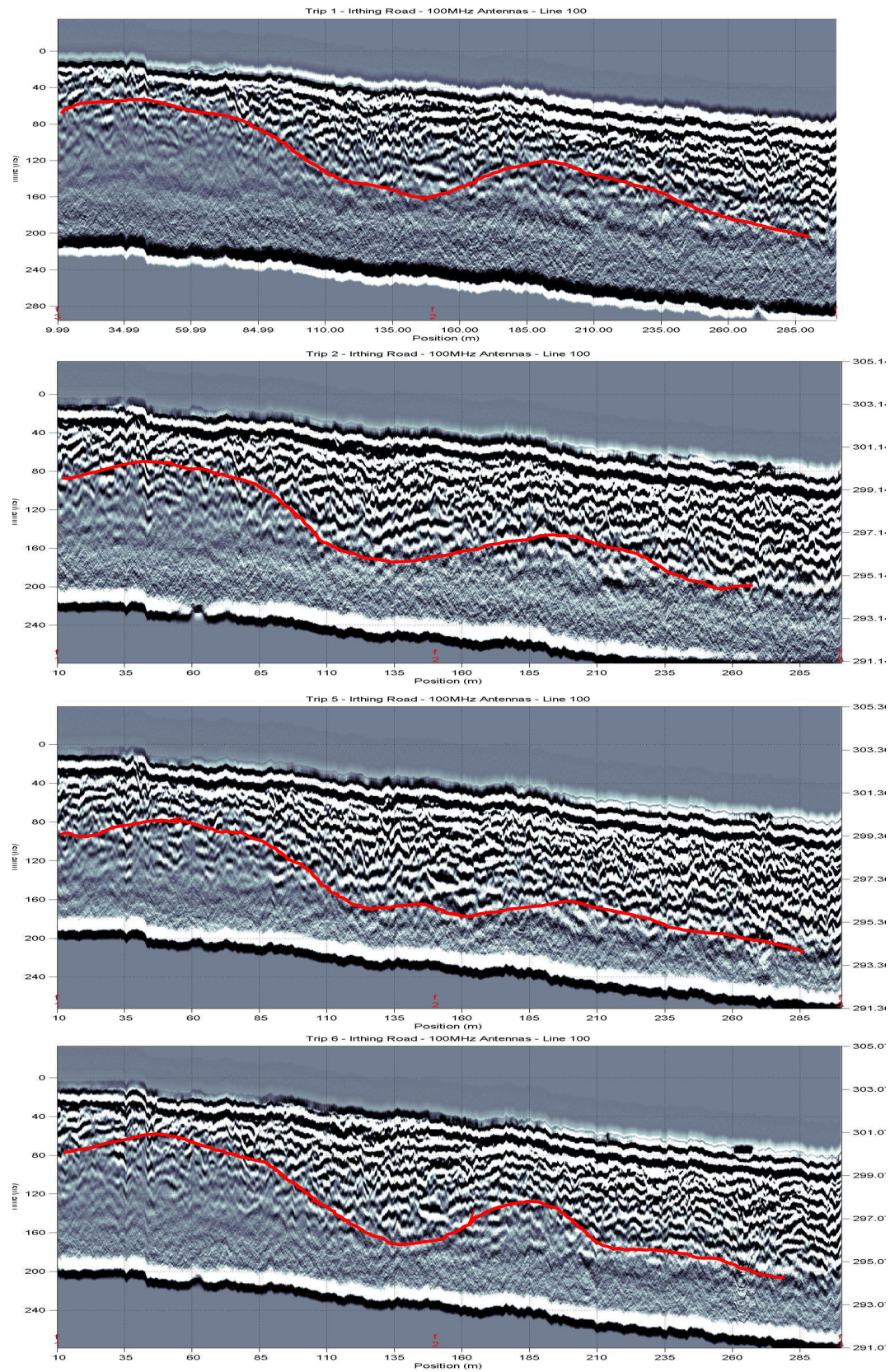


FIGURE 5.41: A collection of all of the 100 MHz radargrams that were recorded along line 100.

5.4 Groundwater Sampling

The groundwater sampling regime and its shortcomings were discussed in chapter 4; however the results do still provide some useful and relevant information. When looking through all of the water sampling results (see Appendix A.2 and A.3) it is important to note that none of the values found in the samples exceed the Ministry of Health Drinking-water Standards for New Zealand guidelines (MOH, 2008).

There are some obvious trends within the water sampling results. The values of ionic concentrations from the Southern and Northern Pits (see Appendix A.2) is on average much higher than those recorded within Irthing Stream. The ionic concentrations recorded within the creek between the cow paddock and the survey area are also higher than those recorded in Irthing Stream. This does suggest that some leachates are being recorded within the sampling, even if their concentration is quite low due to mixing with large volumes of groundwater.

The pore water samples shown in appendix A.3 indicate that on average the ionic concentration recorded within the cow paddock is higher than that of the survey area which did not contain any cattle throughout the year.

The groundwater samples do show that there are obvious differences between the ionic concentrations found within the groundwater beneath the survey area, the surface water, the pore water, and Irthing Stream. This does suggest that the leachate is having an effect upon the water around the wintering site and shows that a complete groundwater sampling survey could give great results.

5.5 Interpretations based upon all data

The amount of data collected throughout the year at the Irthing Road field site was immense. This included over 25 GPR lines, more than 60 EM31 lines and at least 30 DUAL-EM lines. In the previous sections of this chapter a lot of the data has been presented and the temporal changes, or lack thereof, between the data sets have been identified. This section however combines all of this data in an effort to make some accurate interpretations on the system behaviour and the temporal changes that occur within the system throughout the year.

5.5.1 System Temporal Changes

The major point to discuss when it comes to the temporal changes that occurred within the system is to address the cause of these changes. It is important to keep in mind the fact that the geophysics may have simply been the wrong tool for the job in this application, so more subtle changes within the system could have gone unnoticed. Following on from this point it appears that there is no conclusive evidence to suggest that the wintering dairy cattle have any effect upon the geophysical results at this field site. This does not mean that the wintering of dairy cattle on the free draining soils near Lumsden does not affect the shallow groundwater, it simply means that the techniques used in this study do not show any conclusive evidence of increased conductivities within the shallow groundwater that can be linked to farming practises. The water sampling does suggest that ionic concentrations within the groundwater and soil pore water are being affected by the leachate from the wintering cattle.

For a more in depth analysis of the very important conclusion drawn in the previous paragraph it is best to look at the data recorded during the year long study. When comparing the GPR, EM31 and DUAL-EM data from throughout the year it is easiest to use figures that include overlays of all three techniques. This allows easy comparison, both between the techniques and between the different trips throughout the year.

All of the key data recorded throughout the year along line 0 is shown in Figures 5.42, 5.43, 5.44, 5.45, and 5.46. These figures show the temporal changes throughout the year. There is a consistent tendency for the EM31 conductivities to increase as the trips went by and this is shown by an increase in the high point of the EM31 apparent conductivity readings between trip 1 and 6. This increase is between 0.5 and 1 mS/m between Figure 5.42 and Figure 5.46. The issue with this constant increase is that the cause of it cannot be identified. The increase through the year was on the scale of 10 to 20 percent so it could be seen as significant however the origin of this increase is unknown and this was only recorded along line 0.

The data collected along line 50 has been condensed into five overlays (Figures, 5.47, 5.48, 5.49, 5.50, and 5.51). The difference between the trip 1 results (Figure 5.47) and trip 2 results (Figure 5.48) raise an important point. The EM31 apparent conductivity rises by about 0.5 mS/m between these two trips. The most vital thing to remember in this case is that no cattle were in the area when these two trips were conducted. The variation could only have been caused by instrument error, user error or a natural change in the grounds conductivity. The major difference between the two trips was the weather. Trip 1, which records lower conductivities, was held in dry conditions whereas trip 2 data was recorded in heavy rain which had been happening for multiple days

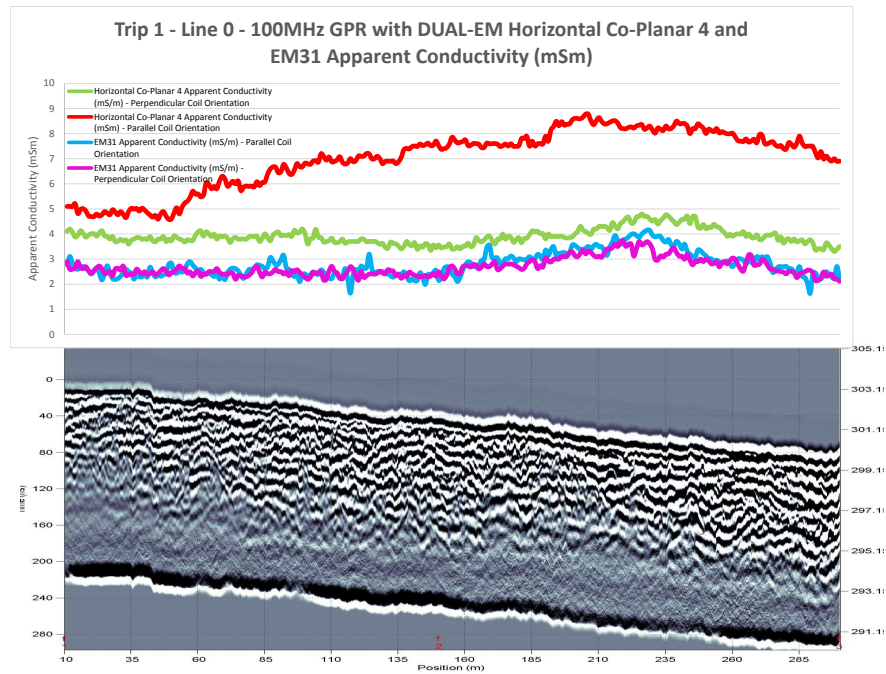


FIGURE 5.42: 100MHz radargram along line 0 from trip 1. This is then overlain with the line 0 EM31 and DUAL-EM data from trip 1.

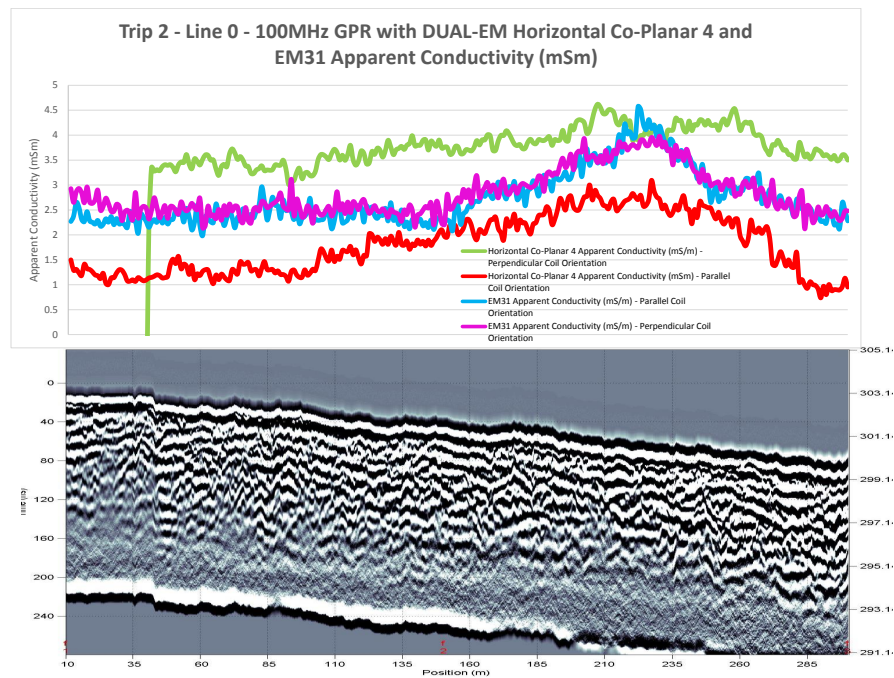


FIGURE 5.43: 100MHz radargram along line 0 from trip 2. This is then overlain with the line 0 EM31 and DUAL-EM data from trip 2.

beforehand. This suggests that there was more water beneath the site and this caused a rise in conductivities along the length of the survey line. It is also important to note that the conductivities increased slightly more at the high point near the 10 metre mark than they did along the rest of the line. This is likely to be linked too a greater increase

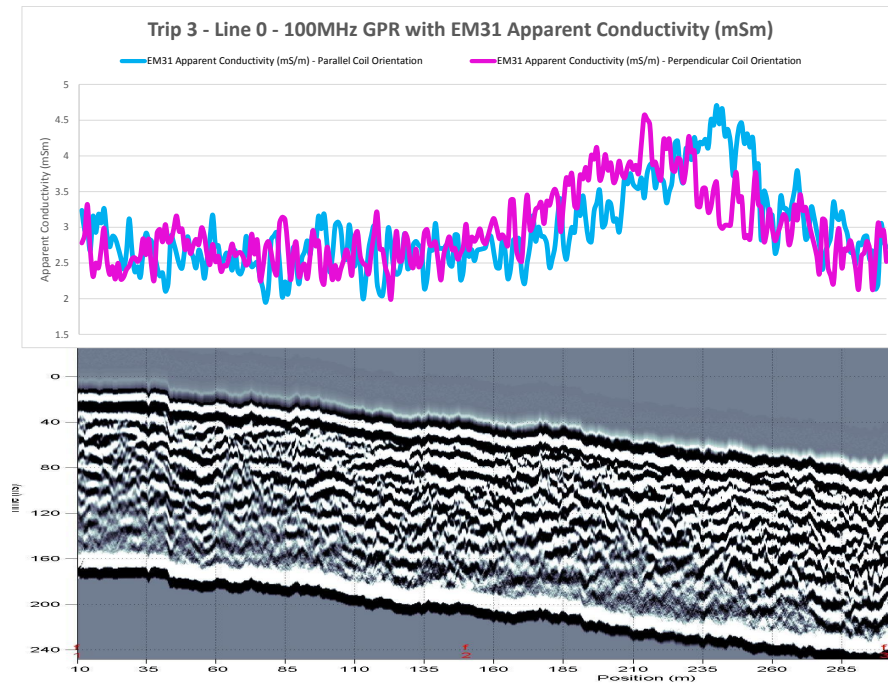


FIGURE 5.44: 100MHz radargram along line 0 from trip 3. This is then overlain with the line 0 EM31 data from trip 3.

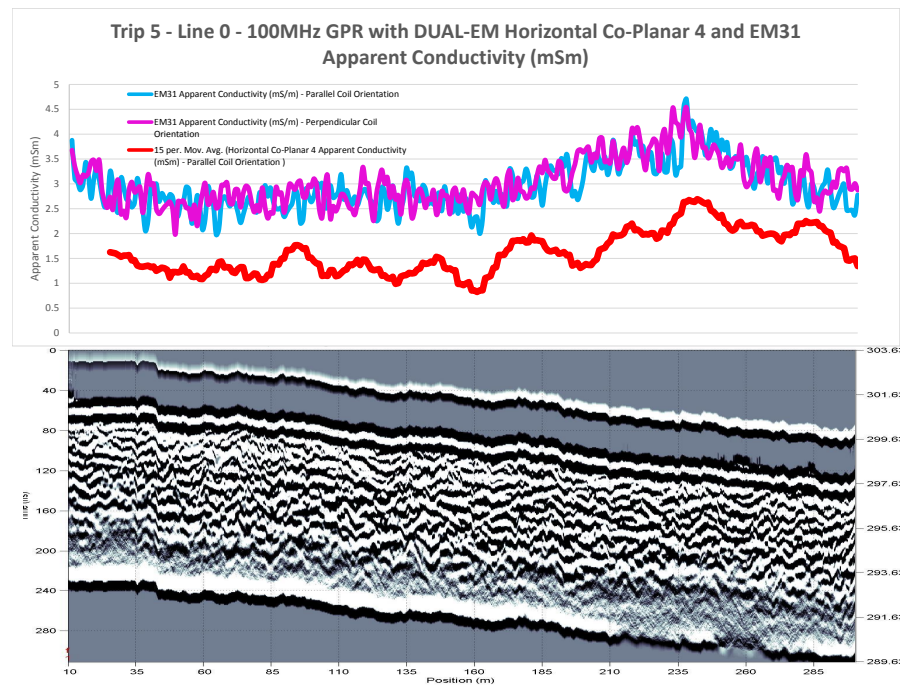


FIGURE 5.45: 100MHz radargram along line 0 from trip 5. This is then overlain with the line 0 EM31 and DUAL-EM data from trip 5.

in the volume of water which is ponding above the fine grained sediments that infill this historic channel.

The data that was collected along line 100 is shown in Figures 5.52, 5.53, 5.54, and 5.55.

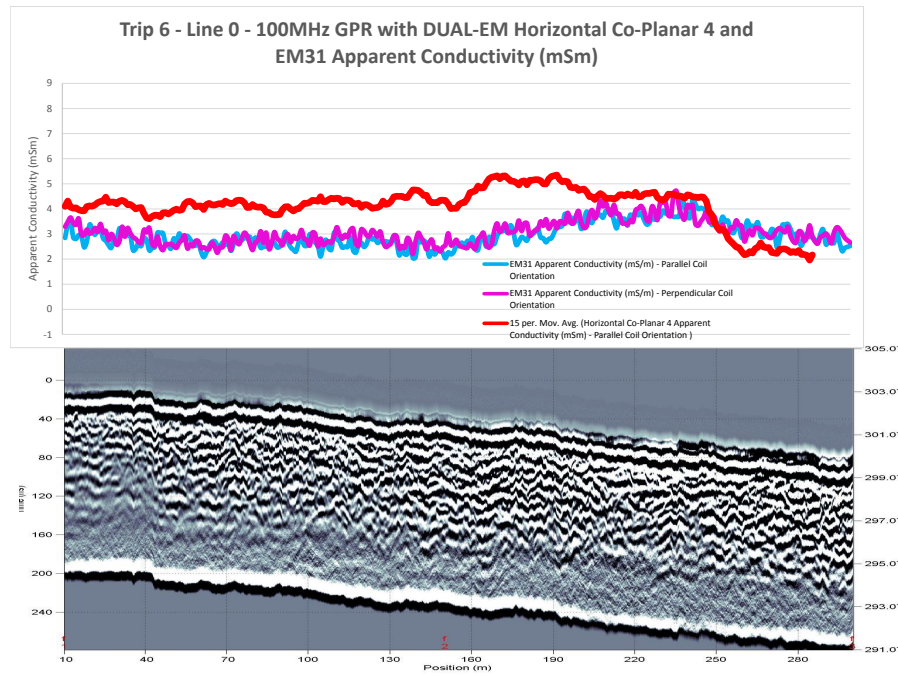


FIGURE 5.46: 100MHz radargram along line 0 from trip 6. This is then overlain with the line 0 EM31 and DUAL-EM data from trip 6.

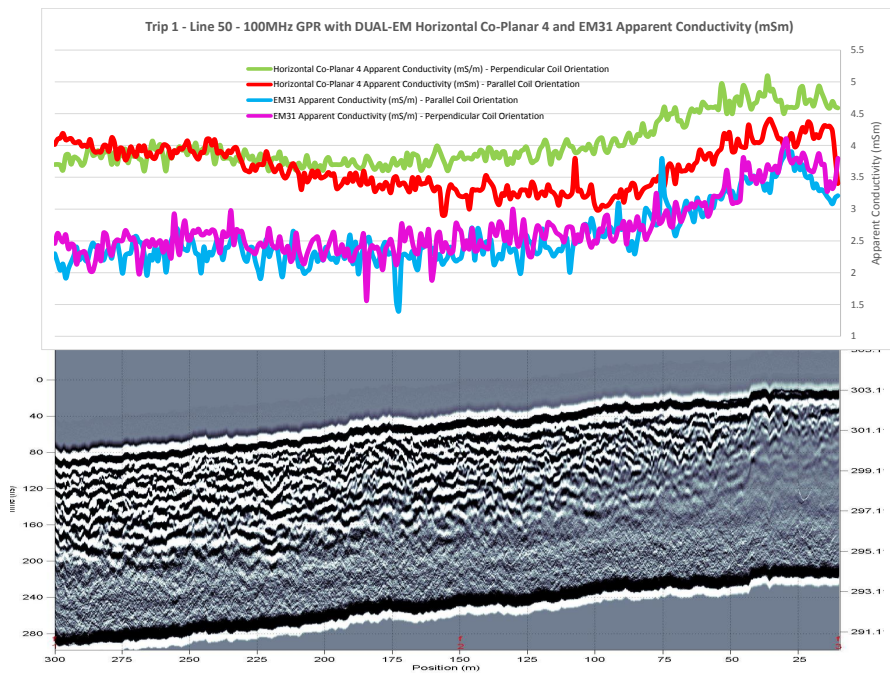


FIGURE 5.47: 100MHz radargram along line 50 from trip 1. This is then overlain with the line 50 EM31 and DUAL-EM data from trip 1.

These figures show a similar tendency as the results of line 50. There appears to be an increase in the EM31 apparent conductivity of about 0.5 mS/m across the length of line 100 between trips 1 and 2. This could potentially be as a result of the heavy rain that was experienced during trip 2.

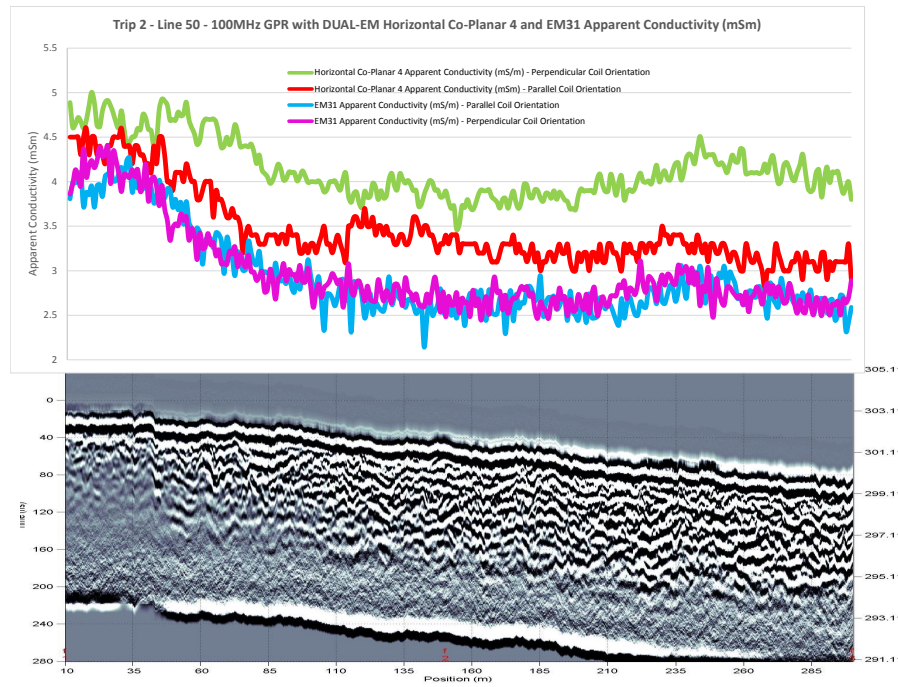


FIGURE 5.48: 100MHz radargram along line 50 from trip 2. This is then overlain with the line 50 EM31 and DUAL-EM data from trip 2.

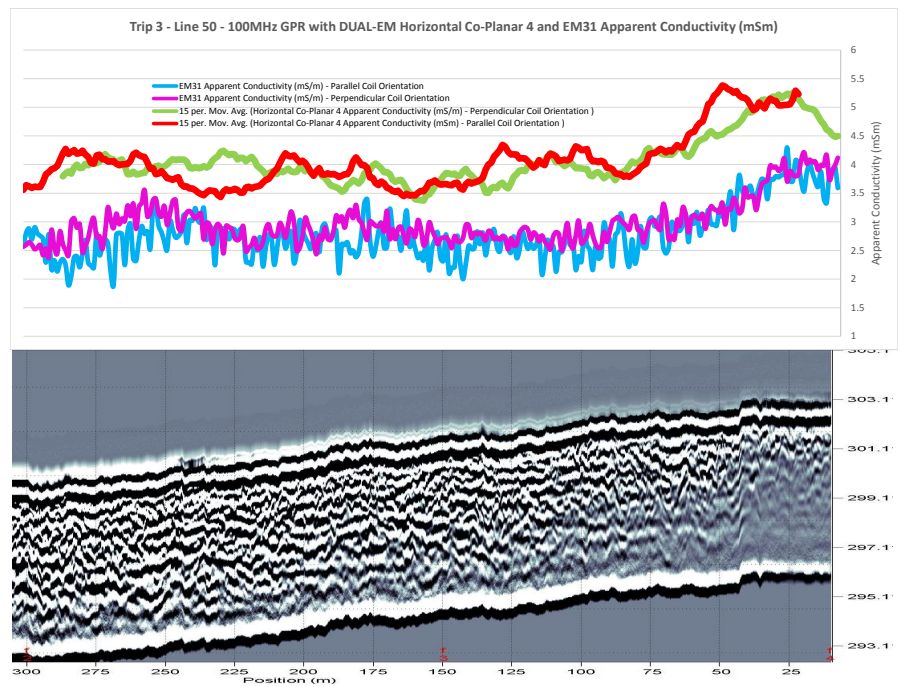


FIGURE 5.49: 100MHz radargram along line 50 from trip 3. This is then overlain with the line 50 EM31 and DUAL-EM data from trip 3.

There was also an effort made to collect data from outside of the field area to perhaps identify other patterns and changes within the system. Figures 5.56 and 5.57 show two different areas that were surveyed. The first figure is showing two examples of EM31 data and one of DUAL-EM data which was recorded within the paddock that held wintering

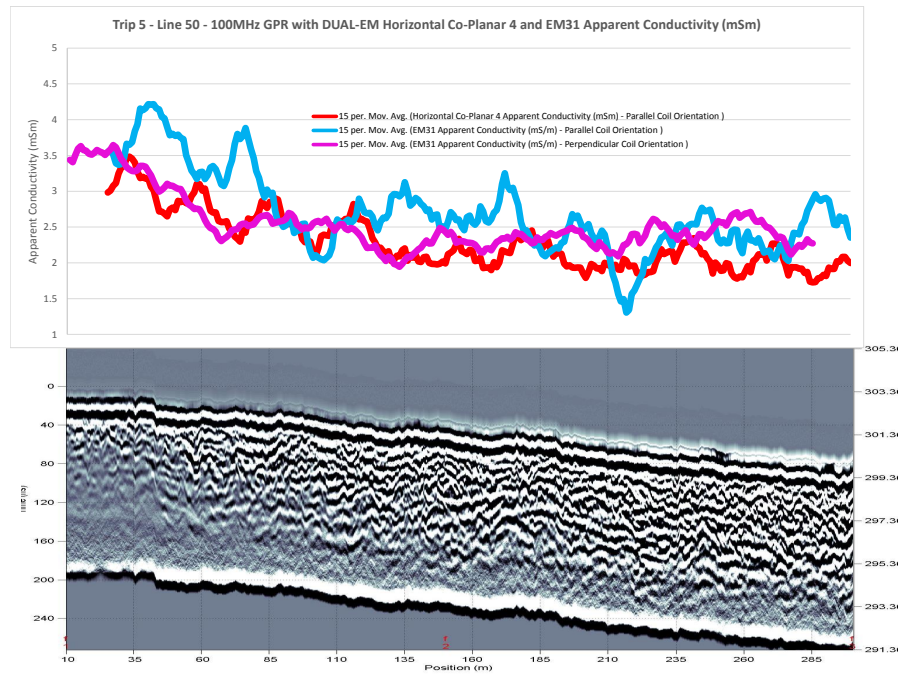


FIGURE 5.50: 100MHz radargram along line 50 from trip 5. This is then overlain with the line 50 EM31 and DUAL-EM data from trip 5.

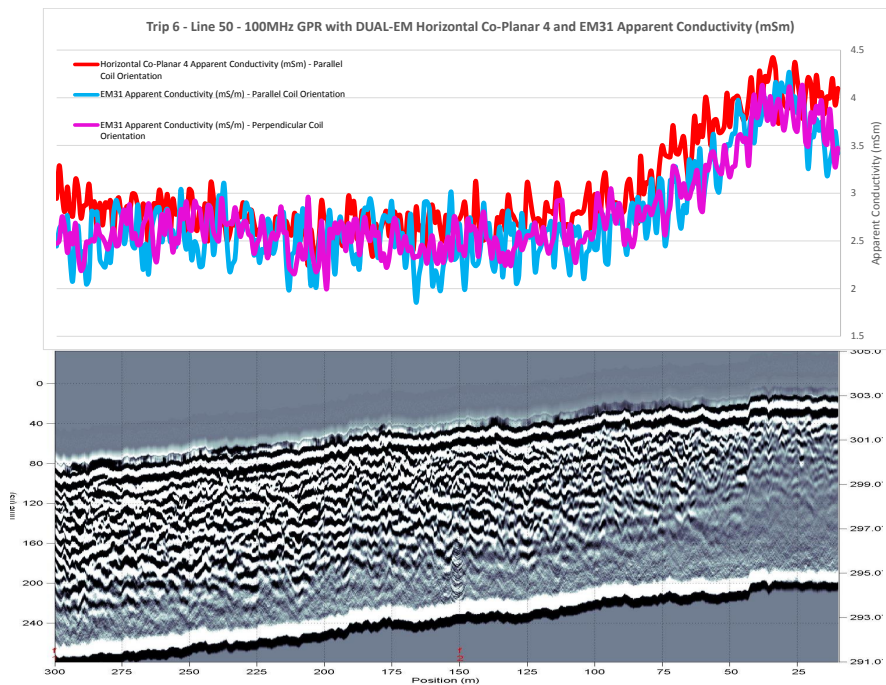


FIGURE 5.51: 100MHz radargram along line 50 from trip 6. This is then overlain with the line 50 EM31 and DUAL-EM data from trip 6.

cows. There is also reference data from line 0 on the figure as to allow a comparison of the conductivities found in and out of the paddock. The EM31 plots appear to be very similar in shape and apparent conductivity readings. There appears to be no evidence that the readings within the paddock are higher than those outside of the paddock. This

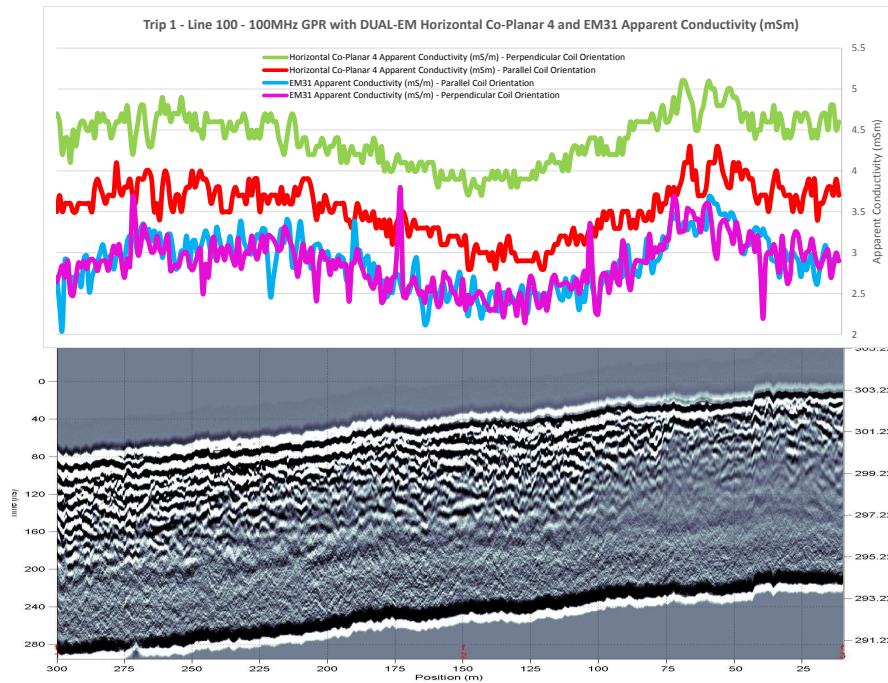


FIGURE 5.52: 100MHz radargram along line 100 from trip 1. This is then overlain with the line 100 EM31 and DUAL-EM data from trip 1.

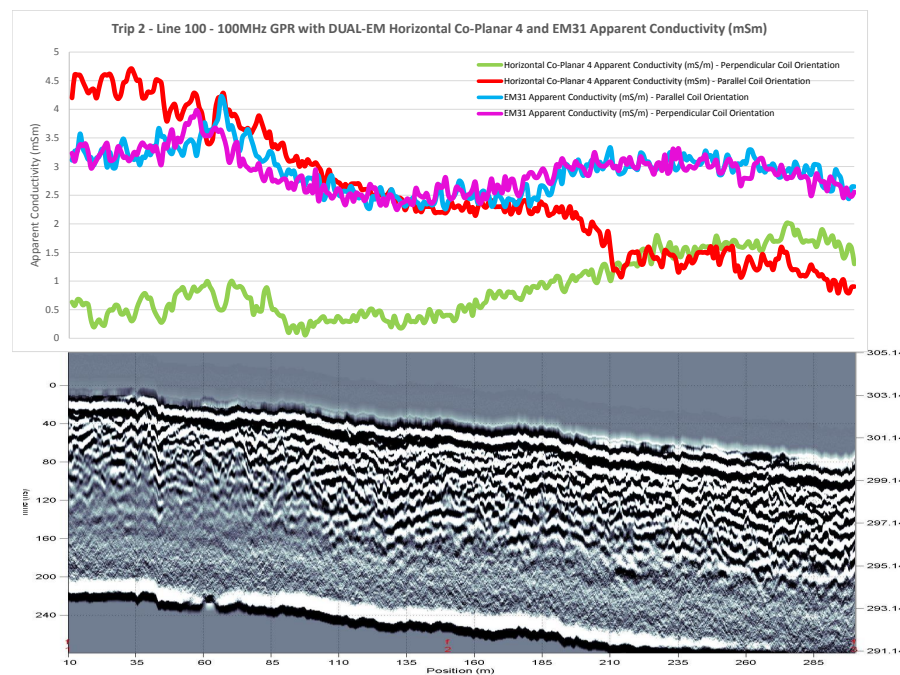


FIGURE 5.53: 100MHz radargram along line 100 from trip 2. This is then overlain with the line 100 EM31 and DUAL-EM data from trip 2.

may appear incorrect when looking at the data because the paddock on average appears to have a large section of high conductivities. It is important to remember that this area is most likely a continuation of the historic channels found beneath the survey area and that the conductivities found within this channel appear to match those that were

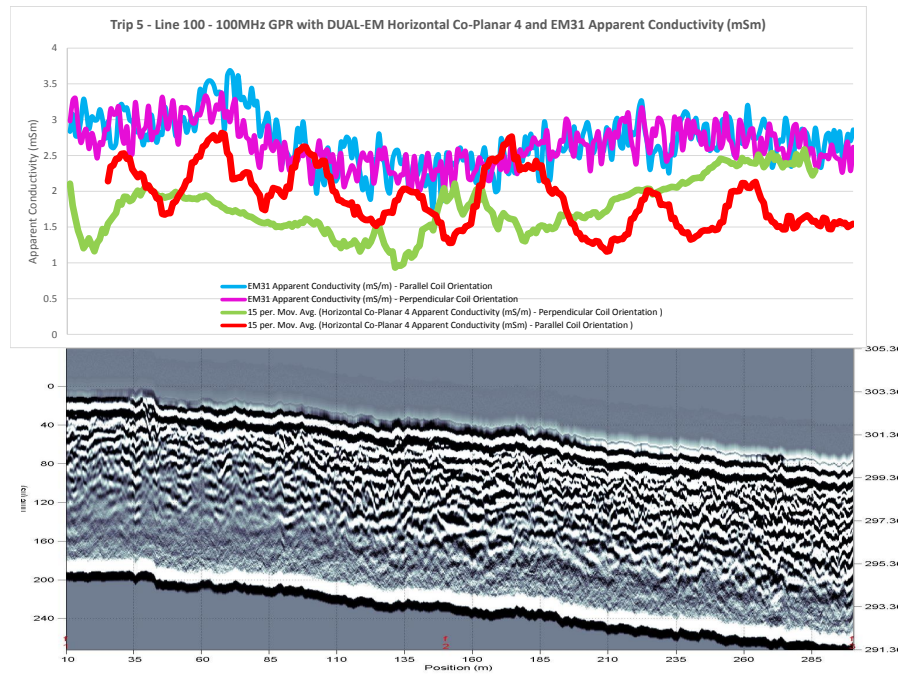


FIGURE 5.54: 100MHz radargram along line 100 from trip 5. This is then overlain with the line 100 EM31 and DUAL-EM data from trip 5.

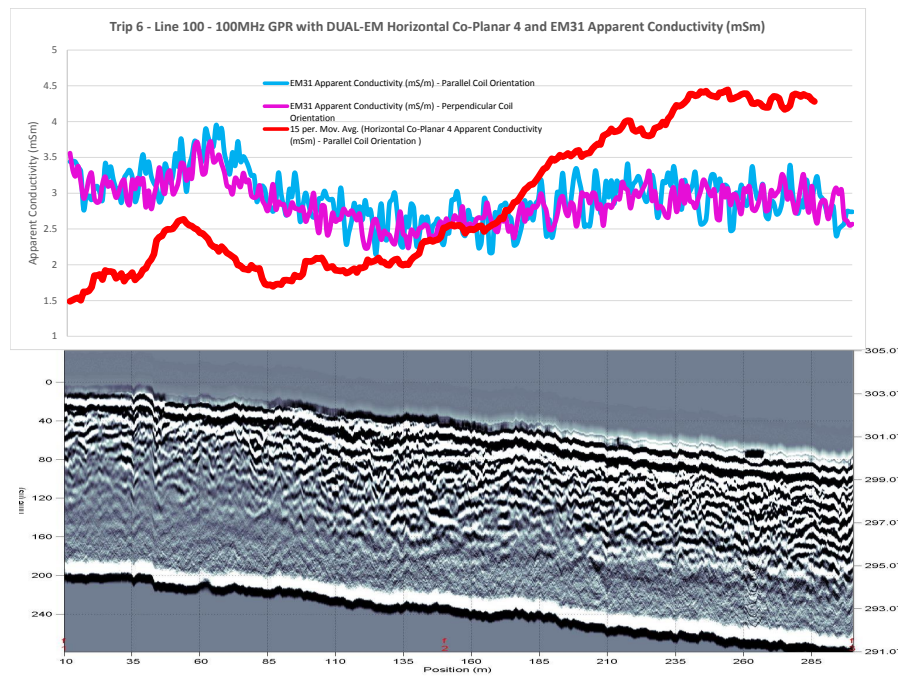


FIGURE 5.55: 100MHz radargram along line 100 from trip 6. This is then overlain with the line 100 EM31 and DUAL-EM data from trip 6.

recorded beneath the survey area.

The DUAL-EM data shown in Figure 5.56 appears to show a huge increase in apparent

conductivity between line 0 and the cow paddock. Due to the huge volume of DUAL-EM survey data that appears to be incorrect it is likely to have been instrument or user error.

Figure 5.57 shows data taken during trip 6 along a line that crosses from the cow paddock into the survey area. The line crossed a culvert which is seen as a dramatic spike in the DUAL-EM data. This line was run in an effort to identify a noticeable difference in conductivities when crossing from the cow paddock to the survey area directly. The DUAL-EM apparent conductivity appears to drop slightly as it crosses into the survey area however the conductivity values appear to be unreasonably high and are not supported by the EM31 results. The data from this area is deemed to be unhelpful but is included to give an example of efforts made to identify noticeable conductivity differences between the two areas.

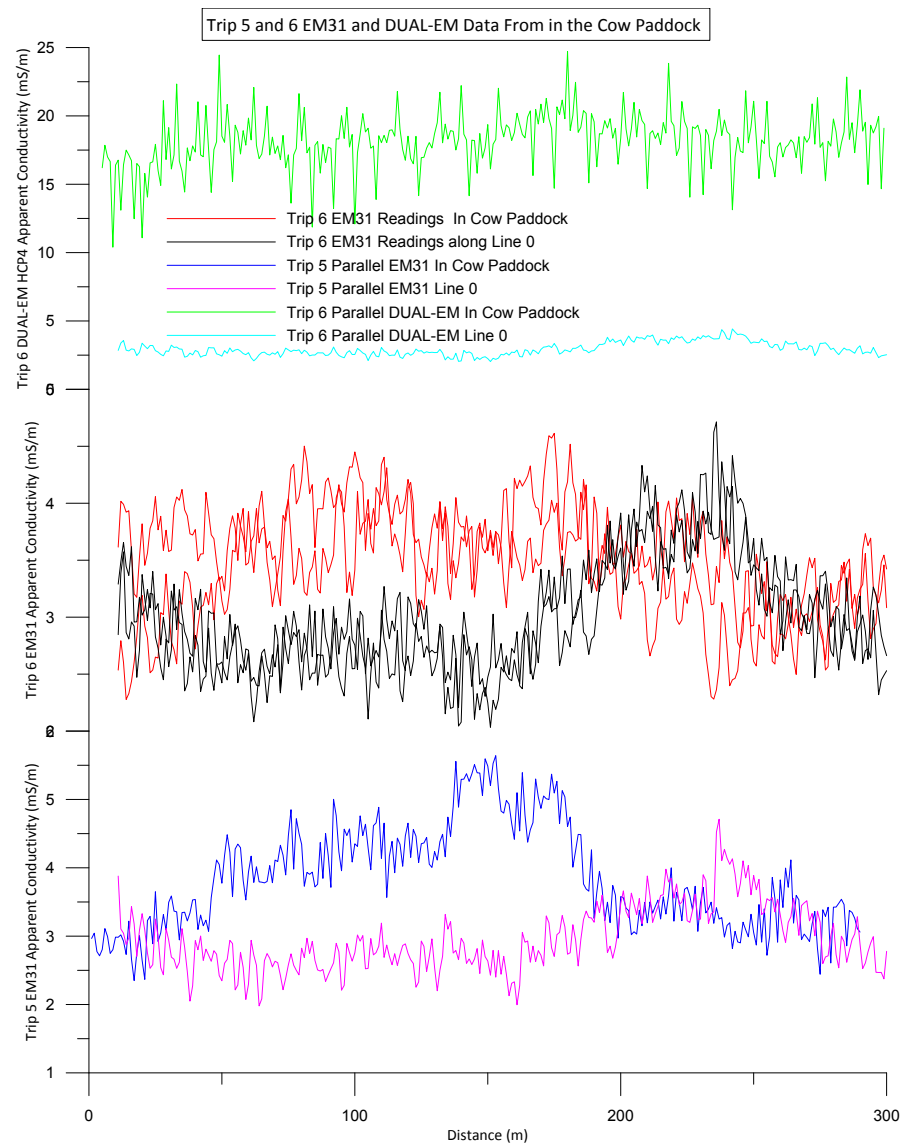


FIGURE 5.56: EM31 and DUAL-EM data recorded in the paddock that contained wintering cows. Reference data from line 0 is also included with each plot.

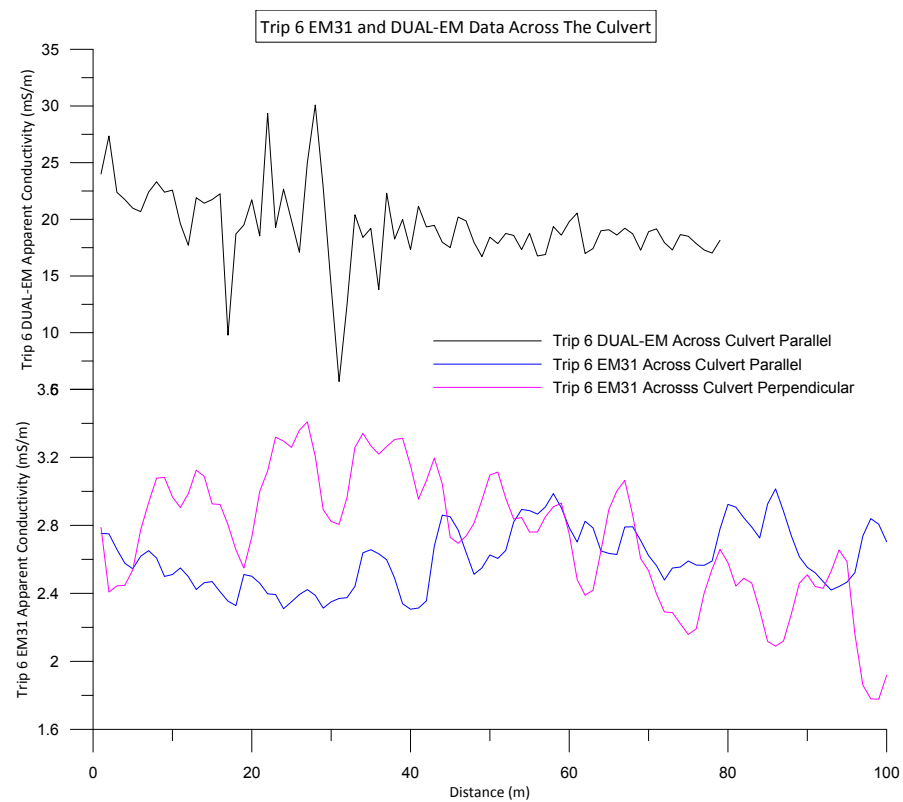


FIGURE 5.57: EM31 and DUAL-EM data recorded by walking between the cow paddock and the survey area in an attempt to see any obvious changes in apparent conductivity.

5.5.2 System Behaviour

The shallow groundwater system at the Irthing Road field site appears to be responsive to rainfall, however shows little response to an input of highly concentrated leachate. The combination of these two ideas points to a system that contains a large amount of water that travels through the ground very quickly. This means that rainfall events rapidly register within the system however due to the large amount of groundwater travelling through the system, even a large source of contamination shows little to no changes in groundwater conductivity. The sheer volume of water and the speed with which it travels through the system means that the large source of contamination is removed very quickly and the actual concentration of contaminants is so small that the geophysics cannot register it.

These characteristics of the groundwater system at Irthing Road explain why rainfall events register in the geophysical results but the contamination is not apparent and does not register as expected. The idea that the high level of contamination would be obvious once the cattle were added to the area would work if the rate at which the groundwater took contaminants away from the area was lower.

The removal of the contaminants from the area by the groundwater is a mixed blessing as it preserves the groundwater system in the immediate area but is undeniably transferring large volumes of contaminants elsewhere.

Chapter 6

Conclusion and Recommendations

6.1 Conclusion

The geophysical techniques and instruments used for this research throughout 2014 have performed well. There is however a commercial interest in this project and there are still important questions around the viability of these techniques and their application to shallow groundwater contamination mapping and monitoring. The conclusion drawn after a year of research and analysis is that all three of the techniques used are viable options for shallow groundwater applications. Each technique however has its own positives and negatives and it is recommended that a combination of techniques is always the best option.

The Geonics Ltd EM31-MK2 device has distinguished itself as a highly reliable instrument that returns consistent results upon which the user can rely. The EM31 has been very important throughout this research and the data it has provided has been key in drawing many of the conclusions from this project. As a stand alone method the EM31 is great for quickly scanning large areas, almost irrespective of the terrain because of its ease of use. The bulk apparent conductivity of the top 5.5 metres of the sub-surface can provide a lot of information when doing shallow groundwater surveys. The potential for the device to quickly and accurately map out preferential flow paths and then monitor areas for conductivity changes is extensive. This could easily be combined with highly targeted shallow groundwater sampling and testing which would allow a complete picture of the shallow groundwater conditions to be obtained. In this application the EM31 has shown itself to be the best value tool with the most consistent results.

The Dualem Inc. DUAL-EM 421s has shown potential throughout the year to be able to out perform the EM31 if it was able to produce consistent results. The DUAL-EM has such potential to be able to provide a depth profile of the apparent conductivities, however the issues with attaining consistent, accurate results has severely impacted its benefit to the research. If the DUAL-EM gets to the point where it can record data at the same level of consistency and reliability as the EM31, across all of its coil spacings, then it will become a far more powerful tool than the EM31 can ever be. Until this point however the device is simply too unreliable for commercial application to be viable.

The Sensors & Software pulseEKKO GPR system performed at a highly consistent level throughout the research. The device saw many hours of hard use in varying conditions from sun and tall grass, through too snow and mud. The GPR results were important throughout this research because they provided data that could be used alongside the EMI data sets that were provided by the EM31 and DUAL-EM. The GPR radargrams showed important information on radar penetration, ground conditions and what rises in EM apparent conductivities were coinciding with. The GPR data is very helpful, but does have some limitations around ease of use due to the difficulty running the device in complex terrain. The GPR worked very well with the EM and the combination of the two allowed accurate delineation of the sub-surface high conductivity pathways. This information could easily be combined with a highly target groundwater sampling regime to produce great results. The GPR is a commercially viable option for shallow groundwater research however it is better suited to the identification of preferential flow paths and sub-surface conditions than to recording changes within the groundwater itself. The use of a shielded, more durable GPR device would also allow it to access more difficult terrain and service more areas.

The study area appears to have such a large volume of water travelling through it that the vast majority of leachate is transported away from the site very quickly. This makes it very difficult to see any changes in the geophysics because the ionic concentrations within the groundwater are not permitted to build up to a high enough level that they register a clear response in the geophysical surveys. This result is positive for the landowner because there is no leachate build up in the immediate vicinity of the highly concentrated agriculture. The high gravel content and hydraulic conductivity of the sub surface allows the leachate to leave the area very quickly. This does however pose a large problem for Environment Southland. The final destination for all of this shallow groundwater pollution is unknown and this could be causing a huge problem if it is collecting in an area further down the hydraulic gradient. This could potentially lead to a contamination problem at a site (most likely a lake, river, or estuary) many kilometres away as leachate from a large catchment, containing free draining soils, is concentrated into one area. The issue then becomes tracking the origin of this leachate and due to

travel times within the groundwater system the damage may not be recognised for years. This delay is also true to remedial strategies which once implemented may not begin to remedy the problem for years as leachate is still travelling through the groundwater system. The problem of where this contamination is going, and in what quantity, needs to be urgently addressed.

6.2 Recommendations

There are several ways to improve future research that have become apparent over the last year. The recommendations are made in reference to further research that could be conducted in this area, and some are based upon mistakes that were made during this research project.

It became obvious towards the latter half of the project that the groundwater sampling program was going to be a vital reference for this research. The lack of establishing a groundwater sampling program did have a negative effect upon the research because there was no way to check what leachate levels were in the shallow groundwater and soil pore water throughout the year. This has led to issues surrounding how much leachate was travelling through the system and in what concentrations. It is recommended that for future work a groundwater sampling program is present and that it is carried out correctly. Access to the groundwater should be a priority and small obstacles that were encountered during this project such as gravel filling the boreholes, need to be overcome immediately.

Three dimensional modelling of the EMI data would also be a great introduction to future work. While it might not be as necessary as water sampling, 3D modelling does help with interpretation and presentation. In this project 3D modelling of the DUAL-EM data may not have been very useful due to the random and inaccurate nature of many of the results. It is also far more time consuming for large areas and would need to be conducted using a towed DUAL-EM device.

Gaining greater access to the sub surface lithology would also help broaden understanding in a project such as this. While in this case there was obvious issues with boring holes into a working farm, future projects should attempt to work around this issue.

6.2.1 Future Research Plan

Future groundwater research is highly recommended in the Lumsden area due to the continued increase of dairy farming in northern Southland. The following six stage research plan briefly outlines a potential method for continuing the research in a way that would provide a solution to the problem of shallow groundwater contamination and its' flow on effects.

Stage 1: Groundwater and land use mapping program: This initial stage would involve mapping the shallow groundwater flow directions for the area on a large scale. This would then be overlain with land use maps showing the areas of highest possible leachate input into the shallow groundwater system.

Stage 2: Groundwater sampling: The next step is to identify where this leachate may possibly be ending up after its journey through the shallow groundwater system. This can be achieved using the mapping which was done in the previous stage to follow the groundwater down gradient. The introduction of water sampling in these areas (lakes, rivers, estuaries) would be aiming to identify where leachate is gathering and in what concentrations.

Stage 3: Geophysical surveys: This step involves starting at the end (areas where contamination is gathering) and working outwards using EMI and GPR surveys to identify the major shallow groundwater flow paths.

Stage 4: Flow path water sampling program: Introducing a sampling program on all of the major shallow groundwater flow paths allows the areas of highest contamination to be identified and remedied first. Some flow paths are expected to be transporting a larger amount of contaminants and these can be identified using this program.

Stage 5: Identifying leachate origins: Using the data collected so far it should be possible to infer as too which sources are causing high levels of leachates to enter the shallow groundwater system. This is done using the land use and groundwater flow direction mapping, combined with the information provided by water sampling across the groundwater flow paths.

Stage 6: Remedies: Once the areas of greatest contaminant contribution are identified it is time to introduce changes that will limit the amount of contaminants finding their way into the groundwater system.

Appendix A

Appendix 1: Supporting Resources

Unit	Terrane	Formation	Description
Q1a	Quaternary	-	Alluvial Terraces and fans - Locally derived, typically bouldery, unconsolidated gravel, sand, and mud in fills most valleys, and forms modern floodplains.
uQa	Quaternary	-	Undifferentiated, variably weathered gravels in alluvial fans or outwash terraces
Q2a	Quaternary	-	Outwash gravels - unweather to slightly weathered
Yc	Caples Terrane	-	Undifferentiated volcaniclastic sandstone and siltstone
Ycu	Caples Terrane	Upper Peak Formation	Thin-bedded graded sandstone and black mudstone
Yc IIA	Caples Terrane	-	Undifferentiated volcaniclastic sandstone and siltstone that's become metamorphosed and deformed towards the centre of the schist belt. This example is a weakly foliated semischist - retains primary appearance and sedimentary texture, although detrital grains are flattened. Metamorphic micas are fine grained (<75 nano metres), and impart a weak cleavage to sandstones. Mudstones have slaty cleavage. Bedding and foliation are equally dominant in outcrop.
Yl	Dun-Mountain – Maitai Terrane	Livingstone Volcanics	Undifferentiated volcanics, dikes, microgabbro, and sediments.
Tmg	Dun-Mountain – Maitai Terrane	Greville Formation	Thin-bedded sandstone and mudstone with sparse ammonites. (contains some Tml - Little Ben Sandstone - Bedded volcaniclastic sandstone with minor siltstone and breccia)

FIGURE A.1: Description of Geological units shown in figure 2.7 (Turnbull, 2000)



Hill Laboratories
BETTER TESTING BETTER RESULTS

R J Hill Laboratories Limited
1 Clyde Street
Private Bag 3205
Hamilton 3240, New Zealand
Tel +64 7 858 2000
Fax +64 7 858 2001
Email mail@hill-labs.co.nz
Web www.hill-labs.co.nz

ANALYSIS REPORT

Page 1 of 3

Client:	Environment Southland	Lab No:	1356589	SUPv1
Contact:	Clint Rissmann	Date Registered:	27-Nov-2014	
	C/- Environment Southland	Date Reported:	09-Dec-2014	
	Private Bag 90116	Quote No:	54752	
	INVERCARGILL 9840	Order No:	EEGWE1	
		Client Reference:	Matt James Field Site	
		Submitted By:	Andrew Little	

Sample Type: Aqueous					
Sample Name:	20145041 25-Nov-2014 11:45 am	20145042 25-Nov-2014 11:10 am	20145045 25-Nov-2014 12:40 pm	20145046 25-Nov-2014 12:09 pm	
Lab Number:	1356589.1	1356589.2	1356589.3	1356589.4	
Sum of Anions	meq/L	1.058 ± 0.037	2.358 ± 0.077	0.387 ± 0.022	0.779 ± 0.032
Sum of Cations	meq/L	1.121 ± 0.047	2.70 ± 0.12	0.432 ± 0.021	0.885 ± 0.039
% Difference in Ion Balance	%	2.9 ± 2.8	6.8 ± 2.8	5.4 ± 3.7	6.4 ± 3.0
pH	pH Units	6.3 ± 0.2	6.7 ± 0.2	7.0 ± 0.2	6.9 ± 0.2
Total Alkalinity	g/m³ as CaCO₃	26.5 ± 1.3	85.8 ± 3.5	14.43 ± 0.88	18.6 ± 1.0
Carbonate Alkalinity	g/m³ as CaCO₃	< 1.0 ± 0.67	< 1.0 ± 0.67	< 1.0 ± 0.67	< 1.0 ± 0.67
Bicarbonate Alkalinity	g/m³ as CaCO₃	26.5 ± 1.3	85.8 ± 3.5	14.42 ± 0.88	18.5 ± 1.0
Total Hardness	g/m³ as CaCO₃	37.1 ± 1.8	93.2 ± 4.3	13.61 ± 0.65	31.0 ± 1.5
Electrical Conductivity (EC)	µS/cm	107 ± 3	212 ± 5	39 ± 2	85 ± 2
Dissolved Boron	g/m³	0.0150 ± 0.0038	0.0204 ± 0.0042	0.0066 ± 0.0034	0.0116 ± 0.0036
Dissolved Calcium	g/m³	8.44 ± 0.53	17.8 ± 1.2	3.49 ± 0.23	8.28 ± 0.52
Dissolved Iodine	g/m³	0.00184 ± 0.00037	0.00579 ± 0.00086	0.00062 ± 0.00028	0.00144 ± 0.00033
Dissolved Iron	g/m³	0.388 ± 0.030	0.685 ± 0.049	0.033 ± 0.014	0.150 ± 0.017
Dissolved Magnesium	g/m³	3.88 ± 0.27	11.82 ± 0.80	1.192 ± 0.082	2.50 ± 0.17
Dissolved Manganese	g/m³	0.421 ± 0.037	1.024 ± 0.089	0.00363 ± 0.00046	0.0345 ± 0.0030
Dissolved Potassium	g/m³	1.69 ± 0.13	1.49 ± 0.12	0.541 ± 0.052	0.855 ± 0.071
Dissolved Sodium	g/m³	6.73 ± 0.73	16.7 ± 1.8	3.31 ± 0.36	5.43 ± 0.59
Bromide	g/m³	< 0.05 ± 0.041	0.056 ± 0.042	< 0.05 ± 0.041	< 0.05 ± 0.041
Chloride	g/m³	4.74 ± 0.45	6.27 ± 0.51	2.24 ± 0.37	8.55 ± 0.62
Fluoride	g/m³	< 0.05 ± 0.041	< 0.05 ± 0.041	< 0.05 ± 0.041	0.061 ± 0.041
Total Nitrogen	g/m³	7.02 ± 0.83	17.4 ± 2.1	0.173 ± 0.062	2.38 ± 0.24
Total Ammoniacal-N	g/m³	0.217 ± 0.019	0.146 ± 0.014	< 0.010 ± 0.0067	0.0184 ± 0.0068
Nitrite-N	g/m³	0.0097 ± 0.0019	< 0.002 ± 0.0014	< 0.002 ± 0.0014	0.0030 ± 0.0014
Nitrate-N	g/m³	0.149 ± 0.020	< 0.002 ± 0.0019	0.0615 ± 0.0078	1.75 ± 0.21
Nitrate-N + Nitrite-N	g/m³	0.159 ± 0.020	< 0.002 ± 0.0014	0.0625 ± 0.0077	1.75 ± 0.21
Total Kjeldahl Nitrogen (TKN)	g/m³	6.86 ± 0.83	17.4 ± 2.1	0.111 ± 0.062	0.630 ± 0.097
Dissolved Reactive Phosphorus	g/m³	< 0.004 ± 0.0027	0.0195 ± 0.0039	< 0.004 ± 0.0027	0.0045 ± 0.0027
Total Phosphorus	g/m³	5.48 ± 0.77	19.9 ± 2.8	0.0075 ± 0.0029	0.0325 ± 0.0053
Reactive Silica	g/m³ as SiO₂	12.50 ± 0.26	19.34 ± 0.40	7.10 ± 0.16	4.69 ± 0.12
Total Sulphide	g/m³	0.0082 ± 0.0032	0.0121 ± 0.0046	0.0031 ± 0.0016	0.0024 ± 0.0015
Sulphate	g/m³	18.4 ± 1.2	22.2 ± 1.4	1.47 ± 0.36	1.98 ± 0.37
Dissolved Organic Carbon (DOC)	g/m³	5.4	4.0	3.4	7.0



This Laboratory is accredited by International Accreditation New Zealand (IANZ), which represents New Zealand in the International Laboratory Accreditation Cooperation (ILAC). Through the ILAC Mutual Recognition Arrangement (ILAC-MRA) this accreditation is internationally recognised.
The tests reported herein have been performed in accordance with the terms of accreditation, with the exception of tests marked *, which are not accredited.

FIGURE A.2: Water sampling results from Environment Southland. Sample 20145041: Southern Pit. Sample 20145042: Northern Pit. Sample 20145045: Irthing Stream. Sample 20145046: Creek between cow paddock and survey area.

Hill Laboratories
BETTER TESTING BETTER RESULTS

R J Hill Laboratories Limited
1 Clyde Street
Private Bag 3205
Hamilton 3240, New Zealand

Tel +64 7 858 2000
Fax +64 7 858 2001
Email mail@hill-labs.co.nz
Web www.hill-labs.co.nz

ANALYSIS REPORT

Page 1 of 3

Client:	Environment Southland	Lab No:	1356588	SUPV1
Contact:	Andrew Little	Date Registered:	28-Nov-2014	
	Private Bag 90116	Date Reported:	16-Dec-2014	
	INVERCARGILL 9840	Quote No:	64978	
		Order No:	4060 1380 414	
		Client Reference:	Matt James Soil	
		Submitted By:	Andrew Little	

Sample Type: Soil

Sample Name:	20145043 25-Nov-2014 11:45 am	20145044 25-Nov-2014 11:10 am		
Lab Number:	1356588.1	1356588.2		
SPLP Sample Weight	g 100	100	-	-
SPLP Extractant Type*	De-ionised Water, pH 5.8 +/- 0.4	De-ionised Water, pH 5.8 +/- 0.4	-	-
SPLP Final pH	pH Units 7.9 ± 0.1	8.0 ± 0.1	-	-

Sample Type: Aqueous

Sample Name:	20145043 [SPLP Extract]	20145044 [SPLP Extract]		
Lab Number:	1356588.3	1356588.4		
Sum of Anions*	meq/L 0.326 ± 0.021	0.276 ± 0.020	-	-
Sum of Cations	meq/L 0.297 ± 0.020	0.247 ± 0.017	-	-
Total Alkalinity*	g/m ³ as CaCO ₃ 8.50 ± 0.75	9.70 ± 0.77	-	-
Total Hardness	g/m ³ as CaCO ₃ 5.47 ± 0.31	2.66 ± 0.16	-	-
Dissolved Boron	g/m ³ 0.074 ± 0.010 #1	0.0546 ± 0.0078 #1	-	-
Dissolved Calcium	g/m ³ 1.81 ± 0.12	0.704 ± 0.056	-	-
Dissolved Iodine	g/m ³ 0.00107 ± 0.00031	0.00052 ± 0.00028	-	-
Dissolved Iron	g/m ³ 0.270 ± 0.023	1.108 ± 0.078	-	-
Dissolved Magnesium	g/m ³ 0.234 ± 0.021	0.218 ± 0.020	-	-
Dissolved Manganese	g/m ³ 0.00259 ± 0.00040	0.0203 ± 0.0018	-	-
Dissolved Potassium	g/m ³ 0.209 ± 0.037	0.159 ± 0.036	-	-
Dissolved Sodium	g/m ³ 3.94 ± 0.43	3.42 ± 0.37	-	-
Bromide*	g/m ³ < 0.05 ± 0.041	< 0.05 ± 0.041	-	-
Chloride	g/m ³ 1.93 ± 0.36	0.61 ± 0.35	-	-
Fluoride*	g/m ³ 0.070 ± 0.041	0.079 ± 0.042	-	-
Total Nitrogen	g/m ³ 1.02 ± 0.12	0.286 ± 0.067	-	-
Total Ammoniacal-N*	g/m ³ < 0.010 ± 0.0067	< 0.010 ± 0.0067	-	-
Nitrite-N*	g/m ³ 0.0042 ± 0.0015	0.0065 ± 0.0016	-	-
Nitrate-N*	g/m ³ 0.814 ± 0.099	0.0546 ± 0.0077	-	-
Nitrate-N + Nitrite-N*	g/m ³ 0.819 ± 0.099	0.0611 ± 0.0075	-	-
Total Kjeldahl Nitrogen (TKN)	g/m ³ 0.205 ± 0.065	0.225 ± 0.066	-	-
Dissolved Reactive Phosphorus	g/m ³ 0.0040 ± 0.0027	0.0180 ± 0.0037	-	-
Total Phosphorus*	g/m ³ 0.0427 ± 0.0066	0.193 ± 0.028	-	-
Reactive Silica*	g/m ³ as SiO ₂ 2.674 ± 0.086	2.517 ± 0.084	-	-
Total Sulphide	g/m ³ < 0.002 ± 0.0014	< 0.002 ± 0.0014	-	-
Sulphate*	g/m ³ 2.08 ± 0.37	2.81 ± 0.38	-	-
Dissolved Organic Carbon (DOC)	g/m ³ 4.6	2.7	-	-



This Laboratory is accredited by International Accreditation New Zealand (IANZ), which represents New Zealand in the International Laboratory Accreditation Cooperation (ILAC). Through the ILAC Mutual Recognition Arrangement (ILAC-MRA) this accreditation is internationally recognised.

The tests reported herein have been performed in accordance with the terms of accreditation, with the exception of tests marked *, which are not accredited.

FIGURE A.3: Water sampling results from Environment Southland. Sample 20145043: Crop Paddock Soil Water. Sample 20145044: Survey Area Soil Water.

Appendix B

Appendix 2: EM31 Results

Trip 1 EM31 Results - Parallel Coil Orientation

Position	Interpolated Conductivity: Line 0 10-300m	Interpolated Conductivity: Line 25 10-300	Interpolated Conductivity: Line 50 10-300m	Interpolated Conductivity: Line 75 10-300m	Interpolated Conductivity: Line 100 10- 300m
	Par	Par	Par	Par	Par
11	2.7679	2.9335	3.212	3.1387	2.8976
12	3.109	3.1161	3.1785	3.041	2.9036
13	2.8321	3.2555	3.083	3.1029	2.9253
14	2.6386	3.241	3.148	3.1446	2.8852
15	2.5927	2.8359	3.1985	3.1013	2.9627
16	2.6808	2.9791	3.266	3.0986	3.0908
17	2.7132	3.0537	3.3085	3.4092	2.9564
18	2.6288	3.0104	3.2914	3.0698	2.8086
19	2.5375	3.2713	3.4001	3.2668	2.6115
20	2.4067	3.3087	3.3328	3.3882	2.699
21	2.5149	2.9992	3.5188	3.011	2.9702
22	2.6448	3.2155	3.4906	3.0976	2.9003
23	2.4509	3.2274	3.5275	3.1828	2.7861
24	2.1683	3.3629	3.699	3.0132	2.9064
25	2.4391	3.5089	3.6178	2.9021	2.7037
26	2.7381	3.142	3.7789	3.0231	2.8987
27	2.4512	3.0931	3.6061	3.009	2.951
28	2.2218	3.4563	3.8966	3.1032	3.0061
29	2.1928	3.0291	3.8934	2.6751	2.9814
30	2.2256	3.278	3.9149	3.0927	2.9071
31	2.3206	3.294	3.8181	3.6128	3.0339
32	2.4544	2.9581	3.741	3.4926	2.8887
33	2.5959	2.8338	3.5954	3.1506	2.6975
34	2.4968	3.0866	3.5093	2.9988	2.8859
35	2.4405	3.1343	3.5863	3.2515	2.8969
36	2.2019	2.8872	3.2619	3.4749	2.9257
37	2.4063	2.7225	3.3985	3.5411	3.1547
38	2.2954	2.8531	3.2946	3.6216	3.1959
39	2.3	2.8659	3.4534	3.8649	3.2926
40	2.4026	3.1051	3.5633	3.6122	3.2073
41	2.2878	2.8006	3.4297	3.5197	3.2919
42	2.6812	3.0112	3.5234	3.7247	3.3009
43	2.4532	2.8539	3.4301	3.3742	3.1939
44	2.2884	2.5357	3.408	3.3624	3.0976
45	2.3946	2.4419	3.4924	3.5286	3.0895
46	2.3157	2.7006	3.5012	3.3994	2.9811
47	2.3697	2.9265	3.3858	3.5057	3.0508
48	2.4358	2.9921	3.1652	3.5143	3.2487
49	2.7892	2.548	3.1761	3.4542	3.3363
50	2.838	2.6841	3.2832	3.5153	3.4597
51	2.4825	2.5054	3.252	3.6293	3.4881
52	2.4346	2.6053	3.3108	3.6053	3.4004
53	2.5192	2.5998	3.2701	3.414	3.4734
54	2.4827	2.5791	3.1578	3.3856	3.4658

55	2.5652	2.4927	3.1969	3.2331	3.4789
56	2.8205	2.4855	3.1852	3.383	3.5915
57	2.9032	2.604	3.0172	3.5882	3.5996
58	2.7623	2.7324	3.2044	3.4941	3.6721
59	2.6476	2.581	3.0508	3.6892	3.6879
60	2.5526	2.5204	2.9461	3.3481	3.2881
61	2.5935	2.2858	2.8793	3.2406	3.4017
62	2.4697	2.3009	3.019	3.3055	3.2913
63	2.402	2.302	3.1732	3.4935	3.2743
64	2.4534	2.4511	2.8081	3.4154	3.2113
65	2.3851	2.5798	2.9114	3.119	3.3617
66	2.3053	2.274	3.0152	3.195	3.363
67	2.3961	2.3057	3.1285	3.0526	3.2751
68	2.2	2.3096	2.9792	3.0211	3.3768
69	2.4002	2.2181	2.7868	2.8948	3.3245
70	2.1777	2.1876	2.7014	2.9003	3.2618
71	2.4646	2.3166	2.5786	2.7887	3.4772
72	2.5966	1.9023	2.7643	2.6717	3.4147
73	2.6456	2.1174	2.9903	2.5832	3.4045
74	2.6157	2.0644	3.0905	2.659	3.2072
75	2.5337	1.8811	3.236	2.7178	3.0526
76	2.3548	1.915	3.7922	2.5996	3.1968
77	2.2288	2.1533	2.795	2.6987	2.9684
78	2.4088	2.3036	2.7472	2.5991	2.9
79	2.5864	2.4047	2.7969	2.923	2.8838
80	2.596	2.1374	2.8906	3.0375	2.754
81	2.6414	2.2996	2.9648	2.6517	3.0491
82	2.7743	1.8454	3.0087	2.5922	3.1717
83	2.7524	1.8097	2.6905	2.7053	2.8861
84	2.7123	2.1655	2.7038	2.6777	2.8748
85	2.6054	2.5186	2.5116	2.6483	2.7063
86	2.6898	2.3305	2.2933	2.7045	2.7819
87	3.0677	2.116	2.495	2.7117	2.723
88	2.9298	2.2524	2.3469	2.5252	2.7582
89	2.7842	2.5337	2.5308	2.304	3.088
90	2.8028	2.2612	2.7887	2.5326	2.9116
91	2.9802	2.1248	2.6859	2.6138	2.7019
92	3.1554	2.3791	3.0999	2.4365	2.9066
93	2.6531	2.6287	2.6431	2.7171	2.7759
94	2.5956	2.7802	2.6466	2.6223	2.6972
95	2.4337	2.4908	2.7201	2.6018	2.6903
96	2.3025	2.5979	2.6834	2.392	2.7559
97	2.4	2.3854	2.571	2.284	2.7497
98	2.1017	2.3159	2.5767	2.5761	2.6596
99	2.3798	2.5314	2.6241	2.6911	2.5704
100	2.4143	2.5037	2.4739	2.5286	2.2899
101	2.3032	2.5087	2.7128	2.2962	2.4299
102	2.3738	2.2983	2.8557	2.3306	2.5627
103	2.496	2.2725	2.628	2.5134	2.776
104	2.4276	2.4042	2.7618	2.3959	2.6522

105	2.3891	2.4019	2.7201	2.1595	2.3996
106	2.5746	2.7749	2.5235	2.4908	2.5269
107	2.4799	3.1746	2.4852	2.4063	2.2986
108	2.3467	2.4435	2.5773	2.7311	2.5245
109	2.2449	2.32	2.3341	2.6922	2.7062
110	2.2201	2.621	2.0069	2.6794	2.5388
111	2.43	2.9894	2.541	2.4678	2.464
112	2.4509	2.5512	2.4714	2.2905	2.6846
113	2.2267	2.3761	2.3448	2.5026	2.4242
114	2.2854	2.3011	2.3715	2.3863	2.436
115	2.6291	2.4007	2.3105	2.4016	2.5502
116	2.1874	2.4529	2.2607	2.4132	2.6735
117	1.6435	2.7531	2.3412	2.321	2.6506
118	2.3914	2.5725	2.4017	2.5613	2.5184
119	2.5863	2.3523	2.4066	2.5799	2.4978
120	2.5193	2.6548	2.6913	1.9793	2.4686
121	2.7251	2.9249	2.3427	2.2705	2.3486
122	2.6407	2.6515	2.2948	2.33	2.494
123	2.6527	2.5067	2.3358	2.5597	2.4993
124	3.2005	2.3998	2.4718	2.4057	2.5082
125	2.6289	2.4233	2.4919	2.5741	2.5531
126	2.4	2.2467	2.5904	2.4226	2.2606
127	2.4975	2.1383	2.4348	2.5488	2.3829
128	2.5002	2.5703	1.9964	2.524	2.5957
129	2.5061	2.3551	2.1322	2.4063	2.5001
130	2.4049	2.0133	2.3633	2.2049	2.4095
131	2.4508	2.0571	2.365	2.2316	2.4053
132	2.3314	1.8738	2.3238	2.653	2.4654
133	2.282	2.2833	2.4742	2.6485	2.3737
134	2.3771	2.3042	2.4576	2.3753	2.4943
135	2.4111	2.1968	2.2193	2.2962	2.5068
136	2.3783	2.2095	2.2922	2.4349	2.3259
137	2.4992	2.3424	2.197	2.5007	2.2866
138	2.3148	2.4676	2.1309	2.4806	2.4675
139	2.1359	2.2672	2.5163	2.4207	2.5252
140	2.2103	2.0448	2.4948	2.4407	2.4872
141	2.1421	2.6008	2.4768	2.4054	2.3033
142	2.1427	2.3118	2.2914	2.1908	2.3779
143	2.4598	2.3113	2.5717	2.5773	2.1951
144	2.292	1.8127	2.6859	2.5251	2.3365
145	1.9898	2.2162	2.1966	2.8606	2.4596
146	2.3867	2.4003	2.7018	2.6366	2.7048
147	2.3784	2.2396	2.4695	2.5819	2.4758
148	2.462	2.1502	2.4009	2.4285	2.2262
149	2.5517	2.2839	2.447	2.4	2.3781
150	2.1552	2.5308	2.241	2.4278	2.4394
151	2.2721	2.5508	2.2093	2.6064	2.7565
152	2.6256	2.3516	2.1834	2.3779	2.6516
153	2.7011	2.5528	2.2431	2.3412	2.4963
154	2.6434	2.318	2.4055	2.509	2.5749

155	2.4	2.3	2.25	2.3	2.45
156	2.3057	2.2052	2.1863	2.4143	2.4072
157	2.1042	2.2752	2.1336	2.4349	2.6213
158	2.267	2.106	2.2894	2.5777	2.5845
159	2.5635	2.4496	2.2123	2.4679	2.4009
160	2.7719	2.4742	2.389	2.3924	2.514
161	2.8926	2.2098	2.3017	2.4	2.507
162	2.8554	2.2124	2.5429	2.3951	2.4358
163	2.7259	2.2291	2.5237	2.3904	2.1768
164	2.6893	2.0077	2.3999	2.413	2.1179
165	2.7453	2.1924	2.3801	2.5448	2.3683
166	2.9487	2.3032	2.0529	2.6015	2.5248
167	2.9828	2.2772	2.1249	2.6019	2.9318
168	3.4676	2.0604	2.3374	2.4021	2.8611
169	3.5561	1.9854	2.2273	2.4691	2.6199
170	3.0531	2.0542	2.2651	2.2082	2.5006
171	3.0497	2.0553	2.2958	2.3298	2.55
172	3.0471	1.9847	2.2576	2.4412	2.5012
173	2.8223	2.0209	1.4075	2.5962	2.6115
174	2.8615	1.8866	1.56	2.6884	2.7329
175	3.0164	2.2709	2.3028	2.4139	2.7371
176	3.015	2.5002	2.3144	2.3358	2.5106
177	3.1227	2.4151	2.2949	2.397	2.535
178	3.0586	2.2312	2.4779	2.4913	2.4596
179	2.8984	1.9967	2.4025	2.4023	2.6133
180	3.0109	2.1343	2.2558	2.3996	2.6647
181	2.9961	2.0075	2.099	2.4236	2.6283
182	2.9741	2.0155	2.1977	2.3074	2.7194
183	3.0035	2.2068	2.3123	2.3002	2.8659
184	3.1	2.0842	2.5537	2.5012	2.5996
185	3.0034	2.3944	2.5194	2.4043	2.9551
186	3.015	2.1007	2.3886	2.434	2.9192
187	3.1898	2.3073	2.2612	2.7091	2.7981
188	3.1311	2.1928	1.9833	2.5415	3.0265
189	2.9685	2.1566	2.4844	2.4476	3.035
190	3.3646	2.2255	2.1383	2.2952	3.3879
191	3.1452	2.57	2.5916	2.4944	2.897
192	3.3785	2.3475	2.373	2.3986	2.6561
193	3.5005	2.4411	2.2217	2.1507	2.6618
194	3.1525	2.4325	2.3119	2.4113	2.9137
195	3.2247	2.5222	2.3006	2.4201	2.9516
196	3.2448	2.1028	2.1612	1.8909	2.9661
197	3.2676	2.5189	2.2328	2.3762	2.8744
198	3.1905	2.4605	2.2094	2.6006	2.8573
199	3.2599	2.324	2.2753	2.6266	2.8931
200	3.5662	2.6046	2.4032	2.6846	3.0143
201	3.5532	2.734	2.1975	2.4678	2.9131
202	3.4554	2.5533	2.2997	2.3408	2.9867
203	3.3946	2.2769	2.1755	2.2068	3.0995
204	3.3913	2.5742	2.3259	2.2927	3.1023

205	3.4383	2.9169	2.2601	2.7313	3.0727
206	3.5079	2.5458	2.0636	2.5578	2.8067
207	3.3975	2.4988	2.0237	2.4534	3.0059
208	3.5289	2.3795	1.9895	2.5008	2.8888
209	3.5928	2.4971	2.0978	2.422	3.1157
210	3.4958	2.3838	2.1025	2.6046	3.3829
211	3.4961	2.4162	2.3861	2.4676	3.1692
212	3.3152	2.6648	2.6565	2.3474	2.9342
213	3.15	2.7835	2.3655	2.3321	2.8299
214	3.4887	2.5426	2.3626	2.5692	3.3282
215	3.6834	2.4951	2.2461	2.5371	3.4078
216	3.9442	2.4436	1.935	2.4049	3.1205
217	3.7434	2.2985	2.1389	2.4811	3.288
218	3.5864	2.6174	2.3972	2.4419	3.1246
219	3.7674	2.7313	2.4023	2.3369	2.9043
220	3.8004	2.91	2.362	2.6002	2.6893
221	3.8844	2.6955	2.2558	2.7371	2.4569
222	3.9859	2.3781	2.5256	2.4756	2.8792
223	4.0121	2.4043	2.2242	2.3085	3.2782
224	3.9402	2.5892	1.9102	2.4105	3.2961
225	3.8724	2.5951	2.0421	2.4368	3.1821
226	4.0019	2.8717	2.18	2.6585	3.2212
227	4.0904	2.899	2.3911	2.7107	3.1057
228	4.1599	2.8854	2.3909	2.4864	2.9835
229	4.1457	2.347	2.1839	2.526	2.9947
230	3.9544	2.3486	2.2187	2.7211	3.0639
231	3.8888	2.6774	2.3764	2.7054	3.1542
232	3.9153	3.0779	2.5584	2.6233	3.3886
233	3.9056	3.09	2.6574	2.5977	3.1591
234	3.7388	3.1565	2.6295	2.5664	2.9058
235	3.6787	3.5326	2.5198	2.3529	2.992
236	3.7869	3.0165	2.4012	2.3086	3.1998
237	3.5638	2.6024	2.3927	2.4668	3.0115
238	3.5429	2.8045	2.2029	2.668	3.0112
239	3.7099	2.9836	2.4245	2.623	3.0385
240	3.6057	2.6659	2.5228	2.312	3.1796
241	3.4024	2.5217	2.4021	2.1597	3.308
242	3.6	2.5045	2.2779	2.2028	2.9551
243	3.3101	2.5181	2.3225	2.443	2.9825
244	3.2031	2.5881	2.1877	2.3082	3.1651
245	3.1123	2.5369	2.407	2.4636	3.2684
246	3.0755	2.8258	1.9955	2.799	3.1673
247	3.3657	2.8151	2.2817	2.5885	3.0432
248	3.3371	2.897	2.306	2.5046	2.9772
249	3.2181	3.0093	2.4854	2.2268	3.151
250	3.1326	3.0926	2.592	2.613	3.1303
251	3.0174	3.0393	2.3534	2.6445	2.8213
252	3.013	3.0736	2.3679	2.4926	3.2027
253	2.9014	3.0003	2.3914	2.4131	2.9886
254	2.9632	2.9295	2.5841	2.5016	3.0217

255	2.8918	3.0111	2.7002	2.5681	2.8684
256	2.8297	3.2118	2.6007	2.5155	2.8
257	2.9113	3.0205	2.519	2.6012	3.0049
258	2.9152	3.0473	2.323	2.3956	3.2224
259	2.8176	2.8844	2.0088	2.5367	3.2224
260	2.6973	2.4768	2.4264	2.5723	3.1225
261	2.8817	3.2444	2.3863	2.4791	2.9391
262	3.0123	4.0866	2.1827	2.5744	3.2335
263	3.01	2.972	2.3992	2.6229	3.144
264	2.952	3.0759	2.1996	2.5935	3.2683
265	2.8078	3.0579	2.2685	2.4339	3.1415
266	2.966	2.7353	1.9561	2.6732	3.2899
267	2.8729	2.9702	2.2969	2.6882	3.1766
268	2.8218	2.9076	2.4601	2.4969	3.3522
269	3.1058	2.899	2.4943	2.0436	3.2781
270	2.9992	2.7067	2.5757	2.4234	2.9894
271	3.1	3.0694	2.5377	2.8704	3.1319
272	3.025	3.1767	2.3119	2.4151	3.2028
273	3.1025	3.1248	2.3017	2.3872	3.2101
274	2.8459	2.9672	2.267	2.4938	3.1375
275	2.4698	2.8827	1.9896	2.3221	2.926
276	2.5621	2.6912	2.2582	2.4075	2.9451
277	2.6922	3.1038	2.4843	2.5764	3.0161
278	2.7029	3.0957	2.4707	2.4163	2.9495
279	2.6962	3.1943	2.2273	2.4575	2.7965
280	2.7122	3.2068	2.3647	2.4449	2.9683
281	2.6259	2.6916	2.3166	2.61	2.8964
282	2.6142	2.375	2.1994	2.2932	2.9531
283	2.4843	2.4658	2.2429	2.0953	3.0993
284	2.4843	2.4772	2.424	2.302	2.9992
285	2.7049	2.5627	2.4022	2.591	2.8921
286	2.3117	2.5026	2.468	2.5045	2.7975
287	2.2783	2.754	2.3533	2.3754	2.7007
288	2.0294	2.5532	2.1868	2.3995	2.5184
289	1.6351	2.4048	2.2125	2.4486	2.961
290	2.452	2.3844	2.3031	2.6804	2.9349
291	2.4488	2.6823	2.2005	2.3983	2.5825
292	2.2537	2.2495	2.4069	2.548	2.7327
293	2.2045	2.3498	2.2698	2.5236	2.6539
294	2.3481	2.7885	2.1669	2.3991	2.702
295	2.5013	2.9248	2.0627	2.3605	2.591
296	2.385	2.4908	1.9144	2.3825	2.9051
297	2.2816	2.4019	2.1378	2.1492	2.919
298	2.2453	2.3842	2.038	2.3782	2.0517
299	2.7112	2.5848	2.1644	2.5555	2.3551
300	2.2	2.4	2.3	2.9	2.7

Trip 1 EM31 Results - Perpendicular Coil Orientation

Position	Interpolated Conductivity: Line 0	Interpolated Conductivity: Line 25	Interpolated Conductivity: Line 50	Interpolated Conductivity: Line 75	Interpolated Conductivity: Line 100
300	2.1109	2.6138	2.4594	2.4568	2.6426
299	2.198	2.5313	2.62	2.3643	2.7453
298	2.2131	2.6147	2.54	2.5326	2.841
297	2.3968	2.6288	2.4831	2.7889	2.6952
296	2.3679	3.1925	2.6	2.5768	2.8991
295	2.3161	3.1122	2.3751	2.5016	2.5024
294	2.4828	3.0507	2.4539	2.4976	2.4729
293	2.2539	2.6645	2.426	2.3416	2.6837
292	2.1544	2.6122	2.1335	2.3215	2.8758
291	2.1477	2.7871	2.3	2.5694	2.8223
290	2.4629	2.7834	2.3206	2.6086	2.8916
289	2.5451	2.5103	2.3311	2.8057	2.8003
288	2.5606	2.4821	2.203	2.6675	2.9072
287	2.49	2.6705	2.0322	2.4163	2.9204
286	2.4565	2.8088	2.025	2.4012	2.8868
285	2.3944	2.482	2.1831	2.4437	2.7766
284	2.2596	2.5416	2.427	2.6005	2.8868
283	2.4478	2.5514	2.1862	2.4908	2.9002
282	2.5075	2.5593	2.6243	2.2091	2.8961
281	2.5097	2.6398	2.6	2.3858	2.78
280	2.4084	2.8081	2.3729	2.5087	2.9309
279	2.4839	2.9137	2.2713	2.0731	3.0825
278	2.5013	2.8394	2.4612	2.4031	2.9856
277	2.5239	2.8869	2.5182	2.6301	3.1007
276	2.5228	2.7125	2.5	2.4423	2.8626
275	2.5996	2.9009	2.5096	2.3905	2.6953
274	2.6016	2.8371	2.6642	2.0618	2.9279
273	2.7602	3.081	2.5981	2.6032	2.8311
272	2.9172	2.9823	2.5168	2.562	3.6728
271	2.9822	3.0639	2.55	2.3591	3.4228
270	2.7891	3.3235	2.4094	2.0631	2.9775
269	2.7737	3.1388	1.9814	2.2524	3.0846
268	2.7553	2.9042	2.1682	2.5815	3.3372
267	3.1342	3.0336	2.4544	2.5121	3.2373
266	3.1713	2.8926	2.5	2.5297	3.1211
265	2.8489	3.1214	2.4081	2.4418	3.0037
264	2.522	3.003	2.5235	2.3979	3.022
263	2.5906	3.1159	2.4267	2.3989	3.2002
262	2.7827	2.8306	2.4737	2.4857	3.0405
261	2.9822	3.0212	2.5	2.402	2.9905
260	3.0414	3.1029	2.3201	2.5131	3.064
259	2.9464	3.0854	2.4931	2.1525	3.2091
258	2.8128	2.8737	2.344	2.4919	2.7785
257	2.8898	3.0203	2.2376	2.4412	2.8241

256	2.8594	3.0757	2.925	2.5453	2.8518
255	2.6878	2.8482	2.516	2.4977	2.8246
254	2.8927	3.7027	2.2816	2.5288	2.9572
253	2.8272	3.0048	2.6291	2.2727	3.0018
252	2.8098	3.1529	2.818	2.3208	2.9948
251	2.9373	3.2025	2.525	2.49	2.8665
250	3.004	3.2069	2.5135	2.5664	2.7844
249	2.8997	3.0979	2.6595	2.3797	2.8588
248	3	3.0918	2.631	2.5071	2.9681
247	2.8984	2.9191	2.6874	2.5235	3.0459
246	2.918	3.0911	2.6	2.505	2.4931
245	2.7674	3.1456	2.5971	2.4738	2.858
244	2.959	2.8996	2.6509	2.6899	2.6998
243	3.1847	2.9906	2.6171	2.4668	3.0917
242	2.9958	2.9836	2.6759	2.3317	3.1896
241	3.1134	2.8346	2.65	2.3887	2.9029
240	3.115	2.8704	2.4763	2.4646	3.0177
239	3.2556	2.9967	2.311	2.4795	3.0571
238	3.4526	3.0933	2.639	2.5896	2.9071
237	3.3595	2.7496	2.5669	2.6615	3.084
236	3.2066	2.7688	2.6	2.4153	3.0282
235	3.1888	3.0112	2.9778	2.4004	2.9119
234	3.0761	2.9999	2.4424	2.2431	2.8513
233	3.1286	3.1145	2.6771	2.3572	3.1785
232	2.9606	3.4028	2.6414	2.6289	2.811
231	2.9815	2.9558	2.65	2.4356	2.9316
230	3.3957	2.8554	2.4834	2.3253	3.0143
229	3.6051	3.0898	2.3819	2.4815	2.9898
228	3.6946	3.0889	2.3592	2.6125	3.2065
227	3.6248	2.8165	2.3239	2.502	3.0379
226	3.5607	2.7786	2.3	2.606	2.918
225	3.7026	2.9328	2.4287	2.613	3.0541
224	3.4117	2.9113	2.468	2.4944	3.2062
223	3.118	2.8047	2.4042	2.6918	3.0047
222	3.5988	2.8412	2.4687	2.4538	3.2105
221	3.5938	2.5973	2.7	2.1295	3.1989
220	3.5065	2.4824	2.4616	2.2661	3.1605
219	3.72	2.4252	2.399	2.6229	3.1017
218	3.693	2.6038	2.3941	2.3987	3.0227
217	3.5001	2.7061	2.569	2.736	3.0567
216	3.6004	2.706	2.35	2.6604	3.3097
215	3.4633	3.0219	2.3172	2.5695	3.2632
214	3.3925	2.8943	2.4153	3.6351	3.1474
213	3.4044	2.6998	2.1753	2.4488	3.0706
212	3.2556	2.8238	2.2473	2.2241	2.9382
211	3.0743	2.7205	2.625	2.4027	2.7063
210	3.1086	2.3914	2.3681	2.4823	2.9179
209	3.0907	2.5579	2.2143	2.3984	3.1051
208	3.1446	2.603	2.1365	2.5714	2.8956
207	3.2619	2.4757	2.2838	2.4453	2.8899

206	3.3246	2.4571	2.4	2.5966	3.0556
205	3.2037	2.6936	2.5018	2.412	2.7484
204	3.3599	2.6461	2.5414	2.5176	2.4065
203	3.2317	2.4062	2.5619	2.397	2.8775
202	3.0934	2.5169	2.3611	2.3539	3.018
201	3.1294	2.6135	2.2	2.3559	2.9354
200	3.282	2.5487	2.3252	2.7022	2.9178
199	3.2683	2.5916	2.427	2.3477	2.7285
198	3.109	2.4974	2.5486	2.5095	2.9022
197	3.0979	2.8316	2.6301	2.7586	2.802
196	3.1011	2.938	2.3	2.2968	2.9255
195	2.9987	2.4408	2.3189	2.6853	2.8315
194	3.0016	2.2498	2.4431	2.7505	2.8651
193	2.9947	2.5736	2.2589	2.6478	2.8437
192	2.8817	2.5215	2.3754	2.6031	2.4014
191	2.9217	2.4665	2.2	2.3602	2.8644
190	3.0441	2.5081	2.1911	2.42	2.8738
189	2.6828	2.7597	2.3319	2.6001	3.0418
188	2.7423	2.437	2.3922	2.8511	2.8897
187	2.6189	2.3993	2.4215	3.0083	2.797
186	2.9046	2.3189	2.6	2.6225	2.697
185	2.9717	2.3117	1.5611	2.6846	2.713
184	2.9018	2.3645	2.2953	2.5119	2.6186
183	2.8185	2.51	2.427	2.4939	2.5619
182	2.6303	2.503	2.3809	2.396	2.6784
181	2.5855	2.1588	2.4	2.8343	2.8156
180	2.661	2.1286	2.2639	2.7337	2.3922
179	2.716	2.2414	2.0446	2.5022	2.4331
178	2.7767	2.3256	2.3624	2.2605	2.6816
177	2.8054	2.0967	2.4439	2.3709	2.5168
176	2.7968	2.4042	2.525	2.8491	2.6924
175	2.8075	2.1548	2.3384	2.7639	2.7081
174	2.7211	2.3036	2.1202	2.3928	3.2205
173	2.6144	2.2412	2.3012	2.5322	3.7811
172	2.5806	2.2797	2.7735	2.5219	2.4712
171	2.8886	2.3693	2.5	2.6118	2.4447
170	2.8054	2.1059	2.6415	2.5446	2.5775
169	2.6996	2.4403	2.7001	2.4014	2.6175
168	2.704	2.4127	2.4725	2.4036	2.7
167	2.8004	2.2199	2.3171	2.3913	2.5763
166	2.6808	2.1723	2.3	2.502	2.4888
165	2.6074	2.0949	2.6135	2.6269	2.5216
164	2.7533	2.0729	2.4412	2.4338	2.384
163	2.7844	1.8998	2.4232	2.4965	2.5779
162	2.6852	2.1409	2.6713	2.2799	2.5254
161	2.7205	2.3975	1.9	2.3466	2.6916
160	2.7381	2.3641	2.1054	2.2091	2.4511
159	2.6887	2.2161	2.5753	2.6995	2.3344
158	2.4393	2.007	2.6369	2.5626	2.4008
157	2.4145	2.2858	2.3325	2.7162	2.7535

156	2.6106	3	2.475	2.5162	2.7
155	2.7262	2.5366	2.3918	2.4942	2.6711
154	2.6607	2.3051	2.3033	2.5325	2.523
153	2.3589	2.0696	2.3458	2.0563	2.5137
152	2.207	2.2656	2.7749	2.2199	2.3937
151	2.3248	2.3734	2.7	2.7078	2.3709
150	2.4926	2.3961	2.6395	2.4779	2.6757
149	2.3179	2.4519	2.3693	2.3002	2.3039
148	2.4309	2.7024	2.5062	2.444	2.4786
147	2.3265	2.4829	2.3713	2.4358	2.3777
146	2.2913	2.3182	2.7	2.496	2.4431
145	2.3501	2.5144	2.3451	2.6717	2.477
144	2.3019	2.4553	2.3508	2.3462	2.5251
143	2.2998	2.4786	2.5057	2.507	2.4858
142	2.3259	2.7069	2.4129	2.7215	2.3968
141	2.351	2.5192	2.4	2.6322	2.3552
140	2.4156	2.4196	2.3777	2.4972	2.2895
139	2.4786	2.2357	2.7592	2.4966	2.3081
138	2.3065	2.1049	2.6641	2.5216	2.296
137	2.3662	2.4019	2.5855	2.2992	2.6142
136	2.2297	2.6127	2.8	2.5177	2.4368
135	2.3875	2.3988	2.7424	2.7837	2.2097
134	2.3456	2.4832	2.5019	2.545	2.3879
133	2.5171	2.4704	2.6416	2.5341	2.5467
132	2.5382	2.5903	2.467	2.2398	2.4003
131	2.5802	2.0659	3	2.2848	2.3993
130	2.4291	2.3095	2.6314	2.4146	2.2291
129	2.4435	2.5908	2.4143	2.5837	2.5031
128	2.5223	2.5586	2.5394	2.6047	2.3931
127	2.432	2.5467	2.8378	2.6096	2.1404
126	2.4127	2.3772	2.5	2.5033	2.4875
125	2.4087	2.1985	2.2691	2.495	2.7112
124	2.4056	2.5122	2.2549	2.5816	2.6486
123	2.33	2.4511	2.5251	2.6009	2.4454
122	2.2676	2.7243	2.7343	2.5399	2.325
121	2.5065	2.3711	2.7	2.4505	2.3651
120	2.1578	2.3977	2.5644	2.5285	2.5034
119	2.3152	2.3155	2.5402	2.4952	2.2916
118	2.5888	2.4322	2.7885	2.4861	2.4601
117	2.7012	2.6873	2.7604	2.5933	2.6723
116	2.5221	2.7022	2.725	2.3626	2.7262
115	2.3915	2.5973	2.6349	2.4524	2.6168
114	2.2136	2.491	2.6012	2.0262	2.598
113	2.2481	2.4702	2.5632	2.5098	2.6202
112	2.4383	2.5926	2.4825	2.4634	2.636
111	2.5152	2.5481	2.7	2.5731	2.6134
110	2.7127	2.5723	2.724	2.4279	2.5482
109	2.5244	2.7982	2.7007	2.4066	2.5956
108	2.1988	2.7365	2.4569	2.5334	2.6783
107	2.1633	2.8925	2.5996	2.558	2.4984

106	2.4776	2.6834	2.5	2.482	2.6497
105	2.4719	2.5073	2.7439	2.7906	2.7781
104	2.4223	2.6085	2.7357	2.5012	2.6456
103	2.4684	2.8198	2.517	2.5986	3.3603
102	2.2776	2.7602	2.3972	2.452	2.7542
101	2.1942	2.6464	2.5	2.4716	2.2803
100	2.2705	2.6048	2.4663	2.6	2.2452
99	2.3652	2.6006	2.6873	2.3913	2.6718
98	2.468	2.6884	2.645	2.2108	2.7466
97	2.5721	2.8725	2.8721	2.7349	2.7359
96	2.5081	2.9536	2.9	2.6825	2.5079
95	2.539	2.7862	2.5591	2.7185	2.7067
94	2.3347	2.7049	2.492	2.4826	2.8733
93	2.4884	2.6209	2.5485	2.6853	2.6499
92	2.4039	2.591	2.6967	2.792	2.6089
91	2.4974	2.5272	2.7	2.2971	3.1357
90	2.5002	2.7978	2.8019	2.5032	3.0297
89	2.6003	2.8018	2.4471	2.5868	2.6765
88	2.4911	2.8192	2.7946	2.6088	2.5427
87	2.4168	2.9162	2.6714	2.7617	2.7912
86	2.4178	2.5014	2.7	2.807	2.9001
85	2.4759	2.6123	2.8834	2.7258	2.9011
84	2.2857	2.7328	2.6795	2.6001	2.8975
83	2.4767	2.5791	2.7409	3.4772	2.8876
82	2.7181	2.4539	2.5251	2.9151	2.8774
81	2.6376	2.9247	2.6	2.785	3.229
80	2.4516	2.6652	2.691	2.695	2.9369
79	2.3538	2.4805	2.8309	2.9182	3.0615
78	2.2922	2.6064	3.2518	2.9032	3.0037
77	2.2974	2.7093	2.7768	2.7979	3.0973
76	2.3262	2.691	2.8	2.7411	3.0346
75	2.3463	2.7553	2.9172	2.9741	3.178
74	2.1931	2.8928	2.9705	2.9045	3.1521
73	2.4258	2.7935	2.7503	3.1451	3.4341
72	2.4593	2.6178	2.7209	2.9342	3.6893
71	2.3866	2.7886	3.1	3.2233	3.6061
70	2.4044	2.5418	2.9803	3.1945	3.2523
69	2.3943	2.3615	2.8036	2.9927	3.2616
68	2.4753	2.3982	2.8802	3.2127	3.2718
67	2.6234	2.691	3.0165	3.2443	3.539
66	2.5098	2.7336	3	3.4977	3.512
65	2.4978	2.5987	3.0874	3.7293	3.4964
64	2.5008	2.1591	3.0252	3.0523	3.4053
63	2.3991	2.5122	3.1095	3.3755	3.4094
62	2.3941	2.7065	3.1042	3.4662	3.2518
61	2.3081	2.6998	3.05	3.3988	3.5319
60	2.5233	2.6875	3.1005	3.1976	3.6018
59	2.4571	2.786	2.8876	3.092	3.5896
58	2.3269	2.7074	2.9601	2.8832	3.3519
57	2.491	2.7064	3.1982	3.3924	3.0398

56	2.4366	2.6492	3.2	3.7263	2.9327
55	2.6199	2.7504	3.1961	3.6506	3.3138
54	2.6232	2.8533	3.2365	3.3996	3.3868
53	2.7305	2.7338	3.3383	3.5241	3.3952
52	2.6076	2.5929	3.6145	3.5651	3.3013
51	2.4889	2.6303	3.3	3.301	3.2279
50	2.4579	2.7647	3.0916	3.4801	3.111
49	2.3689	2.8618	3.1017	3.4712	3.3721
48	2.5232	2.9903	3.1046	3.4971	3.2378
47	2.6232	3.0264	3.1484	3.51	3.0009
46	2.536	2.9486	3.8	3.4173	3.0818
45	2.4238	2.8458	3.6142	3.4135	3.0891
44	2.3837	3.1498	3.7294	3.8292	3.257
43	2.4912	3.2058	3.4749	3.9303	3.2155
42	2.4204	3.0962	3.5166	3.641	3.0095
41	2.3876	2.9713	3.4	3.6492	3.2071
40	2.4994	3.4451	3.6091	3.8144	2.8065
39	2.4033	3.1065	3.4301	3.6808	2.193
38	2.4956	3.0662	3.5062	3.5851	2.9396
37	2.5988	3.2002	3.6977	3.4942	3.0081
36	2.393	3.0824	3.625	3.6439	2.9924
35	2.4065	3.1828	3.62	3.4536	3.1014
34	2.3786	3.3376	3.6764	3.4017	2.9386
33	2.3479	3.4857	3.5765	3.0901	2.7632
32	2.724	3.309	3.8526	3.2853	3.2043
31	2.5628	3.3011	4	3.3007	2.8634
30	2.6315	3.3337	4.1039	3.2399	2.619
29	2.606	3.368	3.8186	3.0916	2.7059
28	2.336	3.2529	3.7208	3.2165	3.1398
27	2.5	3.5965	3.7837	3.3871	3.2587
26	2.4533	3.419	3.8	3.1619	3.2115
25	2.4173	3.8024	3.7296	2.797	3.0153
24	2.612	3.5185	3.8815	3.1349	2.9051
23	2.7242	3.5289	3.8077	3.2107	3.0013
22	2.6438	3.8961	3.6351	3.21	3.0274
21	2.5408	3.5944	3.6	3.3766	3.1703
20	2.428	3.847	3.5905	3.3004	3.0047
19	2.5352	3.9366	3.7388	3.3589	2.8635
18	2.6983	3.644	3.8751	3.0641	2.8108
17	2.6191	3.392	3.6994	3.1291	2.9006
16	2.6572	3.5019	3.7	3.1494	2.981
15	2.8999	3.5009	3.28	3.3294	3.0329
14	2.6531	3.4116	3.4339	3.2988	2.6985
13	2.5981	3.6035	3.3197	3.2789	2.8267
12	2.5977	3.5513	3.4402	3.123	2.9972
11	2.9	3.75	3.8	3.2	2.9

Trip 2 EM31 Results - Parallel Coil Orientation

Position	Interpolated Conductivity: Line 0	Interpolated Conductivity: Line 25	Interpolated Conductivity: Line 50	Interpolated Conductivity: Line 75	Interpolated Conductivity: Line 100
11	2.2681	3.6039	3.8079	3.1903	3.1093
12	2.375	3.5931	3.9924	3.1699	3.2714
13	2.6504	3.7948	3.986	3.3654	3.2767
14	2.551	3.8226	4.0485	3.1389	3.5738
15	2.3108	3.9104	4.1014	3.1126	3.3196
16	2.2651	4.072	3.7167	3.0785	3.226
17	2.4673	3.7175	3.8785	3.0543	3.1225
18	2.2793	3.7744	3.8533	2.9326	3.1615
19	2.2533	3.9291	3.9516	2.82	3.0222
20	2.2157	4.177	3.7127	2.8705	3.148
21	2.2905	3.9888	3.9535	3.0334	3.1731
22	2.1727	3.7663	3.9653	2.9926	3.305
23	2.2098	3.9477	3.8337	3.0885	3.2617
24	2.3235	3.9522	4.0622	3.0297	2.9841
25	2.2546	3.6491	4.0861	2.8871	3.2501
26	2.3676	3.7855	4.1236	2.7942	2.9865
27	2.2029	3.9301	4.0099	2.9773	2.9809
28	2.3289	3.7342	4.0136	3.0031	3.2154
29	2.2165	3.3828	4.0845	3.0423	3.372
30	2.2506	3.5713	4.1607	3.1484	3.4852
31	2.2014	3.495	4.0415	3.415	3.3338
32	2.1483	3.5118	4.2397	3.3888	3.1563
33	2.4726	3.2988	4.2694	3.3584	3.1496
34	2.2909	3.4257	3.8815	3.4767	3.1196
35	2.2733	3.5694	4.0635	3.5185	3.1752
36	2.0289	3.4534	3.9295	3.5565	3.0263
37	2.4164	3.2894	3.9932	3.5376	3.1631
38	2.3578	3.512	3.9183	3.503	3.1573
39	2.2693	3.298	4.0727	3.4102	3.2819
40	2.1505	3.2795	3.9371	3.4799	3.2025
41	2.2467	3.0917	3.939	3.4616	3.356
42	2.3055	3.5166	3.7591	3.8153	3.3566
43	2.2522	3.213	3.8129	3.6502	3.667
44	2.4199	3.4257	4.0177	3.7704	3.5308
45	2.2358	3.599	3.8613	3.7848	3.5232
46	2.3525	3.2594	3.816	3.8773	3.3895
47	2.2167	3.2117	3.9229	3.7484	3.2643
48	2.3057	3.2007	3.911	3.61	3.2258
49	2.3143	3.4604	3.7119	3.4602	3.3831
50	2.5064	3.2175	3.8037	3.3866	3.3418
51	2.4077	2.9513	3.6832	3.5016	3.2706
52	2.4705	2.7986	3.7673	3.5098	3.1954
53	2.2559	2.9921	3.521	3.4883	3.3806
54	2.5313	2.8009	3.7778	3.4776	3.4382

55	2.3657	2.971	3.5429	3.4151	3.4683
56	2.0974	2.8204	3.4771	3.3387	3.3967
57	2.2538	3.0044	3.4075	3.2714	3.1875
58	2.5982	2.8141	3.4821	3.1377	3.4494
59	2.1815	2.9108	3.4212	3.0039	3.6313
60	1.9834	3.1449	3.0724	3.0237	3.7684
61	2.37	2.5456	3.3476	3.1871	3.5796
62	2.3277	2.8276	3.3416	3.1664	3.6358
63	2.2629	3.0293	3.3622	3.0658	3.6497
64	2.2464	2.8047	3.259	2.8011	3.7449
65	2.6215	2.4975	3.4254	2.5705	3.8541
66	2.3946	2.7048	3.4116	2.5281	4.2194
67	2.375	2.7352	3.3311	2.7753	4.1549
68	2.1846	2.6354	2.9674	2.8405	3.9162
69	2.3337	2.4864	3.3702	2.7155	3.6521
70	2.509	2.9334	3.2522	2.6894	3.7177
71	2.3485	2.7824	3.1441	2.7514	3.5628
72	2.1387	2.6118	2.9441	2.6026	3.3619
73	2.3535	2.4967	3.2117	2.4615	3.2742
74	2.2901	2.829	3.1033	2.4861	3.5163
75	2.5247	2.68	3.0024	2.3583	3.571
76	2.3246	2.6472	3.0152	2.4978	3.6502
77	2.3503	2.8357	3.3317	2.5657	3.5051
78	2.4139	2.891	3.2011	2.6791	3.3567
79	2.3374	2.8208	3.0946	2.6763	3.1972
80	2.4797	3.2615	3.0692	2.6264	3.1622
81	2.5992	2.9273	3.2185	2.2979	3.0907
82	2.9669	2.8357	2.9553	2.3025	3.105
83	2.669	3.1619	2.9896	2.3382	3.1567
84	2.2988	2.9709	2.9737	2.5134	3.2652
85	2.4983	2.9125	2.9703	2.4253	3.2234
86	2.7574	2.7813	2.872	2.5124	3.0314
87	2.5931	2.82	3.0876	2.6226	3.0312
88	2.5819	2.8602	2.9	2.3311	2.9216
89	2.3279	2.8209	2.884	2.3087	2.8063
90	2.6999	2.8341	2.8943	2.1858	2.8445
91	2.4896	2.8695	2.8575	2.3231	2.9449
92	2.527	3.0003	3.0001	2.2537	2.8695
93	2.4601	2.9063	2.8089	2.3016	2.9237
94	2.3069	2.7276	2.759	2.1016	2.7421
95	2.5423	3.0084	2.9729	1.9327	2.773
96	2.2259	2.9924	2.7905	2.1265	2.7504
97	2.3273	2.509	2.9697	2.1483	2.6657
98	2.3725	2.7936	2.8758	2.1659	2.7942
99	2.4632	2.9249	3.124	2.2111	2.797
100	2.7328	2.8751	2.9468	2.3086	2.7866
101	2.2575	2.9248	2.7978	2.297	2.7084
102	2.3124	2.9971	2.8118	2.185	2.8421
103	2.2899	3.0245	2.9314	2.2152	2.5631
104	2.3027	2.7782	2.6424	2.2395	2.4185

105	2.3185	3.1084	2.3285	2.2006	2.5291
106	2.5061	2.81	2.7372	2.1102	2.7803
107	2.3992	2.7958	2.7387	2.3695	2.8394
108	2.1203	2.7832	2.6894	2.369	2.5852
109	2.2777	2.8022	2.6053	2.2545	2.5525
110	2.579	2.7893	2.7102	2.3424	2.4837
111	2.5706	2.6637	2.8615	2.2101	2.5657
112	2.2417	2.5226	2.9008	2.1354	2.5687
113	2.2581	2.6466	2.6651	2.1072	2.5604
114	2.3084	2.8288	2.8036	2.1805	2.6565
115	2.5232	2.858	2.3079	2.2363	2.5734
116	2.3321	2.7267	2.873	2.4779	2.5105
117	2.5188	2.6773	2.8161	2.4079	2.4469
118	2.5921	2.573	2.8717	2.4614	2.4928
119	2.548	2.7489	2.7042	2.3466	2.4348
120	2.2545	2.6753	2.4683	2.2817	2.2919
121	2.5807	2.705	2.5859	2.3117	2.2699
122	2.439	2.4861	2.746	2.3263	2.4756
123	2.5613	2.4049	2.5079	2.3758	2.4287
124	2.3857	2.5307	2.6383	2.4352	2.5611
125	2.3304	2.5386	2.5993	2.3244	2.6335
126	2.4166	2.352	2.5574	2.2501	2.4818
127	2.3905	2.6201	2.5462	2.2957	2.4044
128	2.5334	2.9995	2.6903	2.4199	2.4731
129	2.2798	2.9132	2.9327	2.374	2.6001
130	2.6475	2.6273	2.6245	2.2358	2.4885
131	2.2921	2.5759	2.7041	2.3694	2.469
132	2.4041	2.6813	2.768	2.2234	2.4142
133	2.2071	2.7604	2.681	2.2216	2.3649
134	2.503	2.905	2.7584	2.2541	2.3033
135	2.1703	2.6179	2.5889	2.2178	2.3521
136	2.2582	2.5193	2.673	2.1161	2.3764
137	2.12	2.6412	2.673	2.3402	2.4577
138	2.311	2.7848	2.6143	2.0216	2.3907
139	2.2617	2.6686	2.5198	2.2183	2.3525
140	2.2671	2.5727	2.5558	2.3451	2.2655
141	2.3167	2.7739	2.61	2.4335	2.3829
142	2.18	2.8097	2.1422	2.2503	2.3408
143	2.2477	2.7234	2.4683	2.2547	2.3685
144	2.1456	2.5091	2.7158	2.2186	2.3239
145	2.2999	2.7949	2.5011	2.4105	2.3688
146	2.1063	2.7276	2.5512	2.3255	2.5589
147	2.2895	2.7058	2.6208	2.4814	2.6686
148	2.3546	2.8953	2.7979	2.4627	2.3407
149	2.3077	2.9122	2.5305	2.6072	2.2553
150	2.3163	2.716	2.5431	2.6656	2.3939
151	2.3021	2.6031	2.6704	2.3665	2.4389
152	2.2615	2.905	2.499	2.4094	2.4731
153	2.0829	2.7751	2.5922	2.1853	2.5655
154	2.5529	2.8137	2.466	2.0286	2.7467

155	2.595	2.5935	2.635	2.3685	2.705
156	2.2094	2.623	2.6297	2.4029	2.5089
157	2.4187	2.6334	2.3812	2.2931	2.4643
158	2.4675	2.6516	2.6272	2.3885	2.4378
159	2.5847	2.7372	2.7472	2.1192	2.4595
160	2.5599	2.6442	2.7042	2.2488	2.5301
161	2.6615	1.9088	2.7752	2.1861	2.3533
162	2.6751	2.5945	2.6329	2.4034	2.5268
163	2.6744	2.4739	2.7817	2.2636	2.5758
164	2.859	2.4559	2.5156	2.2462	2.5073
165	2.7697	2.4365	2.4484	2.2199	2.4825
166	2.8628	2.519	2.7876	2.1658	2.3041
167	2.7946	2.5273	2.5336	2.2859	2.3594
168	2.7273	2.497	2.5085	2.2588	2.5467
169	2.8799	2.3881	2.5167	2.3635	2.483
170	3.0612	2.7715	2.6984	2.427	2.4075
171	2.9162	2.5654	2.7162	2.5304	2.2959
172	2.8333	2.582	2.2933	2.6628	2.4337
173	2.7223	2.67	2.5944	2.5425	2.4247
174	2.9663	2.8135	2.7746	2.3823	2.4083
175	2.8921	2.3835	2.4351	2.3405	2.3301
176	3.0718	2.5895	2.7335	2.4135	2.3891
177	2.7118	2.5978	2.5801	2.5537	2.5099
178	2.783	2.5162	2.6425	2.4993	2.6731
179	2.9654	2.4971	2.6381	2.4308	2.6799
180	2.5823	2.5225	2.8011	2.3725	2.3139
181	2.8836	2.9127	2.8274	2.3802	2.4188
182	2.9293	2.6235	2.772	2.4244	2.4551
183	3.0874	2.7201	2.6614	2.2323	2.423
184	2.9482	2.8635	2.7108	2.307	2.6541
185	2.7762	2.8493	2.9429	2.1804	2.661
186	3.0176	2.7407	2.493	2.3654	2.6071
187	3.1983	3.1144	2.636	2.5247	2.5049
188	3.0272	2.9656	2.6991	2.5713	2.522
189	3.0719	2.5796	2.696	2.4331	2.7067
190	2.8796	2.9064	2.7126	2.4301	2.8305
191	3.2335	2.7748	2.571	2.4836	2.9295
192	3.1189	3.1016	2.5993	2.2813	2.6977
193	3.1019	3.1446	2.6828	2.274	3.0325
194	3.1734	3.0526	2.7027	2.486	3.0268
195	3.2662	3.3194	2.4409	2.532	2.9274
196	3.1109	3.0325	2.7713	2.5036	2.8523
197	3.1358	3.001	2.5367	2.4435	2.9368
198	3.3106	3.2347	2.4965	2.3926	3.1199
199	3.399	3.3381	2.4432	2.5716	2.9385
200	3.6658	3.0528	2.6037	2.6026	2.8429
201	3.1681	3.104	2.6003	2.5872	3.0277
202	3.4934	3.2023	2.4196	2.4914	3.0201
203	3.7297	3.0671	2.7412	2.4996	3.1127
204	3.3952	3.0243	2.4736	2.4001	3.0483

205	3.5823	3.2608	2.4683	2.3713	2.9222
206	3.6311	3.2019	2.4889	2.142	3.0792
207	3.4392	3.1843	2.6933	2.2162	2.9554
208	3.5881	3.1155	2.6507	2.4053	3.0622
209	3.554	3.1092	2.5696	2.3447	3.239
210	3.4421	3.0775	2.6382	2.3732	3.3234
211	3.7445	2.9931	2.6065	2.6113	2.9819
212	3.5643	3.2795	2.5254	2.4226	3.005
213	3.3639	3.3162	2.4384	2.7175	2.8746
214	3.6962	3.2721	2.3907	2.4806	2.8754
215	4.013	3.3207	2.6878	2.4125	2.9083
216	3.6534	3.3949	2.4667	2.3884	3.0041
217	4.2201	3.2693	2.6293	2.3993	2.9974
218	4.0258	3.1747	2.7078	2.3074	3.0076
219	4.0694	3.0873	2.6083	2.4501	2.9736
220	3.9363	3.4837	2.5075	2.4618	2.9495
221	3.9649	3.3499	2.4993	2.3054	3.236
222	4.5705	3.2402	2.6495	2.4933	3.2085
223	4.5128	3.3437	2.5989	2.3432	3.0738
224	4.2111	3.4103	2.5893	2.3402	3.0817
225	4.109	3.3717	2.7934	2.3454	2.9732
226	4.3135	3.2187	2.8092	2.3875	2.9746
227	4.1336	3.5753	2.7551	2.4187	2.9521
228	4.2008	3.3638	2.6298	2.5401	3.0601
229	3.9668	3.4173	2.8652	2.3288	2.9528
230	4.1807	3.3816	2.6556	2.3047	3.0336
231	4.0248	3.422	2.6306	2.2366	3.1342
232	3.8521	3.5167	2.7343	2.251	3.2467
233	3.6876	3.2963	2.8389	2.2289	3.0437
234	3.9179	3.4409	2.804	2.3151	2.9392
235	3.8645	3.473	2.6541	2.3895	2.9821
236	3.6235	3.2882	2.777	2.3888	3.093
237	3.4923	3.5696	3.0596	2.3462	3.2274
238	3.6954	3.633	2.8386	2.3716	3.1109
239	3.5652	3.5055	2.6906	2.5016	3.1803
240	3.3816	3.4406	2.9768	2.3647	3.1167
241	3.5619	3.5642	2.8596	2.2218	3.0766
242	3.4555	3.5143	2.9898	2.3352	3.0723
243	3.4034	3.4355	2.8604	2.4829	3.034
244	3.1282	3.6305	3.053	2.5297	3.0952
245	3.2119	3.6331	2.8641	2.3661	3.2751
246	3.4121	3.4876	2.634	2.2723	3.1783
247	2.9855	3.712	2.8746	2.3303	3.1924
248	3.1008	3.628	2.9472	2.2761	3.0775
249	2.655	3.7686	2.8134	2.2899	3.2532
250	2.8239	3.674	2.7133	2.2443	2.8655
251	2.9617	3.5276	2.9679	2.4648	2.8589
252	2.6684	3.7349	2.9209	2.5708	3.0003
253	2.7791	3.6263	3.0507	2.3418	3.2028
254	2.7383	3.8181	2.816	2.2915	3.1114